EXCESS CENTROSOMES IN ENDOTHELIAL CELLS: CAUSES AND EFFECTS

Zhixian Yu

A dissertation submitted to the faculty at the University of North Carolina at Chapel Hill in partial fulfillment of the requirements for the degree of Doctor of Philosophy in the Curriculum in Genetics and Molecular Biology in the UNC Graduate School.

Chapel Hill
2016

Approved by:

Victoria Bautch

Jean Cook

Kimryn Rathmell

Stephen Rogers

Qing Zhang

ABSTRACT

Zhixian Yu: Excess Centrosomes in Endothelial Cells: Causes And Effects
(Under the direction of Victoria Bautch)

Tumor endothelial cells, which line the interior surface of tumor blood vessels, were considered genetically normal until recent findings showed that they can be aneuploid, and have compromised p53 signaling and excess centrosomes. However, the causes and effects of centrosome over-duplication and compromised p53 signaling in endothelial cells remain elusive. In this dissertation, I designed and performed various experiments to investigate these questions. I found that some BMP ligands induced BMPR1A-dependent excess centrosomes in primary human endothelial cells, likely though SMAD signaling. In addition, hypoxia and abrogated p53 signaling, but not inflammation, promoted centrosome over-duplication. These results contribute to our understanding of tumor microenvironment. I also demonstrated that excess centrosomes induced p53-dependent senescence in primary endothelial cells, indicating that the response of centrosome over-duplication is dependent on whether cells have intact cell cycle. This is the first evidence linking excess centrosomes and senescence, and may also help explain the abnormal morphology and function in tumor vasculature. Finally, I showed that loss of p53 induced angiogenesis *in vitro* by promoting endothelial cell migration and proliferation, but not in mouse retina vessels. In summary, my thesis work helps understand the causes and effects of centrosome over-duplication in endothelial cells, contributing to the studies on tumor microenvironment.

To everyone who made this dissertation possible.

ACKNOWLEDGEMENTS

It has been more than five years since my first day as a student at UNC. My graduate career was not a pleasant journal, but I feel so lucky that so many people have made it less miserable.

First I want to thank my committee, who provided so much productive advice and helped me through my whole graduate career. I am grateful for their time despite of their extremely busy schedule. Their suggestions have improved me and made me a better scientist.

Special thanks go to my mentor Dr. Vicki Bautch, without whom my degree would be impossible, for her guidance and support. She taught me how to critically think about my project, and pushed me to continue despite of unexpected failure. She was always supportive when I applied for fellowships, and encouraged me to pursue new directions in my project. Talking about science with her is always challenging and satisfying. She also provided so much help with my scientific writing, and is very rigorous about them. Most importantly, she built a wonderful lab to work in, and I met so many great people in her lab.

Dr. Erich Kushner is a smart and productive scientist who offered so much help to me. His initial findings in tumor endothelial cells are the foundation for my major story. He also built so many tools which made my research significantly easier. Dr. Kevin Mouillesseaux is also a great scientist who was my mentor when I was first rotating in this lab. His work contributed to my research paper about centrosome over-duplication. Diana Chong helped me with retina dissection, which is part of my work in Chapter IV.

Besides research, all Bautch lab members have been very good friends to me. I especially thank Diana who listened to my complaint and frustration. She is always a very positive person who encouraged me to overcome sadness. Talking to her gave me hope and made me feel confident. She also took me to hospitals when I had surgeries, and I cannot ask more than that. Jess Nesmith is also a very positive and strong person, who acted as a model for me to deal with my negative feelings about my disease and surgeries, and helped me stay on top of everything. Without her, I probably would never notice the deadlines for so many things, including my thesis.

Finally, I want to thank my friends outside lab, especially Li-chung Tsao and Jie-Yu Liu who are very good friends in GMB. I am thankful that we can prepare for qualify exams, attend seminars and go to genetics retreat together. Our lunch time together was always relaxing and full of joy. I also want to thank my friends who drove me to surgeries or took care of me when I had trouble doing that, specifically Diana, Li-chung, Luke Ferro and Ruiwei Liang. My time with other friends outside the lab has also made my graduate life more colorful.

TABLE OF CONTENTS

LIST OF FIGURES

LIST OF ABBREVIATIONS

BD	Basic domain
BMP	Bone morphogenetic protein
BMPR1A	Type 1A BMP receptor
BMPR1B	Type 1B BMP receptor
BMPR2	Type 2 BMP receptor
BrdU	Bromodeoxyuridine
BSA	Bovine serum albumin
CIN	Chromosome instability
DBD	DNA binding domain
DFO	Desferrioxamine
DOX	Doxycycline
EC	Endothelial cells
EGM-2	Endothelial growth medium-2
H3K9Me3	Tri-methylation of lysine 9 on histone 3
HBMEC	Human brain microvascular endothelial cells

HMVEC-L	Human lung microvascular endothelial cells
HRP	Horseradish peroxidase
HUAEC	Human umbilical artery endothelial cells
HUVEC	Human umbilical vein endothelial cells
IL	Interleukin
LPS	Lipopolysaccharide
MAPK	Mitogen-activated protein kinase
MEF	Mouse embryonic fibroblasts
MTOC	Microtubule organization center
NEC	Normal mouse endothelial cells
NTD	N-terminal transactivation domain
PCM	Pericentriolar materials
Plk4	Polo-like kinase 4
pp53	Phosphorylated p53
PRD	Pro-rich domain

PTM	Post-translational modifications
SA-β-gal	Senescence-associated β-galactosidase
SAC	Spindle assembly checkpoint
SAHF	Senescence associated heterochromatic foci
SASP	Senescence-associated secretory phenotype
shRNA	Short-hairpin RNA
Tet-Plk4	Tetracyclin-inducible Plk4-expressing
TD	Tetramerization domain
VEGF	Vascular endothelial growth factor

LIST OF SYMBOLS

β	Beta
γ	Gamma
σ	Sigma
μ	Micro
X	Chi

CHAPTER I-General Introduction

A. Tumor angiogenesis and tumor endothelial cells

My thesis work started with the observed abnormalities in tumor endothelial cells (EC), and I tested the effects of several tumor environmental factors on EC. This section summarizes basic understanding about tumor EC and their environment.

Blood vessels, whose inner surfaces are lined by endothelial cells (EC), support tissue growth by providing oxygen/nutrients and carrying away the metabolic waste. The growth of blood vessels can be divided into two consecutive steps: vasculogenesis and angiogenesis [1]. During vasculogenesis, embryonic angioblasts differentiate, migrate and coalesce to form a primitive vascular network, which is then expanded by angiogenesis to form mature vessels [1,2]. As the major method of vessel expanding and growth, angiogenesis is defined as the process that new vessels form from pre-existing ones. Upon the stimulation of angiogenic factors, such as vascular endothelial growth factor (VEGF-A) [3], some EC in pre-existing vessels respond and become tip cells, and begin to migrate towards the stimuli. EC adjacent to tip cells follow the migration of tip cells to support sprout elongation [4] [2]. At the final stage, tip cells anastomose with cells from neighboring sprouts and build vessel lumens, which allows for blood flow [2].

Similar to normal tissues, solid tumors, specifically those with a diameter larger than 2 mm, require blood vessels for their growth [5]. To induce angiogenesis in the tumor compartment, tumor cells and tumor stromal cells secrete various angiogenic factors, including VEGF-A [6], Interleukin-8 (IL-8) [7,8] and bone morphogenetic protein 2 (BMP-2) [9,10], to recruit blood vessels from the surrounding environment. Tumor vasculature is morphologically

and functionally distinct from normal vasculature. Tumor vessels appear tortuous and leaky, and have irregular blood flow [11]. Therefore although most tumors are highly vascularized, the tumor environment does not acquire sufficient blood supply and become hypoxic, leading to a more clinically aggressive phenotype [12,13].

Despite the morphological and functional abnormalities, tumor EC were originally considered genetically normal and stable because most tumor vessels are recruited from their normal counterparts [14,15]. However, recent studies indicate that tumor EC, similar to tumor cells, have genetic abnormalities such as aneuploidy [16,17]. In line with this, ~30% of tumor endothelial cells possess excess centrosomes (>2 centrosomes/cell), which can contribute to the genetic abnormalities in these cells [17,18]. Previous studies in our lab demonstrated that high levels of VEGF-A induce excess centrosomes in EC [19]. However, it is not known whether other tumor environmental factors contribute to excess centrosomes in EC. In addition, the effects of excess centrosomes on EC cell cycle remain elusive.

B. Centrosomes

I found that several tumor environmental factors induce excess centrosomes in EC. This section summarizes the structure, regulations and common abnormalities of centrosomes.

Centrosomes are important organelles involved in multiple aspects of cell function. A canonical centrosome is comprised of two centrioles and their surrounding pericentriolar material (PCM) **(Fig. 1.1)**. A typical human centriole is ~500 nm long and ~250 nm wide, and it is has a cylinder structure formed by 9 radially symmetric triplet microtubules [20-22]. At the innermost core of the proximal end of a centriole, there is a cartwheel structure containing a central hub with 9 emanating spokes connecting with outside microtubules [23,24]. At the distal

end of a centriole, there are 9 doublet microtubules, which are modified and associated with subdistal and distal appendages [25].

Over 150 proteins are involved in building the centrosome [21,26]. Sas-6, which can self-assemble to ring-like structures, exists at the cartwheel core of a centriole, and helps dictate the nine-fold symmetry structure [27,28]. Another protein, Sas-5 (or the orthologue protein STIL in human), is also present at the cartwheel structure, and cooperates with Sas-6 to assist the cartwheel formation [29,30]. Sas-4 (or the human homolog CPAP), is recruited to the central cartwheel structure by Sas-6 and Sas-5, and promotes centriolar microtubule polymerization [31,32]. Centrioles are surrounded by the PCM containing hundreds of proteins [33], and serve as the dominant microtubule organization center in the cell.

Normally centrosomes are duplicated once and only once in each cell cycle, reminiscent of DNA replication. A typical G1 phase cell has 1 newly born centrosome, which has two centrioles orienting orthogonally to each other. New procentrioles begin to form near each centriole at G1/S phase, and they continue to elongate throughout G2 phase until reaching similar size to their mother centrioles. Before mitosis, the fibrous tether between two newly formed centrosomes will be severed to allow them to migrate to opposite ends of the cell and to set up the mitotic spindle [22]. After cell division, each new daughter cell will inherit one centrosome to maintain homeostasis.

The signaling pathways controlling centrosome duplication are complex and not yet fully understood. It is believed that the CDK2/cyclin E complex, which initiates S phase and promotes DNA replication [34-36], licenses centrosome duplication [37-39]. The exact mechanism of how CDK2/cyclin E initiates centrosome duplication remains elusive, although several downstream targets are implicated, including nucleophosmin (NPM) [40], Mps1 [41], and CP110 [42].

The centriole assembly process begins with the activation of polo-like kinase 4 (Plk4). Activated Plk4 localizes at the proximal end of the mother centriole, and recruits downstream structural proteins such as Sas-6, which triggers the assembly of the cartwheel structure and also the whole centriole by further recruiting other proteins like Sas-5 and Sas-4 [43-45]. Because of its central function in initiating new centriole formation, down-regulation of Plk4 inhibits centrosome duplication [46], and over-expression leads to centrosome over-duplication (>2 centrosomes/cell) [43]. However, the exact mechanisms how cells regulate Plk4 activity during cell cycle are not fully understood. It seems that Plk4 regulates its own phosphorylation to maintain homeostatic Plk4 levels and centrosome numbers, and phosphorylated Plk4 is degraded through a SCF-Slimb/βTrCP-E3 ubiquitin ligase-dependent mechanism [47-50].

Centrosomes mainly function as the primary microtubule organization center (MTOC) to nucleate microtubules which participate in numerous cellular functions such as defining cell polarity [51], cell migration [52], protein transportation [53], and most importantly mitosis [54]. Therefore centrosome abnormalities can lead to cellular defects in both interphase and mitosis. Recent results from our lab showed that excess centrosomes affect microtubule nucleation and dynamics, contributing to disrupted interphase behavior [18,55]. During mitosis, the two newly separated centrosomes localize at different poles of a cell to assist the formation of a mitotic spindle, which ensures the proper and accurate segregation of chromosomes. As a result, centrosome abnormalities, such as centrosome over-duplication which occurs frequently in most tumor cells [56], can compromise chromosome segregation.

The idea that centrosome over-duplication is correlated with tumorigenesis dates back to more than 100 years ago, first proposed by the German biologist Theodor Boveri [21], and it was demonstrated that centrosome over-duplication is strongly associated with aneuploidy and

chromosome instability (CIN), which refers to the phenotype that cells constantly undergo chromosome missegregation and fail to maintain chromosome stability [57-59]. Originally it was believed that excess centrosomes (>2 centrosomes/cell) lead to the formation of multipolar spindles to induce CIN because excess centrosomes and multipolar spindles are frequently detected in tumors with CIN [60,61]. However, most daughter cells from multipolar division do not survive because they lack sufficient genetic information [62]. Therefore, the idea of multipolar spindle-induced CIN creates a paradox, which is resolved by recent literature demonstrating that centrosome over-duplicated cells still undergo classic bi-polar cell division by clustering centrosomes [62]. In this model, daughter cells develop low-level of aneuploidy and CIN from merotelic attachment without compromising their fitness. However, most of these findings were based on results in tumor cells, and the effects of excess centrosomes on primary cells remain elusive.

C. p53

I found that excess centrosomes activate p53 and phosphorylates p53 at ser33 in EC. This section summarizes the structure, regulations and functions of p53.

p53 is a tumor suppressor protein which does not function correctly in most human cancers, and is mutated in about 50% of tumors [63]. It was first identified as a target protein of the T antigen of the virus SV40, which induces tumor development [64-67]. Originally, p53 was considered as an oncogene because it was over-expressed in some tumor cells [68,69]. However, later examinations of p53 in both tumors and normal cells revealed the tumor suppressing function of p53, and demonstrated that highly-expressed p53 in tumor cells are actually p53 mutants [70,71].

Human p53 is a transcription factor with 393 amino acids, which can be divided to 5 major domains: the N-terminal transactivation domain (NTD), the Pro-rich domain (PRD), the central DNA binding domain (DBD), the tetramerization domain (TD) and the C-terminal basic domain (BD) [72,73]. NTD interacts with many transcriptional factors such as $TF_{II}D$ and $TF_{II}H$ to promote target gene expression [74,75]. DBD binds DNA, and confers specificity in selecting target genes. The consensus binding sequences of DBD are 5'-RRRC(A/T)(T/A)GYYY-(n)-RRRC(A/T)(T/A)GYYY-3', where n=0-13, and R and Y stand for purine and pyrimidine, respectively [76]. TD is required for p53 tetramerization [77,78], which is essential for DNA binding, protein interaction and post-translational modifications (PTM) [79].

MDM2 is a well-known regulator of p53, although other regulators have been reported. MDM2 functions as the E3 ubiquitin-protein ligase, binds TAD of p53, and mark p53 for proteasomal degradation [80,81]. Increased levels of MDM2, frequently detected in some tumor types, result in enhanced degradation of p53, and contribute to tumor development [82,83]. Interestingly, MDM2 is also a downstream target of p53, creating a feedback loop to auto-regulate its own levels [84]. This delicate system ensures that the steady-state levels of p53 are precisely controlled until it is activated by stress signaling.

p53 can be activated by several cell stress signals such as DNA damage [85,86], deregulated oncogene expression [87] and hypoxia [88]. p53 activation requires its stabilization, which is dependent on the PTM on p53. Phosphorylation of p53 is usually considered as the first step of p53 stabilization by blocking the physical association between p53 and MDM2, and inhibiting the ubiquitination of p53 [89]. For example upon DNA damage, several kinases (e.g. ATM and ATR) will phosphorylate p53 at Ser15 and Ser20 to alleviate its inhibition by MDM2, and to stabilize and activate p53 [90-93]. Another amino acid, Ser46, can also be phosphorylated

upon stress stimulation, and this particular phosphorylation event seems critical for p53-induced apoptosis and replicative senescence [94,95]. Furthermore, osmotic shock induces p38-dependent Ser33 phosphorylation [96], which is also involved in oncogene-induced senescence [97].

Although some results suggest that p53 can function without its transcriptional activation activity [98,99], activated p53 mainly affects cell behavior by inducing the expression of various downstream target genes such as p21 [100], 14-3-3σ [101], Puma [102] and p53AIP1 [94]. These targets are differentially involved in various p53 activation-dependent effects.

One important function of p53 is to induce cell cycle arrest, serving as an important cell cycle checkpoint mechanism. p53 can use multiple pathways to arrest stress-stimulated cells, and the signaling is extremely complex. Mainly p53 arrests cells at G1/S and G2/M transition. p21, the downstream target of p53, can bind and inhibit CDK2/cyclin E, which is required for G1/S progression [103], therefore arresting cells at G1 phase. p53 can also promotes G2/M arrest by inhibiting Cdc2 via p21, 14-3-3σ and several other targets [104].

In addition to cell cycle arrest, stress-induced p53 promotes apoptosis, i.e. programmed cell death, by activating the expression of multiple pro-apoptotic proteins like Puma [102] and p53AIP1[94], which initiate the apoptotic pathway. Another important outcome of p53 activation is permanent cell cycle arrest, i.e. senescence [105] (see below). It seems that whether cells undergo cell-cycle arrest, apoptosis or senescence is dependent on cell type and stress, and the mechanisms for differential cell destiny are not fully understood [106].

Recent evidence suggests that loss of centrosome integrity activates p53. Loss of centrosome integrity via down-regulation of important centrosome proteins induces p53-dependent cell cycle arrest [107,108]. In addition, inhibition of centrosome assembly by

knocking out Sas-4 activates p53-dependent apoptosis in mouse embryos [109]. These findings suggest that p53 is critically involved in a "centrosome integrity checkpoint" to ensure a complete centrosome structure and function.

Loss of p53 can induce centrosome over-duplication. In 1996, results from Vande Woude group demonstrated that centrosome over-duplication is frequently detected in mouse embryonic fibroblasts (MEF) from p53 knockout mice, indicating that p53 is involved in regulating centrosome duplication [110]. Two theories may explain the p53 loss-induced centrosome over-duplication: p53 controls the initiation of centrosome duplication, and/or p53 serves as a surveillance mechanism for over-duplicated centrosomes.

It is not surprising that p53 may be involved in the initiation of centrosome duplication because p53 upregulates p21, which inhibits CDK2/cyclin E, the initiator of centrosome duplication. In support with this pathway, p21 deficiency induces centrosome over-duplication by triggering a bona fide centriole over-duplication phenotype [111,112]. In addition, re-introduction of p21 in $p53^{-/-}$ cells partially rescued their centrosome duplication cycles [113].

However, there are contradictory results about whether cells have a p53-dependent surveillance mechanism for centrosome over-duplication. In 2001, Andreassen et al. demonstrated that cells possess a p53-dependent tetraploid checkpoint which responds to centrosome over-duplication and tetraploid genome resulting from failed cytokinesis [114]. However, this notion was later questioned by other findings showing "tetraploid checkpoint" may be an artifact of drug overdose and a side effect of DNA damage [115,116]. In line with the idea that no checkpoint detects centrosome over-duplication, cells with excess centrosomes tend to routinely undergo bipolar cell division and produce viable daughter cells [62]. However, several recent results suggest that cells may actually have a p53-depdendent mechanism for

monitoring extra centrosomes. Induction of extra centrosomes by over-expressing a CDK6 activator induces p53-dependent apoptosis [117]. In addition, extra centrosomes induced by Plk4 over-expression seem to stabilize and activate p53 [49,118]. However, the mechanisms and effects of excess centrosomes-induced p53 stabilization remain elusive.

D. Senescence

I found that excess centrosomes induce p53-dependent senescence in primary EC, establishing the first link between excess centrosome and senescence. This section summarizes current understandings of senescence.

Cellular senescence denotes permanent cell cycle arrest. Unlike quiescent cells, senescent cells cannot go back to the cell cycle regardless of nutrient level or differentiation status. Senescence was first noticed and identified by Hayflick who found that cells have a doubling potential of ~50 passages in culture, referred as the Hayflick limit [119,120]. It was later found that the Hayflick limit is caused by shortened telomeres because DNA polymerases cannot fully replicate the lagging strands [121,122]. Shortened telomeres trigger a DNA damage response (DDR), which finally induces p53-dependent senescence [123,124].

Besides telomere shortening, ectopic expression of oncogenes can also induce senescence. In 1997, Serrano et al. demonstrated that enforced expression of oncogenic Ras in primary human or rodent cells induces premature senescence [87], which is contradictory to the general perception of oncogene functions. Later studies showed that over-expression of BRAF or loss of tumor suppressors such as PTEN can also induce senescence [125,126], indicating that oncogene-induced senescence (OIS) is a general mechanism in cells to prevent cell transformation. It has been shown that the p38 MAPK contributes to oncogene-induced

senescence partially by phosphorylating p53 at Ser33 [97]. In addition to telomere shortening and oncogene over-expression, several genotoxic chemicals induce senescence, such as H_2O_2 [127], etoposide [128], and hydroxyurea [129].

Although there are no definite markers for cellular senescence, it is now well-accepted that senescence is a complicated and complex cellular program which alters cellular morphology, signaling and behaviors in multiple ways. First, most senescent cells, such as those induced by oncogene expression and H_2O_2, tend to have large and flat morphology [87,127]. Another prominent feature of senescence is the expression of senescence-associated β-galactosidase (SA-β-gal), which can be detected by chemical reaction at pH 6 [130]. SA-β-gal activity is expressed from a lysosomal protein GLB1, which has optimal activity at pH 4.5 but markedly lower activity at pH 6 [131]. Because senescent cells accumulates high amount of GLB1, the cumulative activity of GLB1 becomes readily detectable at pH 6, representing the SA-β-gal activity [132]. However, no evidence suggests that SA-β-gal/increased GLB1 contributes to senescence progression [131]. Some senescent cells demonstrate senescence associated heterochromatic foci (SAHF) in their nuclei. In 2003, Narita et al. first described this phenotype, and demonstrated that histone H3 with methylated Lys 9 are concentrated in these SAHF [133], which is supported by following reports [134-136]. However, similar to SA-β-gal, SAHF is dispensable for senescence, and its occurrence depends on specific cell type and stress signals [137].

Both SA-β-gal and SAHF seem to accompany the outcome of senescence without contributing to its development, but two other senescence markers, p53 and p16, are critically involved in senescence progression. As mentioned above, p53 is involved in senescence by mediating DNA damage response [123,124]. Additionally, p53 participates in oncogene-induced

senescence using similar mechanisms through DNA damage response [138]. p21, a downstream target of p53, is also involved in senescence. Ectopic expression of p21 induced premature senescence [139], and lack of p21 bypassed senescence in human fibroblasts [140]. Besides p53/p21, another CDK inhibitor, p16, is also critical for senescence. p16 blocks the cell cycle at G1/S transition by binding and inhibiting CDK4/cyclin D and CDK6/cyclin D [141]. It is up-regulated in several senescence scenarios, including those induced by telomere shortening [142,143] and oncogene over-expression [87]. In addition, ectopic expression of p16 induces premature senescence [139], and loss/inactivation of p16 extend the lifespan of human mammary epithelial cells [144,145]. Although it is not entirely clear how p16 and p53 interact with each other to participate in senescence program, the general concept is that DNA damage response or other stresses first activate p53 to induce transient cell cycle arrest, which progresses to stable and permanent arrest by inducing and maintaining p16 expression [146].

It is not completely known why cells undergo senescence instead of apoptosis. One possible explanation may be related to the senescence-associated secretory phenotype (SASP) in senescent cells. It was shown that senescent cells demonstrate a strong inflammatory phenotype especially in fibroblasts [147], and many inflammatory-related factors are secreted by senescent cells, such as IL-1α/β [148,149], IL-6 [150], and IL-8 [151]. Therefore senescent cells can contribute to inflammatory response via SASP, therefore promoting cell proliferation, migration, and differentiation [152].

Centrosome abnormalities (excess centrosomes and loss of centrosomes) are associated with, and sometimes contributes to, cell cycle arrest or senescence. Some replicatively and prematurely senescent MEF have excess centrosomes because of unidentified mechanisms [153]. In addition, down-regulation of centrosomal structural proteins, such as PCM-1 and γ-tubulin,

induces p53-dependent cell cycle arrest and senescence [107]. Inhibition of two other proteins, Aurora A and TACC3, which promote centrosome maturation, leads to premature senescence in tumor cells [154,155]. Therefore, centrosome abnormalities are associated with cellular senescence, but whether centrosome over-duplication leads to senescence remain to be elucidated.

E. Summary

Centrosome over-duplication is ubiquitously associated with *bona fide* tumor cells, and has been recently documented in tumor EC as well. The outcomes of centrosome over-duplication in tumor EC are not completely understood, but may contribute to the abnormalities of tumor vasculature and the potential drug resistance in tumor angiogenic therapy. Recent evidence suggests that centrosome over-duplication activates a p53 stress pathway, although the exact mechanisms remain elusive. Better understanding of these pathways will contribute to further studies of centrosome function and its implications for disease.

F. Figure

Figure 1.1. Structure of a centrosome

A centrosome is comprised of two centrioles and the surrounding pericentriolar material (PCM, yellow). A centriole is a cylinder structure formed by 9 radially symmetric triplet microtubules. At the proximal end of a centriole, there is a cartwheel structure (red) with 9 triplet microtubules (green). At the distal end of a centriole, there are 9 doublet microtubules, which are modified and associated with subdistal and distal appendages (blue).

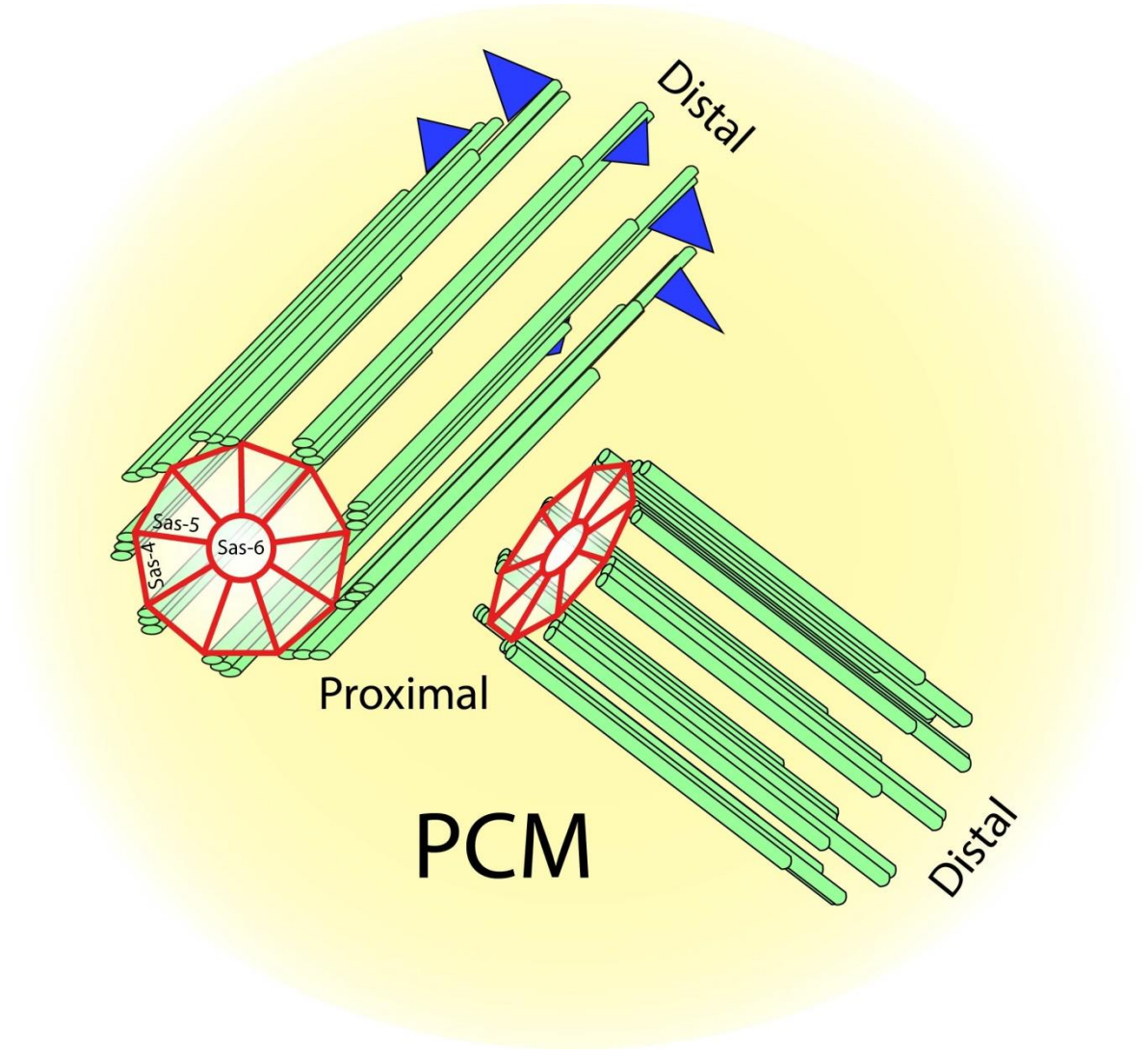
Distal
Sas-5
Sas-6
Sas-4
Proximal
PCM
Distal

REFERENCES

1. Potente M, Gerhardt H, Carmeliet P (2011) Basic and therapeutic aspects of angiogenesis. Cell 146: 873-887.

2. Carmeliet P, Jain RK (2011) Molecular mechanisms and clinical applications of angiogenesis. Nature 473: 298-307.

3. Gerhardt H, Golding M, Fruttiger M, Ruhrberg C, Lundkvist A, et al. (2003) VEGF guides angiogenic sprouting utilizing endothelial tip cell filopodia. J Cell Biol 161: 1163-1177.

4. Gerhardt H (2008) VEGF and endothelial guidance in angiogenic sprouting. Organogenesis 4: 241-246.

5. Folkman J (1971) Tumor angiogenesis: therapeutic implications. N Engl J Med 285: 1182-1186.

6. Ferrara N, Davis-Smyth T (1997) The biology of vascular endothelial growth factor. Endocr Rev 18: 4-25.

7. Koch AE, Polverini PJ, Kunkel SL, Harlow LA, Dipietro LA, et al. (1992) Interleukin-8 as a Macrophage-Derived Mediator of Angiogenesis. Science 258: 1798-1801.

8. Waugh DJJ, Wilson C (2008) The Interleukin-8 Pathway in Cancer. Clinical Cancer Research 14: 6735-6741.

9. Hatakeyama S, Gao YH, Ohara-Nemoto Y, Kataoka H, Satoh M (1997) Expression of bone morphogenetic proteins of human neoplastic epithelial cells. Biochemistry and Molecular Biology International 42: 497-505.

10. Langenfeld EM, Langenfeld J (2004) Bone Morphogenetic Protein-2 stimulates angiogenesis in developing tumors. Molecular Cancer Research 2: 141-149.

11. Narang AS, Varia S (2011) Role of tumor vascular architecture in drug delivery. Adv Drug Deliv Rev 63: 640-658.

12. Vaupel P, Kallinowski F, Okunieff P (1989) Blood-Flow, Oxygen and Nutrient Supply, and Metabolic Microenvironment of Human-Tumors - a Review. Cancer Research 49: 6449-6465.

13. Hockel M, Schlenger K, Aral B, Mitze M, Schaffer U, et al. (1996) Association between tumor hypoxia and malignant progression in advanced cancer of the uterine cervix. Cancer Research 56: 4509-4515.

14. Holash J, Maisonpierre PC, Compton D, Boland P, Alexander CR, et al. (1999) Vessel cooption, regression, and growth in tumors mediated by angiopoietins and VEGF. Science 284: 1994-1998.

15. Dudley AC (2012) Tumor endothelial cells. Cold Spring Harb Perspect Med 2: a006536.

16. Akino T, Hida K, Hida Y, Tsuchiya K, Freedman D, et al. (2009) Cytogenetic abnormalities of tumor-associated endothelial cells in human malignant tumors. Am J Pathol 175: 2657-2667.

17. Hida K, Hida Y, Amin DN, Flint AF, Panigrahy D, et al. (2004) Tumor-associated endothelial cells with cytogenetic abnormalities. Cancer Research 64: 8249-8255.

18. Kushner EJ, Ferro LS, Liu JY, Durrant JR, Rogers SL, et al. (2014) Excess centrosomes disrupt endothelial cell migration via centrosome scattering. J Cell Biol 206: 257-272.

19. Taylor SM, Nevis KR, Park HL, Rogers GC, Rogers SL, et al. (2010) Angiogenic factor signaling regulates centrosome duplication in endothelial cells of developing blood vessels. Blood 116: 3108-3117.

20. Jana SC, Marteil G, Bettencourt-Dias M (2014) Mapping molecules to structure: unveiling secrets of centriole and cilia assembly with near-atomic resolution. Curr Opin Cell Biol 26: 96-106.

21. Gonczy P (2015) Centrosomes and cancer: revisiting a long-standing relationship. Nat Rev Cancer 15: 639-652.

22. Fu J, Hagan IM, Glover DM (2015) The centrosome and its duplication cycle. Cold Spring Harb Perspect Biol 7: a015800.

23. Guichard P, Desfosses A, Maheshwari A, Hachet V, Dietrich C, et al. (2012) Cartwheel architecture of Trichonympha basal body. Science 337: 553.

24. Guichard P, Hachet V, Majubu N, Neves A, Demurtas D, et al. (2013) Native architecture of the centriole proximal region reveals features underlying its 9-fold radial symmetry. Curr Biol 23: 1620-1628.

25. Paintrand M, Moudjou M, Delacroix H, Bornens M (1992) Centrosome Organization and Centriole Architecture - Their Sensitivity to Divalent-Cations. Journal of Structural Biology 108: 107-128.

26. Jakobsen L, Vanselow K, Skogs M, Toyoda Y, Lundberg E, et al. (2011) Novel asymmetrically localizing components of human centrosomes identified by complementary proteomics methods. EMBO J 30: 1520-1535.

27. Kitagawa D, Vakonakis I, Olieric N, Hilbert M, Keller D, et al. (2011) Structural Basis of the 9-Fold Symmetry of Centrioles. Cell 144: 364-375.

28. van Breugel M, Hirono M, Andreeva A, Yanagisawa H, Yamaguchi S, et al. (2011) Structures of SAS-6 Suggest Its Organization in Centrioles. Science 331: 1196-1199.

29. Arquint C, Sonnen KF, Stierhof YD, Nigg EA (2012) Cell-cycle-regulated expression of STIL controls centriole number in human cells. Journal of Cell Science 125: 1342-1352.

30. Tang CJC, Lin SY, Hsu WB, Lin YN, Wu CT, et al. (2011) The human microcephaly protein STIL interacts with CPAP and is required for procentriole formation. Embo Journal 30: 4790-4804.

31. Schmidt TI, Kleylein-Sohn J, Westendorf J, Le Clech M, Lavoie SB, et al. (2009) Control of Centriole Length by CPAP and CP110. Current Biology 19: 1005-1011.

32. Kohlmaier G, Loncarek J, Meng X, McEwen BF, Mogensen MM, et al. (2009) Overly Lona Centrioles and Defective Cell Division upon Excess of the SAS-4-Related Protein CPAP. Current Biology 19: 1012-1018.

33. Andersen JS, Wilkinson CJ, Mayor T, Mortensen P, Nigg EA, et al. (2003) Proteomic characterization of the human centrosome by protein correlation profiling. Nature 426: 570-574.

34. Koff A, Giordano A, Desai D, Yamashita K, Harper JW, et al. (1992) Formation and activation of a cyclin E-cdk2 complex during the G1 phase of the human cell cycle. Science 257: 1689-1694.

35. Ohtsubo M, Theodoras AM, Schumacher J, Roberts JM, Pagano M (1995) Human cyclin E, a nuclear protein essential for the G1-to-S phase transition. Mol Cell Biol 15: 2612-2624.

36. Lukas J, Herzinger T, Hansen K, Moroni MC, Resnitzky D, et al. (1997) Cyclin E-induced S phase without activation of the pRb/E2F pathway. Genes Dev 11: 1479-1492.

37. Lacey KR, Jackson PK, Stearns T (1999) Cyclin-dependent kinase control of centrosome duplication. Proc Natl Acad Sci U S A 96: 2817-2822.

38. Matsumoto Y, Hayashi K, Nishida E (1999) Cyclin-dependent kinase 2 (Cdk2) is required for centrosome duplication in mammalian cells. Current Biology 9: 429-432.

39. Meraldi P, Lukas J, Fry AM, Bartek J, Nigg EA (1999) Centrosome duplication in mammalian somatic cells requires E2F and Cdk2-cyclin A. Nat Cell Biol 1: 88-93.

40. Okuda M, Horn HF, Tarapore P, Tokuyama Y, Smulian AG, et al. (2000) Nucleophosmin/B23 is a target of CDK2/Cyclin E in centrosome duplication. Cell 103: 127-140.

41. Fisk HA, Winey M (2001) The mouse Mps1p-like kinase regulates centrosome duplication. Cell 106: 95-104.

42. Chen ZH, Indjeian VB, McManus M, Wang LY, Dynlacht BD (2002) CP110, a cell cycle-dependent CDK substrate, regulates centrosome duplication in human cells. Dev Cell 3: 339-350.

43. Habedanck R, Stierhof YD, Wilkinson CJ, Nigg EA (2005) The Polo kinase Plk4 functions in centriole duplication. Nat Cell Biol 7: 1140-1146.

44. Kleylein-Sohn J, Westendorf J, Le Clech M, Habedanck R, Stierhof YD, et al. (2007) Plk4-induced centriole biogenesis in human cells. Dev Cell 13: 190-202.

45. Rodrigues-Martins A, Riparbelli M, Callaini G, Glover DM, Bettencourt-Dias M (2007) Revisiting the role of the mother centriole in centriole biogenesis. Science 316: 1046-1050.

46. Bettencourt-Dias M, Rodrigues-Martins A, Carpenter L, Riparbelli M, Lehmann L, et al. (2005) SAK/PLK4 is required for centriole duplication and flagella development. Current Biology 15: 2199-2207.

47. Guderian G, Westendorf J, Uldschmid A, Nigg EA (2010) Plk4 trans-autophosphorylation regulates centriole number by controlling betaTrCP-mediated degradation. J Cell Sci 123: 2163-2169.

48. Rogers GC, Rusan NM, Roberts DM, Peifer M, Rogers SL (2009) The SCF Slimb ubiquitin ligase regulates Plk4/Sak levels to block centriole reduplication. J Cell Biol 184: 225-239.

49. Holland AJ, Fachinetti D, Zhu Q, Bauer M, Verma IM, et al. (2012) The autoregulated instability of Polo-like kinase 4 limits centrosome duplication to once per cell cycle. Genes Dev 26: 2684-2689.

50. Cunha-Ferreira I, Bento I, Pimenta-Marques A, Jana SC, Lince-Faria M, et al. (2013) Regulation of autophosphorylation controls PLK4 self-destruction and centriole number. Curr Biol 23: 2245-2254.

51. Siegrist SE, Doe CQ (2007) Microtubule-induced cortical cell polarity. Genes Dev 21: 483-496.

52. Etienne-Manneville S (2013) Microtubules in Cell Migration. Annual Review of Cell and Developmental Biology, Vol 29 29: 471-499.

53. Vale RD (1987) Intracellular-Transport Using Microtubule-Based Motors. Annual Review of Cell Biology 3: 347-378.

54. Vicente JJ, Wordeman L (2015) Mitosis, microtubule dynamics and the evolution of kinesins. Exp Cell Res 334: 61-69.

55. Kushner EJ, Ferro LS, Yu Z, Bautch VL (2016) Excess centrosomes perturb dynamic endothelial cell repolarization during blood vessel formation. Mol Biol Cell 27: 1911-1920.

56. Chan JY (2011) A clinical overview of centrosome amplification in human cancers. Int J Biol Sci 7: 1122-1144.

57. Giehl M, Fabarius A, Frank O, Hochhaus A, Hafner M, et al. (2005) Centrosome aberrations in chronic myeloid leukemia correlate with stage of disease and chromosomal instability. Leukemia 19: 1192-1197.

58. Lingle WL, Barrett SL, Negron VC, D'Assoro AB, Boeneman K, et al. (2002) Centrosome amplification drives chromosomal instability in breast tumor development. Proc Natl Acad Sci U S A 99: 1978-1983.

59. Nam HJ, Chae S, Jang SH, Cho H, Lee JH (2010) The PI3K-Akt mediates oncogenic Met-induced centrosome amplification and chromosome instability. Carcinogenesis 31: 1531-1540.

60. Sato N, Mizumoto K, Nakamura M, Maehara N, Minamishima YA, et al. (2001) Correlation between centrosome abnormalities and chromosomal instability in human pancreatic cancer cells. Cancer Genetics and Cytogenetics 126: 13-19.

61. Pihan GA, Purohit A, Wallace J, Malhotra R, Liotta L, et al. (2001) Centrosome defects can account for cellular and genetic changes that characterize prostate cancer progression. Cancer Research 61: 2212-2219.

62. Ganem NJ, Godinho SA, Pellman D (2009) A mechanism linking extra centrosomes to chromosomal instability. Nature 460: 278-282.

63. Vogelstein B, Lane D, Levine AJ (2000) Surfing the p53 network. Nature 408: 307-310.

64. DeLeo AB, Jay G, Appella E, Dubois GC, Law LW, et al. (1979) Detection of a transformation-related antigen in chemically induced sarcomas and other transformed cells of the mouse. Proc Natl Acad Sci U S A 76: 2420-2424.

65. Lane DP, Crawford LV (1979) T antigen is bound to a host protein in SV40-transformed cells. Nature 278: 261-263.

66. Linzer DI, Levine AJ (1979) Characterization of a 54K dalton cellular SV40 tumor antigen present in SV40-transformed cells and uninfected embryonal carcinoma cells. Cell 17: 43-52.

67. Chou JY, Martin RG (1975) DNA infectivity and the induction of host DNA synthesis with temperature-sensitive mutants of simian virus 40. J Virol 15: 145-150.

68. Cattoretti G, Rilke F, Andreola S, D'Amato L, Delia D (1988) P53 expression in breast cancer. Int J Cancer 41: 178-183.

69. van den Berg FM, Tigges AJ, Schipper ME, den Hartog-Jager FC, Kroes WG, et al. (1989) Expression of the nuclear oncogene p53 in colon tumours. J Pathol 157: 193-199.

70. Finlay CA, Hinds PW, Tan TH, Eliyahu D, Oren M, et al. (1988) Activating Mutations for Transformation by P53 Produce a Gene-Product That Forms an Hsc70-P53 Complex with an Altered Half-Life. Mol Cell Biol 8: 531-539.

71. Finlay CA, Hinds PW, Levine AJ (1989) The P53 Proto-Oncogene Can Act as a Suppressor of Transformation. Cell 57: 1083-1093.

72. Chen JD (2016) The Cell-Cycle Arrest and Apoptotic Functions of p53 in Tumor Initiation and Progression. Cold Spring Harb Perspect Med 6.

73. Kamada R, Yoshino W, Nomura T, Chuman Y, Imagawa T, et al. (2010) Enhancement of transcriptional activity of mutant p53 tumor suppressor protein through stabilization of tetramer formation by calix[6]arene derivatives. Bioorganic & Medicinal Chemistry Letters 20: 4412-4415.

74. Liu X, Miller CW, Koeffler PH, Berk AJ (1993) The p53 activation domain binds the TATA box-binding polypeptide in Holo-TFIID, and a neighboring p53 domain inhibits transcription. Mol Cell Biol 13: 3291-3300.

75. Leveillard T, Andera L, Bissonnette N, Schaeffer L, Bracco L, et al. (1996) Functional interactions between p53 and the TFIIH complex are affected by tumour-associated mutations. Embo Journal 15: 1615-1624.

76. el-Deiry WS, Kern SE, Pietenpol JA, Kinzler KW, Vogelstein B (1992) Definition of a consensus binding site for p53. Nat Genet 1: 45-49.

77. Friedman PN, Chen XB, Bargonetti J, Prives C (1993) The P53 Protein Is an Unusually Shaped Tetramer That Binds Directly to DNA (Vol 90, Pg 3319, 1993). Proc Natl Acad Sci U S A 90: 5878-5878.

78. Iwabuchi K, Li B, Bartel P, Fields S (1993) Use of the 2-Hybrid System to Identify the Domain of P53 Involved in Oligomerization. Oncogene 8: 1693-1696.

79. Chene P (2001) The role of tetramerization in p53 function. Oncogene 20: 2611-2617.

80. Haupt Y, Maya R, Kazaz A, Oren M (1997) Mdm2 promotes the rapid degradation of p53. Nature 387: 296-299.

81. Honda R, Tanaka H, Yasuda H (1997) Oncoprotein MDM2 is a ubiquitin ligase E3 for tumor suppressor p53. Febs Letters 420: 25-27.

82. Reifenberger G, Liu L, Ichimura K, Schmidt EE, Collins VP (1993) Amplification and Overexpression of the Mdm2 Gene in a Subset of Human-Malignant Gliomas without P53 Mutations. Cancer Research 53: 2736-2739.

83. Buesoramos CE, Yang Y, Deleon E, Mccown P, Stass SA, et al. (1993) The Human Mdm-2 Oncogene Is Overexpressed in Leukemias. Blood 82: 2617-2623.

84. Barak Y, Juven T, Haffner R, Oren M (1993) Mdm2 Expression Is Induced by Wild Type-P53 Activity. Embo Journal 12: 461-468.

85. Fritsche M, Haessler C, Brandner G (1993) Induction of nuclear accumulation of the tumor-suppressor protein p53 by DNA-damaging agents. Oncogene 8: 307-318.

86. Hall PA, McKee PH, Menage HD, Dover R, Lane DP (1993) High levels of p53 protein in UV-irradiated normal human skin. Oncogene 8: 203-207.

87. Serrano M, Lin AW, McCurrach ME, Beach D, Lowe SW (1997) Oncogenic ras provokes premature cell senescence associated with accumulation of p53 and p16(INK4a). Cell 88: 593-602.

88. Graeber TG, Peterson JF, Tsai M, Monica K, Fornace AJ, Jr., et al. (1994) Hypoxia induces accumulation of p53 protein, but activation of a G1-phase checkpoint by low-oxygen conditions is independent of p53 status. Mol Cell Biol 14: 6264-6277.

89. Kruse JP, Gu W (2009) Modes of p53 regulation. Cell 137: 609-622.

90. Banin S, Moyal L, Shieh S, Taya Y, Anderson CW, et al. (1998) Enhanced phosphorylation of p53 by ATM in response to DNA damage. Science 281: 1674-1677.

91. Canman CE, Lim DS, Cimprich KA, Taya Y, Tamai K, et al. (1998) Activation of the ATM kinase by ionizing radiation and phosphorylation of p53. Science 281: 1677-1679.

92. Appella E, Anderson CW (2001) Post-translational modifications and activation of p53 by genotoxic stresses. Eur J Biochem 268: 2764-2772.

93. Shieh SY, Ikeda M, Taya Y, Prives C (1997) DNA damage-induced phosphorylation of p53 alleviates inhibition by MDM2. Cell 91: 325-334.

94. Oda K, Arakawa H, Tanaka T, Matsuda K, Tanikawa C, et al. (2000) p53AIP1, a potential mediator of p53-dependent apoptosis, and its regulation by Ser-46-phosphorylated p53. Cell 102: 849-862.

95. Feng L, Hollstein M, Xu Y (2006) Ser46 phosphorylation regulates p53-dependent apoptosis and replicative senescence. Cell Cycle 5: 2812-2819.

96. Kishi H, Nakagawa K, Matsumoto M, Suga M, Ando M, et al. (2001) Osmotic shock induces G(1) arrest through p53 phosphorylation at Ser(33) by activated p38(MAPK) without phosphorylation at Ser(15) and Ser(20). Journal of Biological Chemistry 276: 39115-39122.

97. Kwong J, Hong L, Liao R, Deng Q, Han J, et al. (2009) p38alpha and p38gamma mediate oncogenic ras-induced senescence through differential mechanisms. J Biol Chem 284: 11237-11246.

98. Haupt Y, Rowan S, Shaulian E, Vousden KH, Oren M (1995) Induction of apoptosis in HeLa cells by trans-activation-deficient p53. Genes Dev 9: 2170-2183.

99. Green DR, Kroemer G (2009) Cytoplasmic functions of the tumour suppressor p53. Nature 458: 1127-1130.

100. el-Deiry WS, Tokino T, Velculescu VE, Levy DB, Parsons R, et al. (1993) WAF1, a potential mediator of p53 tumor suppression. Cell 75: 817-825.

101. Hermeking H, Lengauer C, Polyak K, He TC, Zhang L, et al. (1997) 14-3-3 sigma is a p53-regulated inhibitor of G2/M progression. Mol Cell 1: 3-11.

102. Nakano K, Vousden KH (2001) PUMA, a novel proapoptotic gene, is induced by p53. Mol Cell 7: 683-694.

103. Harper JW, Elledge SJ, Keyomarsi K, Dynlacht B, Tsai LH, et al. (1995) Inhibition of cyclin-dependent kinases by p21. Mol Biol Cell 6: 387-400.

104. Taylor WR, Stark GR (2001) Regulation of the G2/M transition by p53. Oncogene 20: 1803-1815.

105. Rufini A, Tucci P, Celardo I, Melino G (2013) Senescence and aging: the critical roles of p53. Oncogene 32: 5129-5143.

106. Carvajal LA, Manfredi JJ (2013) Another fork in the road--life or death decisions by the tumour suppressor p53. EMBO Rep 14: 414-421.

107. Mikule K, Delaval B, Kaldis P, Jurcyzk A, Hergert P, et al. (2007) Loss of centrosome integrity induces p38-p53-p21-dependent G1-S arrest. Nat Cell Biol 9: 160-170.

108. Srsen V, Gnadt N, Dammermann A, Merdes A (2006) Inhibition of centrosome protein assembly leads to p53-dependent exit from the cell cycle. J Cell Biol 174: 625-630.

109. Bazzi H, Anderson KV (2014) Acentriolar mitosis activates a p53-dependent apoptosis pathway in the mouse embryo. Proc Natl Acad Sci U S A 111: E1491-1500.

110. Fukasawa K, Choi T, Kuriyama R, Rulong S, Vande Woude GF (1996) Abnormal centrosome amplification in the absence of p53. Science 271: 1744-1747.

111. Mantel C, Braun SE, Reid S, Henegariu O, Liu L, et al. (1999) p21(cip-1/waf-1) deficiency causes deformed nuclear architecture, centriole overduplication, polyploidy, and relaxed microtubule damage checkpoints in human hematopoietic cells. Blood 93: 1390-1398.

112. Duensing A, Ghanem L, Steinman RA, Liu Y, Duensing S (2006) p21(Waf1/Cip1) deficiency stimulates centriole overduplication. Cell Cycle 5: 2899-2902.

113. Tarapore P, Horn HF, Tokuyama Y, Fukasawa K (2001) Direct regulation of the centrosome duplication cycle by the p53-p21Waf1/Cip1 pathway. Oncogene 20: 3173-3184.

114. Andreassen PR, Lohez OD, Lacroix FB, Margolis RL (2001) Tetraploid state induces p53-dependent arrest of nontransformed mammalian cells in G1. Mol Biol Cell 12: 1315-1328.

115. Wong C, Stearns T (2005) Mammalian cells lack checkpoints for tetraploidy, aberrant centrosome number, and cytokinesis failure. BMC Cell Biol 6: 6.

116. Uetake Y, Sluder G (2004) Cell cycle progression after cleavage failure: mammalian somatic cells do not possess a "tetraploidy checkpoint". J Cell Biol 165: 609-615.

117. Cuomo ME, Knebel A, Morrice N, Paterson H, Cohen P, et al. (2008) p53-Driven apoptosis limits centrosome amplification and genomic instability downstream of NPM1 phosphorylation. Nat Cell Biol 10: 723-730.

118. Ganem NJ, Cornils H, Chiu SY, O'Rourke KP, Arnaud J, et al. (2014) Cytokinesis failure triggers hippo tumor suppressor pathway activation. Cell 158: 833-848.

119. Hayflick L (1965) The Limited in Vitro Lifetime of Human Diploid Cell Strains. Exp Cell Res 37: 614-636.

120. Kuilman T, Michaloglou C, Mooi WJ, Peeper DS (2010) The essence of senescence. Genes Dev 24: 2463-2479.

121. Harley CB, Futcher AB, Greider CW (1990) Telomeres shorten during ageing of human fibroblasts. Nature 345: 458-460.

122. Baird DM, Rowson J, Wynford-Thomas D, Kipling D (2003) Extensive allelic variation and ultrashort telomeres in senescent human cells. Nat Genet 33: 203-207.

123. d'Adda di Fagagna F, Reaper PM, Clay-Farrace L, Fiegler H, Carr P, et al. (2003) A DNA damage checkpoint response in telomere-initiated senescence. Nature 426: 194-198.

124. Herbig U, Jobling WA, Chen BP, Chen DJ, Sedivy JM (2004) Telomere shortening triggers senescence of human cells through a pathway involving ATM, p53, and p21(CIP1), but not p16(INK4a). Mol Cell 14: 501-513.

125. Michaloglou C, Vredeveld LC, Soengas MS, Denoyelle C, Kuilman T, et al. (2005) BRAFE600-associated senescence-like cell cycle arrest of human naevi. Nature 436: 720-724.

126. Chen ZB, Trotman LC, Shaffer D, Lin HK, Dotan ZA, et al. (2005) Crucial role of p53-dependent cellular senescence in suppression of Pten-deficient tumorigenesis. Nature 436: 725-730.

127. Chen Q, Ames BN (1994) Senescence-like growth arrest induced by hydrogen peroxide in human diploid fibroblast F65 cells. Proc Natl Acad Sci U S A 91: 4130-4134.

128. te Poele RH, Okorokov AL, Jardine L, Cummings J, Joel SP (2002) DNA damage is able to induce senescence in tumor cells in vitro and in vivo. Cancer Research 62: 1876-1883.

129. Yeo EJ, Hwang YC, Kang CM, Kim IH, Kim DI, et al. (2000) Senescence-like changes induced by hydroxyurea in human diploid fibroblasts. Experimental Gerontology 35: 553-571.

130. Dimri GP, Lee X, Basile G, Acosta M, Scott G, et al. (1995) A biomarker that identifies senescent human cells in culture and in aging skin in vivo. Proc Natl Acad Sci U S A 92: 9363-9367.

131. Lee BY, Han JA, Im JS, Morrone A, Johung K, et al. (2006) Senescence-associated beta-galactosidase is lysosomal beta-galactosidase. Aging Cell 5: 187-195.

132. Kurz DJ, Decary S, Hong Y, Erusalimsky JD (2000) Senescence-associated beta-galactosidase reflects an increase in lysosomal mass during replicative ageing of human endothelial cells. Journal of Cell Science 113: 3613-3622.

133. Narita M, Nunez S, Heard E, Lin AW, Hearn SA, et al. (2003) Rb-mediated heterochromatin formation and silencing of E2F target genes during cellular senescence. Cell 113: 703-716.

134. Zhang R, Poustovoitov MV, Ye X, Santos HA, Chen W, et al. (2005) Formation of MacroH2A-containing senescence-associated heterochromatin foci and senescence driven by ASF1a and HIRA. Dev Cell 8: 19-30.

135. Zhang R, Chen W, Adams PD (2007) Molecular dissection of formation of senescence-associated heterochromatin foci. Mol Cell Biol 27: 2343-2358.

136. Di Micco R, Sulli G, Dobreva M, Liontos M, Botrugno OA, et al. (2011) Interplay between oncogene-induced DNA damage response and heterochromatin in senescence and cancer. Nat Cell Biol 13: 292-302.

137. Kosar M, Bartkova J, Hubackova S, Hodny Z, Lukas J, et al. (2011) Senescence-associated heterochromatin foci are dispensable for cellular senescence, occur in a cell type- and insult-dependent manner and follow expression of p16(ink4a). Cell Cycle 10: 457-468.

138. Di Micco R, Fumagalli M, Cicalese A, Piccinin S, Gasparini P, et al. (2006) Oncogene-induced senescence is a DNA damage response triggered by DNA hyper-replication. Nature 444: 638-642.

139. McConnell BB, Starborg M, Brookes S, Peters G (1998) Inhibitors of cyclin-dependent kinases induce features of replicative senescence in early passage human diploid fibroblasts. Curr Biol 8: 351-354.

140. Brown JP, Wei W, Sedivy JM (1997) Bypass of senescence after disruption of p21CIP1/WAF1 gene in normal diploid human fibroblasts. Science 277: 831-834.

141. Serrano M, Hannon GJ, Beach D (1993) A New Regulatory Motif in Cell-Cycle Control Causing Specific-Inhibition of Cyclin-D/Cdk4. Nature 366: 704-707.

142. Hara E, Smith R, Parry D, Tahara H, Steven S, et al. (1996) Regulation of p16(CDKN2) expression and its implications for cell immortalization and senescence. Mol Cell Biol 16: 859-867.

143. Alcorta DA, Xiong Y, Phelps D, Hannon G, Beach D, et al. (1996) Involvement of the cyclin-dependent kinase inhibitor p16 (INK4a) in replicative senescence of normal human fibroblasts. Proc Natl Acad Sci U S A 93: 13742-13747.

144. Brenner AJ, Stampfer MR, Aldaz CM (1998) Increased p16 expression with first senescence arrest in human mammary epithelial cells and extended growth capacity with p16 inactivation. Oncogene 17: 199-205.

145. Huschtscha LI, Noble JR, Neumann AA, Moy EL, Barry P, et al. (1998) Loss of p16(INK4) expression by methylation is associated with lifespan extension of human mammary epithelial cells. Cancer Research 58: 3508-3512.

146. Lasry A, Ben-Neriah Y (2015) Senescence-associated inflammatory responses: aging and cancer perspectives. Trends Immunol 36: 217-228.

147. Shelton DN, Chang E, Whittier PS, Choi D, Funk WD (1999) Microarray analysis of replicative senescence. Curr Biol 9: 939-945.

148. Maier JA, Voulalas P, Roeder D, Maciag T (1990) Extension of the life-span of human endothelial cells by an interleukin-1 alpha antisense oligomer. Science 249: 1570-1574.

149. Kumar S, Millis AJ, Baglioni C (1992) Expression of interleukin 1-inducible genes and production of interleukin 1 by aging human fibroblasts. Proc Natl Acad Sci U S A 89: 4683-4687.

150. Kuilman T, Michaloglou C, Vredeveld LC, Douma S, van Doorn R, et al. (2008) Oncogene-induced senescence relayed by an interleukin-dependent inflammatory network. Cell 133: 1019-1031.

151. Sarkar D, Lebedeva IV, Emdad L, Kang DC, Baldwin AS, et al. (2004) Human polynucleotide phosphorylase (hPNPase(old-35)): A potential link between aging and inflammation. Cancer Research 64: 7473-7478.

152. Coppe JP, Desprez PY, Krtolica A, Campisi J (2010) The Senescence-Associated Secretory Phenotype: The Dark Side of Tumor Suppression. Annual Review of Pathology-Mechanisms of Disease 5: 99-118.

153. Manning JA, Kumar S (2010) A potential role for NEDD1 and the centrosome in senescence of mouse embryonic fibroblasts. Cell Death Dis 1: e35.

154. Schmidt S, Schneider L, Essmann F, Cirstea IC, Kuck F, et al. (2010) The centrosomal protein TACC3 controls paclitaxel sensitivity by modulating a premature senescence program. Oncogene 29: 6184-6192.

155. Huck JJ, Zhang MK, McDonald A, Bowman D, Hoar KM, et al. (2010) MLN8054, an Inhibitor of Aurora A Kinase, Induces Senescence in Human Tumor Cells Both In vitro and In vivo. Molecular Cancer Research 8: 373-384.

CHAPTER II-Tumor-Derived Factors and Reduced p53 Promote Endothelial Cell Centrosome Over-duplication[1]

A. Summary

Approximately 30% of tumor endothelial cells have over-duplicated (>2) centrosomes, which may contribute to abnormal vessel function and drug resistance. Elevated levels of vascular endothelial growth factor A induce excess centrosomes in endothelial cells, but how other features of the tumor environment affect centrosome over-duplication is not known. To test this, we treated endothelial cells with tumor-derived factors, hypoxia, or reduced p53, and assessed centrosome numbers. We found that hypoxia and elevated levels of bone morphogenetic protein 2, 6 and 7 induced excess centrosomes in endothelial cells through BMPR1A and likely via SMAD signaling. In contrast, inflammatory mediators IL-8 and lipopolysaccharide did not induce excess centrosomes. Finally, down-regulation in endothelial cells of p53, a critical regulator of DNA damage and proliferation, caused centrosome over-duplication. Our findings suggest that some tumor-derived factors and genetic changes in endothelial cells contribute to excess centrosomes in tumor endothelial cells.

[1]This chapter is adapted from a paper submitted to *PLOS ONE* in 2016. I performed most of the experiments and wrote the first draft of the manuscript. Dr. Victoria Bautch edited and added to my original draft. Dr. Kevin Mouillesseaux performed the experiments in Fig 2.1 and Supplementary Fig 2.1B. Dr. Erich Kushner provided the immortalized normal endothelial cells.

B. Introduction

Tumor progression requires angiogenesis, a hallmark of cancer development, and tumor vessels enable tumor metastasis by providing a conduit for tumor cell invasion and spread [1,2]. Although tumor vessels are a critical part of the tumor micro-environment, anti-angiogenic therapies have had no effect or provided transitory improvement, indicating that tumor vessels become resistant to angiogenesis inhibitors [3]. Consistent with the lack of effectiveness of anti-angiogenic therapy, recent studies show that endothelial cells (EC) that line tumor vessels have genetic abnormalities such as aneuploidy. Aneuploidy is often associated with excess centrosomes, and up to 30% of tumor EC have excess centrosomes [4-6]. Centrosomes form the microtubule-organizing center (MTOC) in interphase cells to regulate cell migration, polarity, and adhesion, and they form the spindle poles that segregate chromosomes during mitosis [7]. Thus tumor EC acquire permanent structural and genetic alterations via excess centrosomes that likely contribute to the phenotypic and functional abnormalities of tumor blood vessels.

Tumor blood vessels are thought to arise from normal vessels that enter the tumor [8,9], suggesting that the environment is responsible for inducing excess centrosomes in EC. Tumor cells secrete elevated levels of various growth factors [10], and our previous work showed that elevated levels of vascular endothelial growth factor A (VEGF-A) induce centrosome over-duplication in EC [11]. However, the frequency of centrosome over-duplication in tumor-derived EC is significantly higher than that induced by excess VEGF-A [6,11]. Thus other up-regulated signaling pathways in the tumor environment likely contribute to centrosome over-duplication in EC. For example, bone morphogenetic protein (BMP), which is required for appropriate angiogenesis, is up-regulated in certain cancers [12]. Furthermore, different BMP ligands such as

BMP2, BMP4, BMP6 and BMP7 induce angiogenesis [13], and BMP2 and BMP4 promote tumor angiogenesis [13].

In addition to growth factors, the tumor environment is hypoxic and has elevated levels of inflammatory cytokines. The tumor environment is hypoxic in part because of abnormal tumor blood vessels [14]. Hypoxia activates the hypoxia-inducible factor (HIF) family of transcription factors, which further induce expression of numerous downstream targets, including VEGF-A [15]. Inflammation is also a hallmark of the tumor environment and is thought to promote tumor growth [16], perhaps via secretion of angiogenic chemokines such as Interleukin 8 (IL-8) that induce tumor angiogenesis [17]. It is not known whether hypoxia or inflammation promote excess centrosomes in EC.

In this report, we analyzed the effects of specific inputs elevated in the tumor environment on centrosome over-duplication in EC. We found that elevated levels of some BMP ligands are sufficient to induce centrosome over-duplication in EC, using BMP receptor 1A and likely via downstream SMAD signaling. Additionally, hypoxia promoted EC centrosome over-duplication through a VEGF-A-independent mechanism. In contrast, inflammatory mediators did not affect centrosome numbers in EC. In addition to environmental factors, down-regulation of the tumor-suppressor p53 induced centrosome over-duplication in EC. These results indicate that both environmental and genetic factors contribute to centrosome over-duplication in EC, and may contribute to the high frequencies seen in tumor vessels.

C. Materials and Methods

Cell culture

Human umbilical vein endothelial cells (HUVEC, Lonza Group cc-2519), human brain microvascular endothelial cells (HBMEC, Cell Systems ACBRI 376) and human umbilical artery endothelial cells (HUAEC) were cultured in endothelial growth medium-2 (EGM-2, Lonza Group cc-3162). Human lung microvascular endothelial cells (HMVEC-L, Lonza Group cc-2527) were cultured in EGM-2 MV (Lonza Group cc-3102). Normal mouse EC (NEC) were originally isolated from mouse mammary glands and cultured in EGM-2 [6]. Growth factors or lipopolysaccharide (LPS, List Biological Laboratories 201) were added to cultures at indicated concentrations. Exogenous recombinant growth factors used in this study were VEGFA-165 (PeproTech 100-20), BMP2 (R&D Systems 355-BM-010), BMP4 (R&D Systems 314-BP-010), BMP6 (R&D Systems 507-BP-020), BMP7 (R&D Systems 354-BP-010), and Interleukin-8 (IL-8, PeproTech 200-08). VEGF-A and BMP were used at 200 ng/ml, and IL-8 was added at indicated concentrations. Culture medium was replaced daily for 4 days, and cells were maintained at 30-70% confluence. To study signaling, HUVEC were cultured in Opti-MEM for 4 hr before treatment with 200 ng/ml BMP ligands in Opti-MEM for 30 min.

Lipofectamine RNAiMAX (Life Technologies 13778-150) was used for siRNA transfection according to manufacturer protocols. siRNAs were: non-targeting siRNA (Life technologies 4390847), BMPR1A siRNA (Life technologies 4392420-s280), BMPR1B siRNA (Life technologies 4392420-s2043) and BMPR2 siRNA (Life technologies 4390824-s2046).

For hypoxia experiments, HUVEC were cultured in 2% or 3% O_2 for 4 days. 1 μg/ml of recombinant human VEGF Receptor-1 (Flt-1)/Fc (R&D Systems 321-FL-050) was added to medium to block VEGF-A signaling [18], and the medium was changed daily. In general, EC

were immediately fixed with cold MeOH after hypoxic incubation. To test for translocation of HIF1α, EC were recovered in normoxia for 30 min before fixation. Hypoxic-mimetic agent desferrioxamine (DFO) and a hypoxia incubator chamber were kindly provided by Dr. Kimryn Rathmell.

Immunofluorescence and microscopy

HUVEC were fixed in ice cold 100% MeOH for 10 min, then stained as previously described [19]. Briefly, fixed cells were blocked in 5% bovine serum in PBS for 1hr at room temperature (RT), then incubated with mouse anti-human γ-tubulin (1:5000, Sigma-Aldrich T6557), rabbit anti-human pSmad1/5 (1:500, Cell Signaling 9516) or mouse anti-human HIF1α (1:50, Novus biologicals NB100-105) at 4^0C overnight. After washing 3X 5 min in PBS, cells were incubated with secondary antibodies (1:250), including goat-anti-mouse Alexa 488 (Invitrogen A11029) or goat-anti-mouse Alexa 594 (Invitrogen A11005), and DRAQ7 (1:1000, Abcam ab109202) or SYTOX green (1:50,000, Invitrogen S7020), for 2hr at RT. Both primary and secondary antibodies were diluted in 5% bovine serum in PBS. Centrosome numbers were determined using a Zeiss LSM 5 Pascal microscope with a 100X objective.

pSMAD1/5 fluorescence intensities were quantified in ImageJ. Briefly, the DRAQ7 (nucleus) channel from compressed z-stacks was thresholded to segment nuclei and adjusted into a binary image. Intensity analysis was redirected from the binary image to the pSMAD1/5 channel by changing the “Set Measurements” parameter. “Analyze Particles” function was executed to determine pSMAD1/5 intensity in each nucleus.

Western blot

Western blot analysis was performed as previously described, with slight modifications [11]. Briefly, HUVEC lysates were lysed using RIPA buffer supplemented with protease inhibitor (Cell Signaling 5871S). Proteins were separated on a 10% sodium dodecyl sulfate–polyacrylamide gel, transferred to a PVDF membrane (GE Healthcare, RPN303F), and blocked in 5% bovine serum albumin (BSA) in PBS with 1% tween-20 (Sigma P2287) for 1h at RT. Primary antibodies used were: rabbit anti-phospho-Smad1/5 (1:1000, Cell Signaling 9516), rabbit anti-Akt (1:1000, Cell Signaling 9272), rabbit anti-phospho-Akt (Ser473) (1:1000, Cell Signaling 4060), rabbit anti-phospho-ERK1/2 (Thr202/Tyr204) (1:1000, Cell Signaling 4370), rabbit anti-ERK 1/2 (1:1000, Cell Signaling 4695), mouse anti-HIF1α (1:500, Novus biologicals NB100-105), mouse anti-p53 (1:1000, Abcam ab1101) and rabbit anti-p53 (1:500, Abcam ab131442). Membranes were incubated with primary antibodies diluted in 1% BSA overnight at 4^0C. Signal was detected with horseradish peroxidase (HRP) anti-rabbit (1:5000, Invitrogen G-21234) or HRP anti-mouse (1:30,000, Invitrogen 81-6720), and imaged via Clarity Western ECL Substrate (Bio-Rad 170-5061).

Quantitative real-time PCR

HUVEC were collected 48 hr after siRNA transfection, and total RNA was isolated with TRIZOL (Life technologies 15596-026) according to the manufacturer's protocol. 1 μg of RNA was used for synthesizing cDNA with iScript (Bio-Rad 1708891). cDNA products were diluted fivefold. For measuring BMPR1B, BMPR2 and GAPDH, 0.5 ul of diluted samples were used as templates; for BMPR1A, 5 ul of diluted samples were used. RT-PCR was preformed using iTaq universal SYBR Green supermix (Bio-Rad 1725121) in a 7900HT fast RT-PCR system (Applied

Biosystems). Primer sequences were: GAPDH (forward: CCTCAAGATCATCAGCAATGCCTCCT; reverse: GGTCATGAGTCCTTCCACGATACCAA), BMPR1A (forward: AGCTACGCCGGACAATAGAA; reverse: CTATGACAACAGGGGGCAGT), BMPR1B (forward: GCCTGCCATAAGTGAGAAGC; reverse: CTTTCTTGGTGCCCACATTT), and BMPR2 (forward: GGTAAGCTCTTGCCGTCTTG; reverse: ATCTCGATGGGAAATTGCAG).

Lentivirus infection

Human p53–targeted shRNA (clone ID: V3LHS_333920) with pGIPZ vector was obtained from Open Biosystems. Mouse p53–targeted shRNA clone (TRCN0000012360) with pLKO.1 vectors were obtained from the UNC Lenti-shRNA Core facility. shRNA lentiviruses were made by the UNC Lenti-shRNA Core facility. Cells were infected with 100 μl/ml lentivirus in 5 ml medium plus 1μg/ml polybrene (Millipore) overnight at 37°C, then incubated for 4 days before fixation or collection. Virus lacking a target sequence (empty vector) was used as a control.

Statistical analysis

The paired or unpaired two-tailed Student's t-test was used to determine statistical significance in cases with 3 repeats. The X^2 test was used to determine statistical significance in cases with 2 repeats. Error bars represent standard deviation from mean between experiments.

D. Results

Elevated levels of BMP ligands induce excess centrosomes in EC

We began to dissect the different potential inputs to excess centrosome formation from the tumor environment by introducing elevated levels of different signaling pathways or by genetic manipulation of normal EC and assessing effects on centrosome over-duplication. Because BMP ligands regulate angiogenesis and are expressed in the tumor micro-environment, we asked whether elevated BMP signaling regulates centrosome number in EC. HUVEC treated with different BMP ligands were stained with anti-γ-tubulin antibodies to label centrosomes, and EC with different centrosome numbers were clearly identified **(Supp. Fig 2.1A)**. As previously described, EC with 3 or more centrosomes were considered to have excess centrosomes **(Fig 2.1A)** [19]. Exposure to BMP2, BMP6, or BMP7 caused a significant increase in the percentage of HUVEC with excess centrosomes **(Fig 2.1B-C, Fig 2.2A)**. This effect was not observed with BMP4 treatment in HUVEC **(Supp. Fig 2.1B)**, nor upon treatment with BMP2 or BMP6 in HUAEC, HBMEC or HMVEC-L **(Supp. Fig 2.1C-E)**. These results indicate that some but not all BMP ligands induce excess centrosomes, and that different EC isolates respond differently to these ligands.

BMP-induced centrosome over-duplication is BMP receptor type 1A (BMPR1A)-dependent

To understand the mechanism of BMP-induced centrosome over-duplication, we down-regulated BMP receptors in HUVEC. There are several BMP-specific receptors that include type 1A BMP receptor (BMPR1A/ALK3), type 1B BMP receptor (BMPR1B/ALK6), and type 2 BMP receptor (BMPR2) [20]. siRNA targeting of these three receptors efficiently and significantly knock-down their mRNA levels **(Supp. Fig 2.2A-C)**. The increase in EC with

excess centrosomes seen with BMP2 or BMP6 was blocked by BMPR1A knockdown, but not by BMPR1B or BMPR2 knockdown **(Fig 2.2A-B)**. These findings suggest that BMPR1A is required for BMP-induced centrosome over-duplication.

Type 1 and type 2 BMP receptors form hetero-tetramers upon ligand binding that permits phosphorylation of downstream effectors called receptor-regulated SMAD (R-SMAD), including SMAD1 and SMAD5. Phosphorylated R-SMADs bind SMAD4 to translocate into the nucleus and modulate gene expression [20]. To further understand the mechanism of BMP-induced centrosome over-duplication, we examined the phosphorylation of SMAD1/5 by immunofluorescence. The levels of nuclear phospho-SMAD1/5 (pSMAD1/5) were significantly induced by BMP6 treatment in control siRNA, BMPR1B siRNA and BMPR2 siRNA-treated HUVEC, but not in BMPR1A siRNA-treated cells **(Fig 2.2C-D)**, which was also confirmed by western blot **(Fig 2.2E)**. These results suggest that BMPR1A is required for BMP-induced centrosome over-duplication through downstream R-SMAD activation.

Inflammatory mediators do not promote excess centrosomes in EC

Chronic inflammation-associated signaling, which is activated by up-regulation of cytokines, is another characteristic of the tumor environment. IL-8 is a pro-inflammatory cytokine that regulates angiogenesis [21]. To determine if IL-8 promotes centrosome over-duplication in EC, we treated HUVEC with IL-8, which induced ERK phosphorylation in HMVEC **(Supp. Fig 2.3)**; however, these levels of IL-8 did not induce excess centrosomes **(Fig 2.3A)**. To test more general effects of inflammation on centrosome over-duplication, HUVEC were treated with lipopolysaccharide (LPS), a potent pro-inflammatory agent that promotes secretion of a wide range of inflammatory mediators [22]. Consistent with the results of IL-8

treatment, LPS treatment did not induce significant increases in excess centrosomes in HUVEC **(Fig 2.3B)**. These results indicate that IL-8 and LPS do not induce centrosome over-duplication in EC, suggesting that inflammatory mediators are not causative agents in generating excess centrosomes in EC.

Hypoxia induces excess centrosomes in EC

In addition to the complex milieu of cytokines and growth factors, tumor environments are often hypoxic. To determine whether hypoxia induces excess centrosomes in EC, HUVEC were first treated with the oxygen chelating agent desferrioxamine (DFO), which mimics hypoxia in inducing HIF1α accumulation [23]. Treatment with DFO resulted in a 4-fold increase in the frequency of excess centrosomes compared to controls **(Fig 2.4A)**. To further test our hypothesis, HUVEC were cultured in a 2-3% oxygen environment (hypoxia) for 4 days, then fixed and stained to assess the frequency of centrosome over-duplication. Hypoxic incubation led to translocation of HIF1α from the cytoplasm to the nuclear compartment of EC **(S4A Fig 2.)**, and also induced accumulation of HIF1α **(Supp. Fig 2.4B)**, indicating the activation of hypoxia pathways. Incubation in 2% or 3% oxygen significantly promoted centrosome over-duplication compared to normoxic controls **(Fig 2.4B, Supp. Fig 2.4C)**. These results indicate that a hypoxic environment is sufficient to induce excess centrosomes in EC.

Hypoxia up-regulates the production and release of pro-angiogenic cytokines such as VEGF-A in multiple tissues [15]. To determine whether hypoxia-induced centrosome over-duplication in EC requires VEGF-A signaling, HUVEC were incubated in hypoxic conditions with recombinant human soluble VEGF Receptor-1 (Flt-1)/Fc to block VEGF-A signaling. Flt-1/Fc treatment efficiently inhibited ERK phosphorylation induced by VEGF-A **(Supp. Fig 2.4C)**,

but was unable to rescue hypoxia-induced centrosome over-duplication **(Fig 2.4C)**. This result suggests that hypoxia induces excess centrosomes in EC through VEGF-A-independent mechanisms.

Inhibition of p53 signaling induces excess centrosomes in EC

Loss or inactivation of p53 induces excess centrosomes in mouse embryonic fibroblasts [24]. Thus, we tested whether p53 attenuation leads to excess centrosomes in EC. A short-hairpin RNA (shRNA) was used to down-regulate p53 levels in HUVEC **(Supp. Fig 2.5A)**, and HUVEC infected with shRNA had an approximately 3-fold increase in the percentage of excess centrosomes **(Fig 2.5A)**. Previous studies demonstrated that mouse tumor stromal cells, including mouse tumor EC, have an attenuated p53 response [25]. Therefore we asked whether down-regulation of p53 induced excess centrosomes in mouse EC by infecting immortalized normal mouse EC (NEC) [6] with p53 shRNA. Down-regulation of mouse p53 also induced excess centrosomes in NEC **(Supp. Fig2.5B, Fig 2.5B)**. These results suggest that down-regulation of p53 contributes to centrosome over-duplication in tumor EC.

E. Discussion

We previously showed that high levels of the pro-angiogenic growth factors VEGF-A and bFGF promote excess centrosomes in EC [11]. However, the frequency of EC centrosome over-duplication, even with a combination of both VEGF-A and bFGF, was much less than that seen in primary isolates of tumor-derived EC [6], suggesting that other aspects of the tumor environment contribute to pathological centrosome over-duplication. Here we provide evidence that excess centrosomes in EC occur downstream of numerous tumor-related inputs. We found

that the BMP ligands BMP2, BMP6 and BMP7 significantly induced centrosome over-duplication, while inflammatory mediators were ineffective. Hypoxia, which is associated with most solid tumors, induced excess centrosomes in EC through VEGF-A-independent mechanisms. Besides environmental factors, cell-autonomous perturbation of p53 also promoted excess centrosomes in EC. These findings suggest that multiple inputs contribute to the high frequency of tumor vessel-derived EC with excess centrosomes.

Elevated levels of some BMP ligands, similar to high levels of VEGF and FGF ligands, induce excess centrosomes in EC. Interestingly, VEGF and FGF signaling are mediated by VEGF receptor 2 and FGF receptor, respectively, which belong to the tyrosine kinase receptor family [26], whereas BMP signals through serine/threonine kinase receptors [27], suggesting that diverse signaling inputs promote centrosome over-duplication in EC. Our results also show ligand and cell type specificity of BMP in inducing excess centrosomes: BMP2, BMP6 and BMP7, but not BMP4, significantly induced excess centrosomes in HUVEC, whereas BMP2 and BMP6 did not significantly affect centrosome numbers in several other human primary EC.

BMP ligands initiate signal transduction by binding a hetero-tetrameric receptor comprised of two dimers of type 1 and type 2 receptors [20]. Among a group with specificity for TGFβ and/or BMP signaling, BMPR1A, BMPR1B and BMPR2 are specific to BMP ligands [20]. Here we show that knockdown of BMPR1A, but not BMPR1B or BMPR2, inhibits BMP-induced SMAD1/5 phosphorylation and centrosome over-duplication. BMPR1A is critically involved in BMP signaling, and BMPR1A knockout mice are embryonically lethal with severe heart valve and EC defects [28-30]. However, BMPR1B knockout are viable [31]. In line with the *in vivo* data, previous *in vitro* data showed that BMPR1A siRNA, but not BMPR1B siRNA, abrogates SMAD1/5 phosphorylation in human microvascular endothelial cells [32]. These

results are consistent with our findings. Interestingly, BMPR2 knockdown did not inhibit SMAD activation or block BMP ligand-induced centrosome over-duplication, indicating possible redundancy of type 2 receptors in EC. This is also consistent with previous finding that ablation of BMPR2 in pulmonary artery smooth muscle cells allows signaling through ActR2A and does not abolish BMP signaling [33].

Another prominent feature of the tumor environment is a chronic inflammatory response, which is mediated by infiltration of immune system cells [34]. Tumor inflammation is similar to inflammation associated with normal physiological processes such as wound healing [34]. Our results suggest that inflammatory mediators do not induce centrosome over-duplication in EC. Thus, despite being a hallmark of the tumor environment, chronic inflammation is likely not an input for centrosome over-duplication in tumor EC. This finding also suggests that during physiological inflammation, EC do not develop excess centrosomes, therefore maintaining a relatively normal phenotype and function.

Hypoxia upregulates the expression and secretion of growth factors, such as VEGF-A, in the tumor environment [35]. Here we show that hypoxia induces excess centrosomes in EC. However, although hypoxia-induced signaling up-regulates VEGF-A, which promotes centrosome over-duplication [11], our data suggest that hypoxia-induced excess centrosomes in EC are independent of EC-derived VEGF-A. This indicates that, if tumor EC undergo centrosome over-duplication as a result of up-regulated VEGF-A signaling in the tumor environment, the source of the ligand is likely the tumor cells or other non-endothelial stromal cells.

In addition to changes in the tumor environment, tumor EC may also acquire cell-autonomous perturbations that promote centrosome over-duplication. Previous studies showed

that tumor stromal cells, including tumor EC, have attenuated p53 activation in response to stress stimulation [25], and p53 abnormalities have been linked with centrosome over-duplication. For example, mouse embryonic fibroblasts isolated from p53 knock-out mice possess multiple copies of functional centrosomes [24]. Here we show that reduced p53 levels induced excess centrosomes in EC, suggesting that cell autonomous p53 changes contribute to centrosome over-duplication in tumor EC.

Although up to 30% of primary tumor EC have excess centrosomes [6], our results indicate that no single environmental factor or down-regulation of p53 alone achieves such a high percentage of excess centrosomes in EC [11]. It is possible that *in vivo*, several inducing factors combine to achieve the high percentage of excess centrosomes in tumor EC. In summary, we show that multiple environmental inputs and attenuated p53 contribute to centrosome over-duplication in EC. This work contributes to our understanding of both normal and tumor angiogenesis, and provides potential insights for anti-angiogenic therapy.

F. Figures

Figure 2.1. BMP2 and BMP7 induce excess centrosomes in EC.

(A) Representative images of HUVEC with normal (left) and over-duplicated centrosomes (right). HUVEC were stained with γ-tubulin for centrosomes (green) and DRAQ7 for nuclei (blue). (B, C) Frequency of excess centrosomes in HUVEC after treatment with 200 ng/ml BMP2 (B) or BMP7 (C) for 4 days. Error bars, standard deviation from mean. Statistics: two-tailed unpaired Student's t-test. *, $p \leq 0.05$.

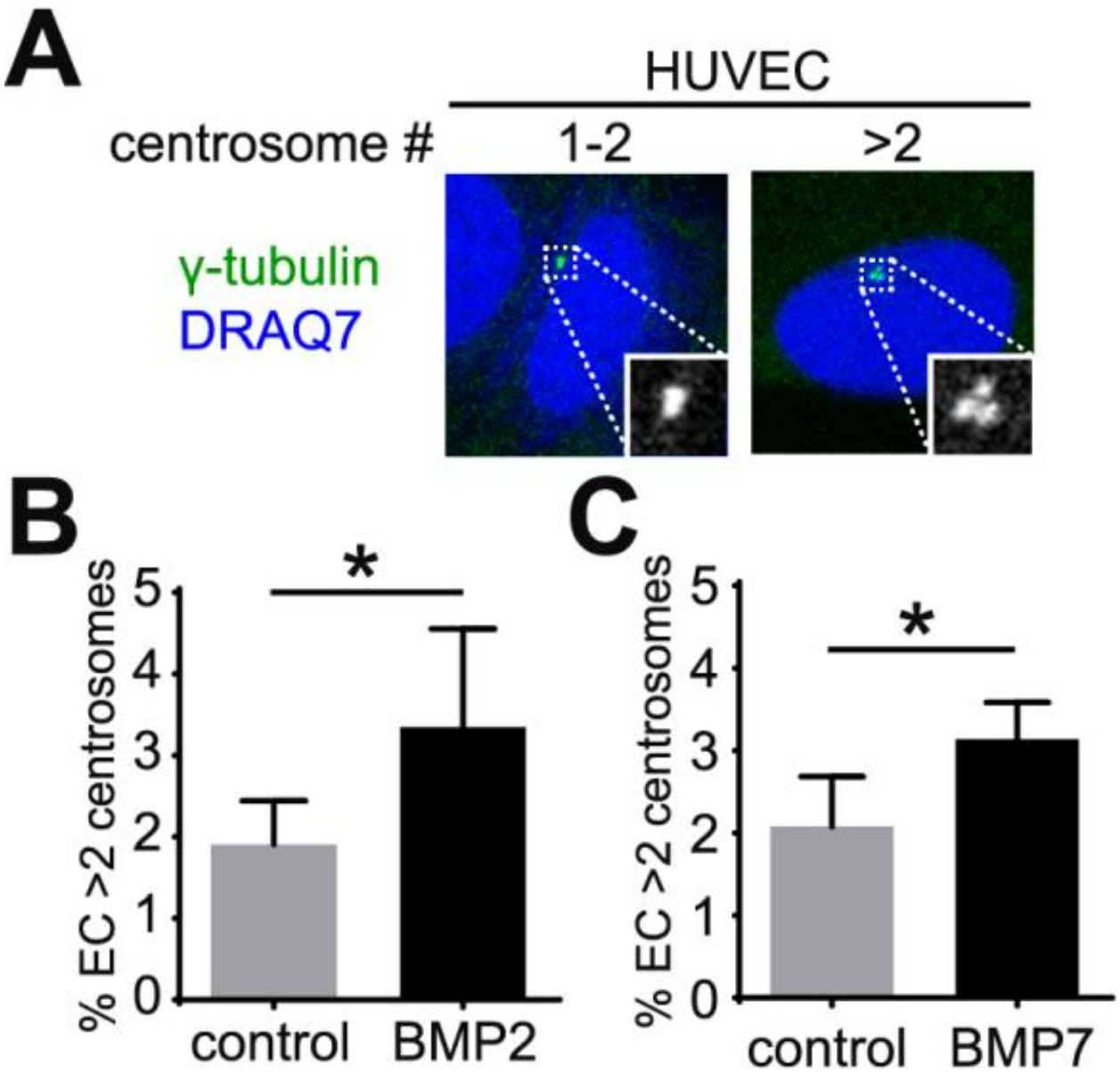
A
HUVEC
centrosome #
1-2
>2
γ-tubulin
DRAQ7
B
% EC >2 centrosomes
0
1
2
3
4
5
*
control
BMP2
C
% EC >2 centrosomes
0
1
2
3
4
5
*
control
BMP7

Figure 2.2. BMP-induced centrosome over-duplication is dependent on BMPR1A.

(A, B) Frequency of excess centrosomes in indicated siRNA-treated HUVEC cultured with vehicle or 200 ng/ml of BMP6 (A) or BMP2 (B) for 4 days. C, non-targeting control siRNA; R1A, BMPR1A siRNA; R1B, BMPR1B siRNA; R2, BMPR2 siRNA. (C) Representative images of HUVEC treated with indicated siRNA and vehicle or BMP6 and stained for phospho-SMAD1/5 (pSMAD1/5, green) and nucleus (DRAQ7, blue). Cells were starved in Opti-MEM for 4 hr, followed by 30 min treatment with vehicle or BMP6. Only the nuclear pSMAD1/5 is shown (see Methods for details of mask). (D) Quantification of nuclear pSMAD1/5 in HUVEC treated as indicated. (E) Western blot of phospho-SMAD1/5 (pSMAD) and total SMAD1 in HUVEC treated as indicated. Cells were starved in Opti-MEM for 4 hr, then treated with vehicle or BMP6 for 30 min. Error bars, standard deviation from mean. Statistics: two-tailed paired (A, B) or unpaired (D) Student's t-test. ns, not significant; *, $p \leq 0.05$; **, $p \leq 0.01$; ***, $p \leq 0.001$.

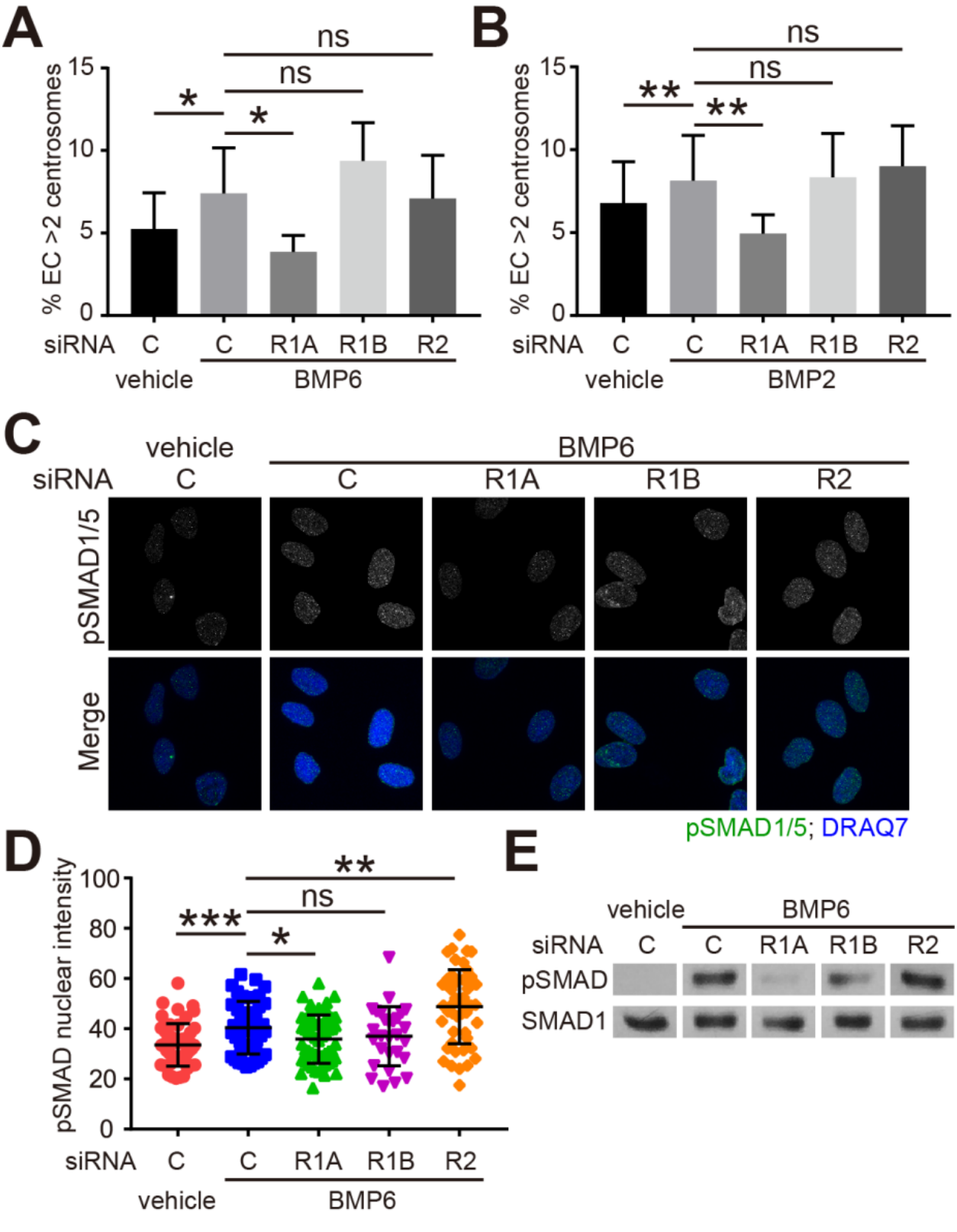
A
% EC >2 centrosomes
15
10
5
0
ns
ns
*
*
siRNA C C R1A R1B R2
vehicle BMP6
B
% EC >2 centrosomes
15
10
5
0
ns
ns
**
**
siRNA C C R1A R1B R2
vehicle BMP2
C
vehicle BMP6
siRNA C C R1A R1B R2
pSMAD1/5
Merge
pSMAD1/5; DRAQ7
D
pSMAD nuclear intensity
100
80
60
40
20
0
**
ns
***
*
siRNA C C R1A R1B R2
vehicle BMP6
E
vehicle BMP6
siRNA C C R1A R1B R2
pSMAD
SMAD1

Figure 2.3. Inflammatory mediators do not induce excess centrosomes in EC.

(A) Frequency of excess centrosomes in HUVEC after treatment with indicated factors for 4 days. (B) HUVEC incubated with 10 ng/ml LPS for 4 days prior to determination of excess centrosome frequency. Results are shown in fold of increase, and each frequency was normalized to its respective control. Error bars, standard deviation from mean. Statistics: Two-tailed unpaired Student's t-test (A), X^2 test (B). *, $p \leq 0.05$; ns, not significant.

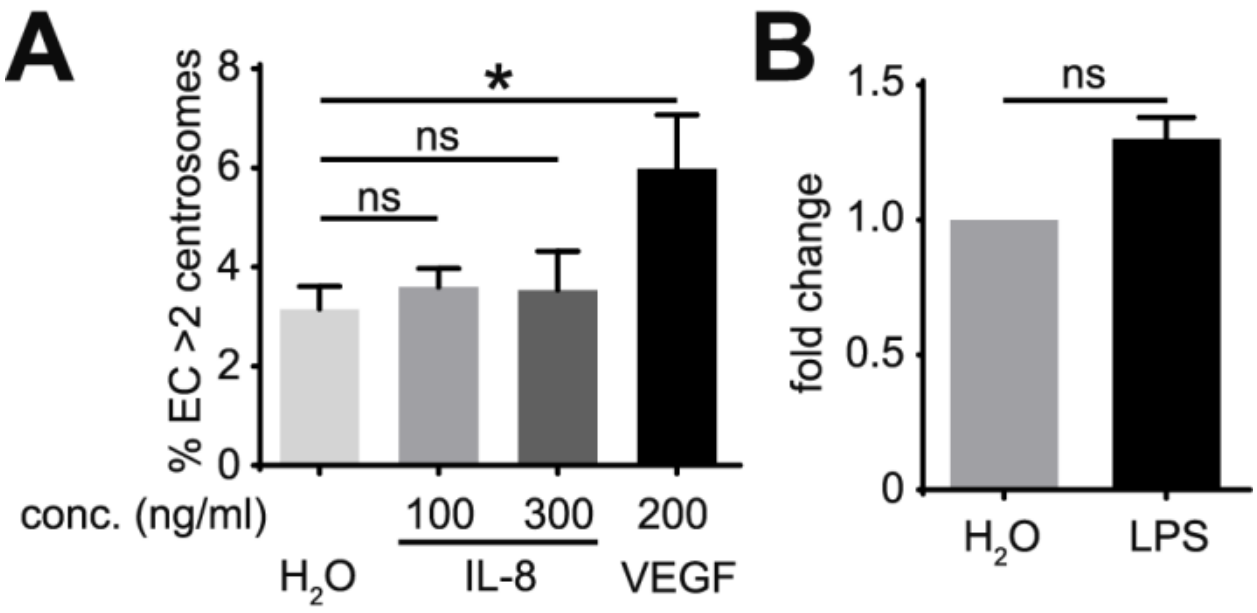
A
% EC >2 centrosomes
0
2
4
6
8
*
ns
ns
conc. (ng/ml)
100
300
200
H2O
IL-8
VEGF
B
fold change
0
0.5
1.0
1.5
ns
H2O
LPS

Figure 2.4. Hypoxia induces excess centrosomes in EC independent of cell-autonomous VEGF-A signaling.

(A) Frequency of excess centrosomes in HUVEC after treatment with 100 μM hypoxic-mimetic agent desferrioxamine (DFO) for 4 days. (B) Frequency of excess centrosomes in HUVEC after 4 days of incubation in 2% oxygen. (C) Frequency of excess centrosomes in HUVEC after incubation in 20% or 2% oxygen for 4 days and indicated treatments. Error bars, standard deviation from mean. Statistics: two-tailed unpaired Student's t-test. *, $p \leq 0.05$; ns, not significant.

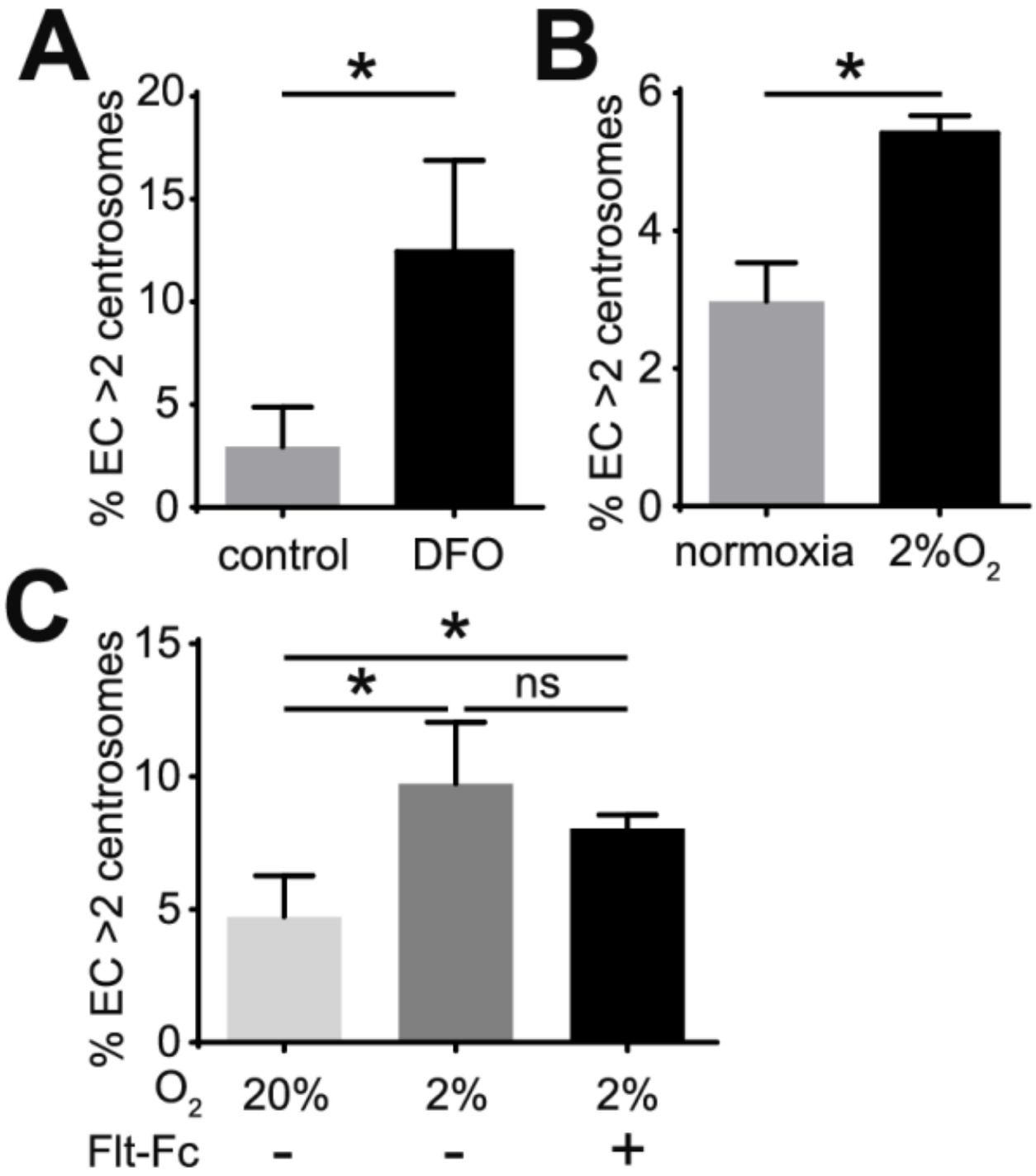
A
*
% EC >2 centrosomes
20
15
10
5
0
control
DFO
B
*
% EC >2 centrosomes
6
4
2
0
normoxia
2%O2
C
*
*
ns
% EC >2 centrosomes
15
10
5
0
O2
20%
2%
2%
Flt-Fc
-
-
+

Figure 2.5. Down-regulation of p53 induces excess centrosomes in EC.

(A) Frequency of excess centrosomes in HUVEC infected with human p53 shRNA. (B) Frequency of excess centrosomes in normal mouse endothelial cells (NEC) infected with mouse p53 shRNA. Error bars, standard deviation from mean. Statistics: two-tailed unpaired Student's t-test. *, $p \leq 0.05$.

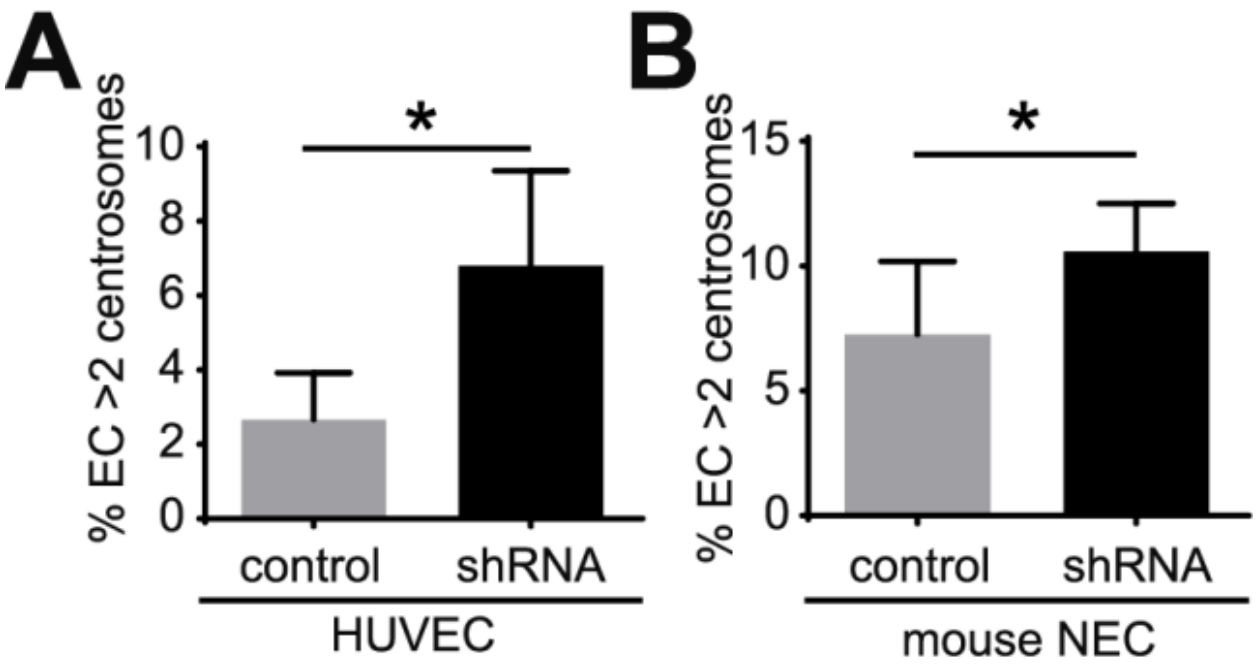
A
% EC >2 centrosomes
10
8
6
4
2
0
*
control
shRNA
HUVEC
B
% EC >2 centrosomes
15
10
5
0
*
control
shRNA
mouse NEC

Supplementary Figure 2.1. Effects of BMP ligands on human primary EC.

(A) Representative images of HUVEC with different centrosome numbers (n). (B) Frequency of excess centrosomes in HUVEC after treatment with 200 ng/ml of BMP4 for 4 days. (C-E) Frequency of excess centrosomes in HUAEC (C), HBMEC(D), or HMVEC-L (E) after treatment with 200 ng/ml of BMP2 or BMP6 for 4 days. Error bars, standard deviation from mean. Statistics: two-tailed unpaired Student's t-test. ns, not significant.

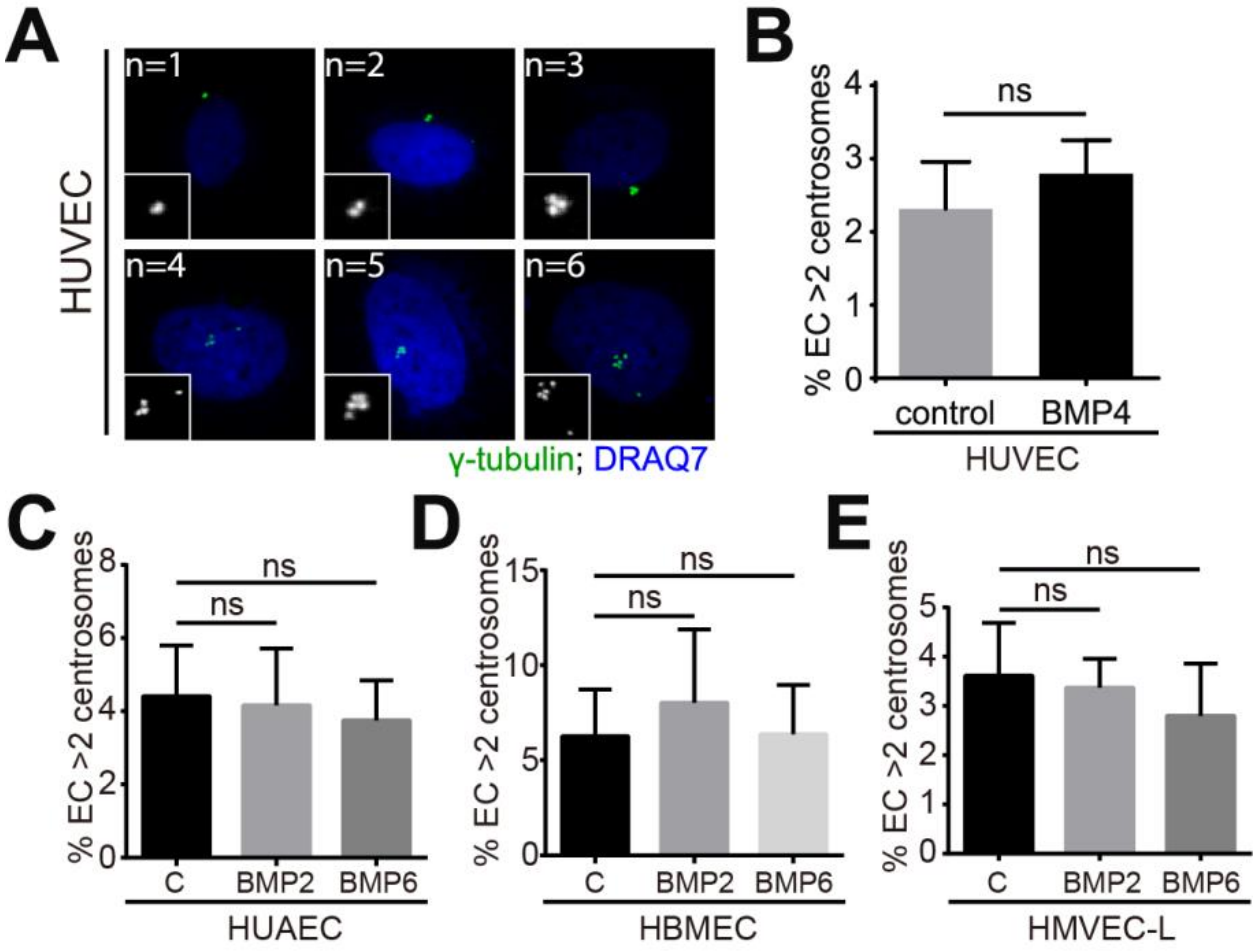
A
HUVEC
n=1
n=2
n=3
n=4
n=5
n=6
γ-tubulin; DRAQ7
B
% EC >2 centrosomes
ns
control
BMP4
HUVEC
C
% EC >2 centrosomes
ns
ns
C
BMP2
BMP6
HUAEC
D
% EC >2 centrosomes
ns
ns
C
BMP2
BMP6
HBMEC
E
% EC >2 centrosomes
ns
ns
C
BMP2
BMP6
HMVEC-L

Supplementary Figure 2.2. Validation of BMP receptor siRNAs.

(A-C) Relative mRNA levels of BMPR1A (A), BMPR1B (B), or BMPR2 (C) in HUVEC treated with indicated siRNAs. Cells were collected 48 hr after siRNA treatment. Error bars: standard deviations from mean. Statistics: two-tailed unpaired. *, $p \leq 0.05$; ***, $p \leq 0.001$.

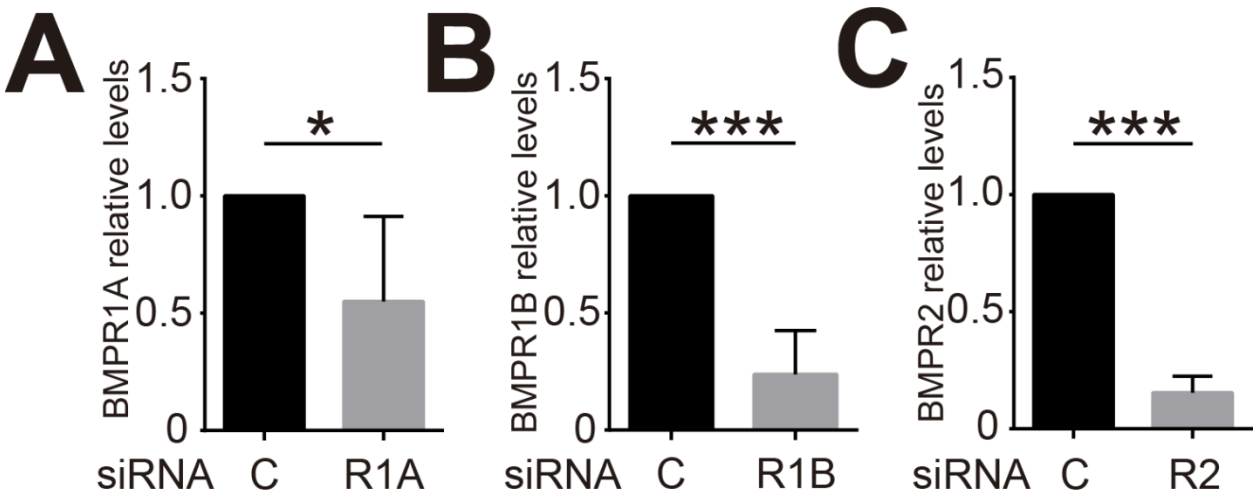
A
BMPR1A relative levels
1.5
1.0
0.5
0
*
siRNA C R1A
B
BMPR1B relative levels
1.5
1.0
0.5
0
***
siRNA C R1B
C
BMPR2 relative levels
1.5
1.0
0.5
0
***
siRNA C R2

Supplementary Figure 2.3. Elevated IL-8 activates ERK phosphorylation.

HMVEC were treated with 200 ng/ml IL-8 or VEGF-A for indicated times, collected, and analyzed for phosphorylated ERK (pERK) and total ERK.

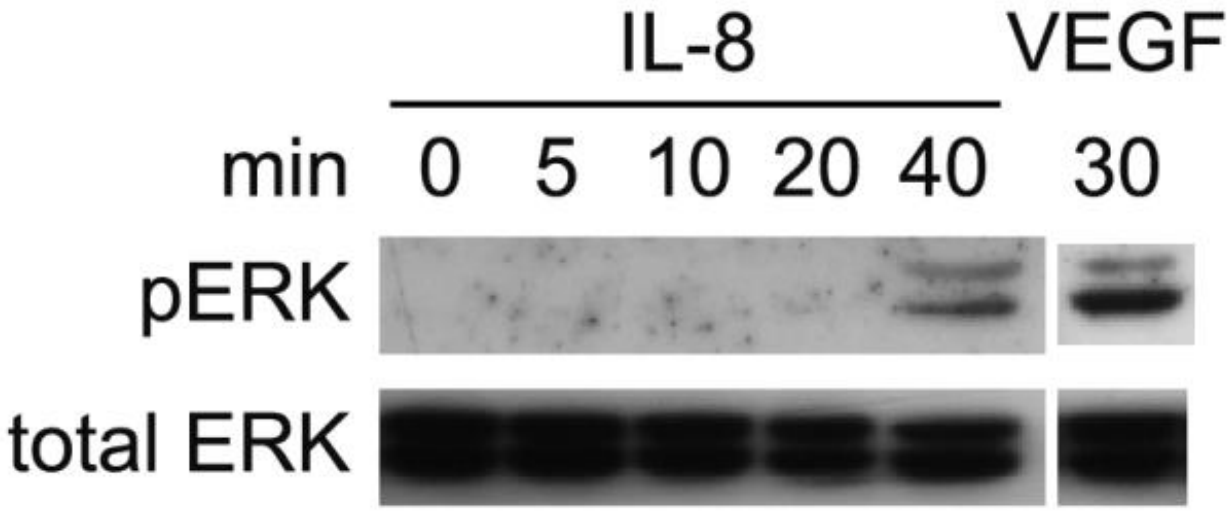
IL-8
VEGF
min
0
5
10
20
40
30
pERK
total ERK

Supplementary Figure 2.4. Hypoxia activates HIF1α and Flt-Fc blocks VEGF-A signaling. (A) HUVEC were MeOH fixed immediately (lower panel) or after 30-min recovery in normoxia (top panel) post-hypoxic incubation, then stained for HIF1α (red) and DRAQ7 (DNA, green). (B) Western blot for HIF1α in HUVEC incubated in normoxia or 2% oxygen. (C) Frequency of excess centrosomes in HUVEC after incubation in 3% O_2 for 4 days. (D) HUVEC were treated with VEGF-A (200 ng/ml) or VEGF-A plus Flt-Fc (1 ug/ml) for 20 min. Cell lysates were collected and blotted for phosphorylated ERK (pERK) and total ERK. Error bars, standard deviation from mean. Statistics: two-tailed unpaired Student's t-test. *, $p \leq 0.05$.

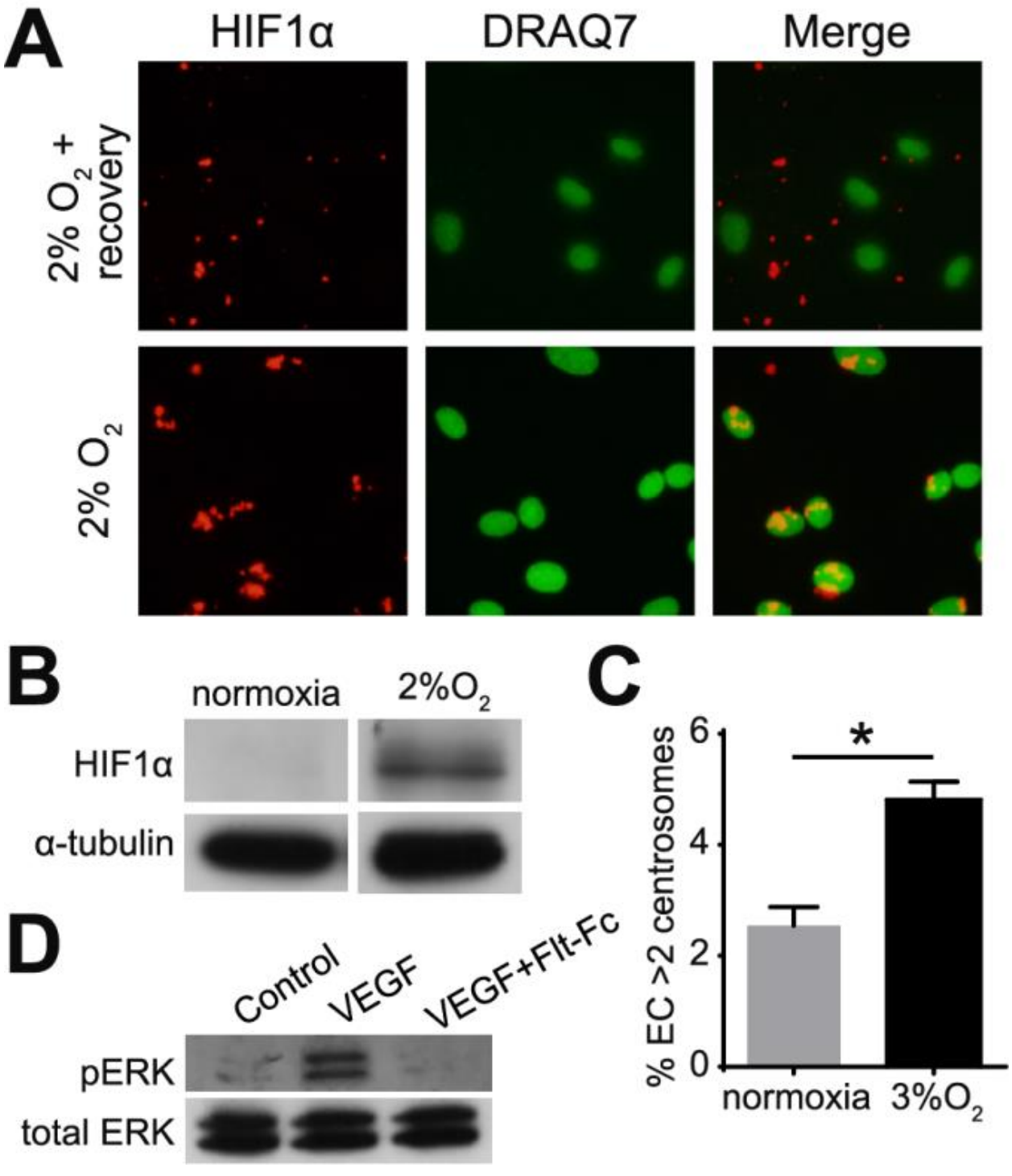
A
HIF1α
DRAQ7
Merge
2% O2 + recovery
2% O2
B
normoxia
2%O2
HIF1α
α-tubulin
C
% EC >2 centrosomes
6
4
2
0
*
normoxia
3%O2
D
Control
VEGF
VEGF+Flt-Fc
pERK
total ERK

Supplementary Figure 2.5. Validation of p53 shRNA.

HUVEC (A) or mouse normal endothelial cells (NEC) (B) were infected with viruses expressing human p53 shRNA or mouse p53 shRNA, respectively. p53 levels were detected by western blot 4 days after viral infection.

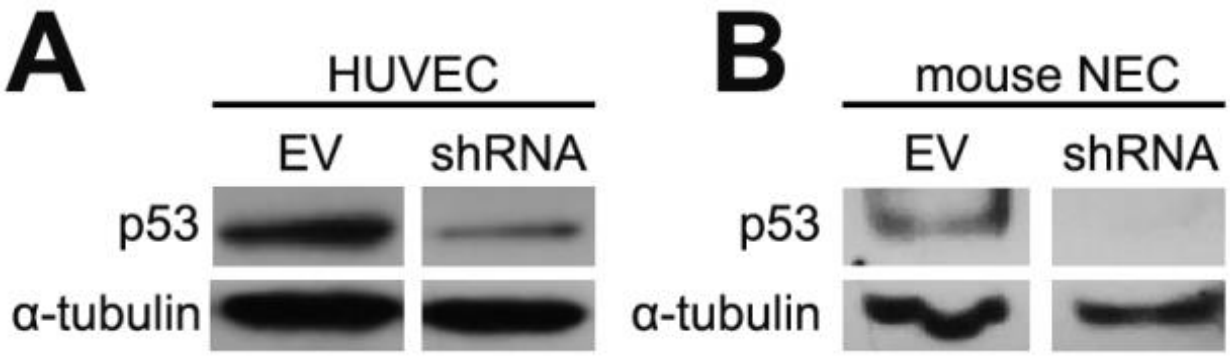
A
HUVEC
EV
shRNA
p53
α-tubulin
B
mouse NEC
EV
shRNA
p53
α-tubulin

REFERENCES

1. Hanahan D, Weinberg RA (2011) Hallmarks of cancer: the next generation. Cell 144: 646-674.

2. Carmeliet P, Jain RK (2000) Angiogenesis in cancer and other diseases. Nature 407: 249-257.

3. Bergers G, Hanahan D (2008) Modes of resistance to anti-angiogenic therapy. Nat Rev Cancer 8: 592-603.

4. Akino T, Hida K, Hida Y, Tsuchiya K, Freedman D, et al. (2009) Cytogenetic abnormalities of tumor-associated endothelial cells in human malignant tumors. Am J Pathol 175: 2657-2667.

5. Hida K, Hida Y, Amin DN, Flint AF, Panigrahy D, et al. (2004) Tumor-associated endothelial cells with cytogenetic abnormalities. Cancer Research 64: 8249-8255.

6. Kushner EJ, Ferro LS, Liu JY, Durrant JR, Rogers SL, et al. (2014) Excess centrosomes disrupt endothelial cell migration via centrosome scattering. J Cell Biol 206: 257-272.

7. Bettencourt-Dias M, Glover DM (2007) Centrosome biogenesis and function: centrosomics brings new understanding. Nat Rev Mol Cell Biol 8: 451-463.

8. Holash J, Maisonpierre PC, Compton D, Boland P, Alexander CR, et al. (1999) Vessel cooption, regression, and growth in tumors mediated by angiopoietins and VEGF. Science 284: 1994-1998.

9. Dudley AC (2012) Tumor endothelial cells. Cold Spring Harb Perspect Med 2: a006536.

10. Zhang X, Nie D, Chakrabarty S (2010) Growth factors in tumor microenvironment. Front Biosci (Landmark Ed) 15: 151-165.

11. Taylor SM, Nevis KR, Park HL, Rogers GC, Rogers SL, et al. (2010) Angiogenic factor signaling regulates centrosome duplication in endothelial cells of developing blood vessels. Blood 116: 3108-3117.

12. Bobinac D, Maric I, Zoricic S, Spanjol J, Dordevic G, et al. (2005) Expression of bone morphogenetic proteins in human metastatic prostate and breast cancer. Croat Med J 46: 389-396.

13. David L, Feige JJ, Bailly S (2009) Emerging role of bone morphogenetic proteins in angiogenesis. Cytokine Growth Factor Rev 20: 203-212.

14. Vaupel P, Harrison L (2004) Tumor hypoxia: causative factors, compensatory mechanisms, and cellular response. Oncologist 9 Suppl 5: 4-9.

15. Liu Y, Cox SR, Morita T, Kourembanas S (1995) Hypoxia regulates vascular endothelial growth factor gene expression in endothelial cells. Identification of a 5' enhancer. Circ Res 77: 638-643.

16. Lu H, Ouyang W, Huang C (2006) Inflammation, a key event in cancer development. Mol Cancer Res 4: 221-233.

17. Yuan A, Chen JJ, Yao PL, Yang PC (2005) The role of interleukin-8 in cancer cells and microenvironment interaction. Front Biosci 10: 853-865.

18. Roberts DM, Kearney JB, Johnson JH, Rosenberg MP, Kumar R, et al. (2004) The vascular endothelial growth factor (VEGF) receptor Flt-1 (VEGFR-1) modulates Flk-1 (VEGFR-2) signaling during blood vessel formation. Am J Pathol 164: 1531-1535.

19. Kushner EJ, Ferro LS, Yu Z, Bautch VL (2016) Excess centrosomes perturb dynamic endothelial cell repolarization during blood vessel formation. Mol Biol Cell 27: 1911-1920.

20. Wang RN, Green J, Wang Z, Deng Y, Qiao M, et al. (2014) Bone Morphogenetic Protein (BMP) signaling in development and human diseases. Genes Dis 1: 87-105.

21. Brat DJ, Bellail AC, Van Meir EG (2005) The role of interleukin-8 and its receptors in gliomagenesis and tumoral angiogenesis. Neuro Oncol 7: 122-133.

22. Martich GD, Boujoukos AJ, Suffredini AF (1993) Response of man to endotoxin. Immunobiology 187: 403-416.

23. An WG, Kanekal M, Simon MC, Maltepe E, Blagosklonny MV, et al. (1998) Stabilization of wild-type p53 by hypoxia-inducible factor 1alpha. Nature 392: 405-408.

24. Fukasawa K, Choi T, Kuriyama R, Rulong S, Vande Woude GF (1996) Abnormal centrosome amplification in the absence of p53. Science 271: 1744-1747.

25. Dudley AC, Shih SC, Cliffe AR, Hida K, Klagsbrun M (2008) Attenuated p53 activation in tumour-associated stromal cells accompanies decreased sensitivity to etoposide and vincristine. Br J Cancer 99: 118-125.

26. Holmes K, Roberts OL, Thomas AM, Cross MJ (2007) Vascular endothelial growth factor receptor-2: structure, function, intracellular signalling and therapeutic inhibition. Cell Signal 19: 2003-2012.

27. Miyazono K, Maeda S, Imamura T (2005) BMP receptor signaling: transcriptional targets, regulation of signals, and signaling cross-talk. Cytokine Growth Factor Rev 16: 251-263.

28. Mishina Y, Suzuki A, Ueno N, Behringer RR (1995) Bmpr encodes a type I bone morphogenetic protein receptor that is essential for gastrulation during mouse embryogenesis. Genes Dev 9: 3027-3037.

29. Gaussin V, Van de Putte T, Mishina Y, Hanks MC, Zwijsen A, et al. (2002) Endocardial cushion and myocardial defects after cardiac myocyte-specific conditional deletion of the bone morphogenetic protein receptor ALK3. Proc Natl Acad Sci U S A 99: 2878-2883.

30. Gaussin V, Morley GE, Cox L, Zwijsen A, Vance KM, et al. (2005) Alk3/Bmpr1a receptor is required for development of the atrioventricular canal into valves and annulus fibrosus. Circ Res 97: 219-226.

31. Yi SE, Daluiski A, Pederson R, Rosen V, Lyons KM (2000) The type IBMP receptor BMPRIB is required for chondrogenesis in the mouse limb. Development 127: 621-630.

32. Upton PD, Long L, Trembath RC, Morrell NW (2008) Functional characterization of bone morphogenetic protein binding sites and Smad1/5 activation in human vascular cells. Mol Pharmacol 73: 539-552.

33. Yu PB, Beppu H, Kawai N, Li E, Bloch KD (2005) Bone morphogenetic protein (BMP) type II receptor deletion reveals BMP ligand-specific gain of signaling in pulmonary artery smooth muscle cells. Journal of Biological Chemistry 280: 24443-24450.

34. Grivennikov SI, Greten FR, Karin M (2010) Immunity, inflammation, and cancer. Cell 140: 883-899.

35. Harris AL (2002) Hypoxia--a key regulatory factor in tumour growth. Nat Rev Cancer 2: 38-47.

CHAPTER III-Excess Centrosomes Induce p53-Dependent Senescence without DNA Damage in Endothelial Cells[2]

A. Summary

Tumor blood vessels support tumor growth and progression. Centrosomes are microtubule organization centers in cells, and up to 30% of tumor endothelial cells often acquire excess (>2) centrosomes. Excess centrosomes are associated with aneuploidy and chromosome instability in tumor cells, but it is not known how untransformed endothelial cells respond to excess centrosomes. We found that the frequency of primary endothelial cells (EC) with excess centrosomes was quickly reduced in a p53-dependent manner. Excess centrosomes in EC were associated with p53 phosphorylation at Ser33, decreased cell proliferation and expression of senescence markers, but independent of DNA damage and apoptosis. EC with excess centrosomes in vascular sprouts also showed Ser33 p53 phosphorylation and expressed senescence markers. Our work shows that non-transformed EC respond differently to excess centrosomes than most tumor cells, and that they undergo senescence in vascular sprouts, suggesting that pathological outcomes of centrosome over-duplication depend on the transformation status of cells.

[2]This chapter is adapted from a manuscript prepared for submission in 2016. I performed all of the experiments and wrote the first draft of the manuscript. Dr. Victoria Bautch edited and added to my original draft. Dr. Erich Kushner originally established the protocol for generating Tet-Plk4 HUVEC.

B. Introduction

Cells rely on cell cycle to proliferate, ensuring an accurate inheritance of genetic information. An active eukaryotic cell cycle is divided into 4 phases: G1, S, G2 and M. Upon stress stimulation, cells can undergo cell cycle arrest as a self-protective mechanism to avoid cell death and to prevent genetic abnormalities [1,2]. Cells can be arrested at several checkpoints, but two major types of cell cycle arrest are the reversible quiescence and the permanent senescence, which share the same characteristic of no cell proliferation, but lead to dramatically different outcomes [3].

Centrosomes, comprised of two barrel-shaped centrioles and surrounding pericentriolar material, are microtubule organizing centers (MTOC) and important for directed cell migration and chromosome segregation during mitosis [4,5]. Centrosome biogenesis is highly regulated to ensure that centrosomes are duplicated once and only once during each cell cycle [6]. Cells in G1 have a single centrosome that is duplicated during S phase to form two centrosomes in G2, and these nucleate the bi-polar spindles at mitosis [7]. Loss of centrosome integrity induces p53-dependent cell cycle arrest likely via senescence [8,9], indicating that cells have a surveillance mechanism that detects and responds to centrosome loss.

Excess centrosomes are frequently found in tumor cells, where they are often associated with aneuploidy [10]. Tumor cells with excess centrosomes either form multi-polar spindles at mitosis that lead to gross aneuploidy, or cluster excess centrosomes to form bipolar spindles that are prone to merotely, the formation of inappropriate connections to spindles of individual chromosomes that can lead to subtle aneuploidy [11]. Although the process of centrosome clustering delays M phase in centrosome over-duplicated cells [12], the merotelic attachment cannot be detected by the spindle assembly checkpoint (SAC), and tumor cells with unresolved merotely progress through the cell cycle [13,14].

It was recently suggested that centrosome over-duplication leads to a p53-dependent checkpoint and growth arrest or apoptosis. Over-expression of a Kaposi's sarcoma herpesviral protein in U2OS cells induced centrosome over-duplication and p53-dependent apoptosis [15], and excess centrosomes in immortalized RPE-1 cells prevented cell proliferation in a p53-dependent manner [16]. Nevertheless, the existence of and the consequences of a p53-dependent "excess centrosome checkpoint" in primary cells are unknown. Non-tumor endothelial cells (EC) derived from the tumor micro-environment have a high frequency of excess centrosomes, likely resulting in part from cell cycle alterations induced by elevated growth factor signaling [17-19]. However, how EC, which are untransformed, respond to excess centrosomes, and whether they have a surveillance mechanism for excess centrosomes remains unclear.

Here we asked how primary EC respond to excess centrosomes. We found that EC with excess centrosomes were cell cycle arrested in a p53-dependent manner, and that excess centrosomes led to Ser33 but not Ser15 p53 phosphorylation, suggesting that the DNA damage response is not invoked. EC with excess centrosomes did not undergo apoptosis, but underwent p53-dependent senescence in culture and in vascular sprouts. Thus we reveal a previously unknown link between excess centrosomes and senescence through p53, and suggest that the response of untransformed cells with intact cell cycle regulation to excess centrosomes is senescence.

C. Methods

Cell culture

Human umbilical vein endothelial cells (HUVEC, Lonza Group) were cultured in endothelial basal medium-2 (EBM-2, Lonza cc-3156) supplemented with the EGM-2 BulletKit (Lonza cc-3162). Tetracyclin-inducible Plk4-expressing HUVEC (Tet-Plk4 or Tet-Plk4$^{1-608}$)

were generated as described [20]. Briefly, P2 HUVEC were infected with 500 μl/ml Plk4-expressing Tet-ON lentiviruses [20] in 5 ml EGM-2 plus 1 μg/ml polybrene (Millipore TR-1003-G) overnight at 37°C. Infected cells were incubated for 4d, followed with 2 μg/ml puromycin for selection. Viruses were produced by the UNC Lenti-shRNA Core Facility.

Tet-Plk4 HUVEC were treated with 0.5-1 μg/ml doxycycline (DOX; Sigma D9891) for 24h to induce centrosome over-duplication. p53 siRNA (Life technologies, 4427038-s605) transfection utilized RNAi Max (Life technologies, 13778-075) according to manufacturer's protocols. Senescence was induced using H_2O_2 (Fisher scientific H325), etoposide (Sigma E1383), or hydroxyurea (Sigma H8627). Briefly, HUVEC were incubated with 100 μM H_2O_2 in EGM-2 for 2h/day for 3 consecutive days, and fixed/collected 2d post H_2O_2 treatment. HUVEC were incubated with etoposide (50 μM) or hydroxyurea (400 μM) for 6d, and fixed/collected immediately after treatment.

Immunofluorescence

HUVEC (in dishes or on gelatin-coated cover slips) were fixed in cold 100% MeOH for 10 min, then stained as described previously [17]. Briefly, fixed cells were blocked in 5% bovine serum at RT for 1h, then incubated with primary antibodies at 4°C overnight. Cells were washed 3X 5 min with PBS after primary antibodies, then incubated with secondary antibodies and the DNA dye DRAQ7 (1:1000, Abcam ab109202) for 2h at RT. Cells were washed 3X 10 min with PBS before mounting with VECTASHIELD mounting medium (Vector Laboratories H-1000). Both primary and secondary antibodies were diluted in 5% bovine serum in PBS. Images were acquired using an Olympus FV1200 confocal microscope. Immunofluorescence intensity was quantified using ImageJ. Primary antibodies were: anti-γ-tubulin (1:5000, Sigma T6557), anti-

phospho-p53 (Ser33) (1:250, Cell signaling 2526), anti-cleaved-caspase3 (1:400, Cell signaling 9664), anti-pericentrin (1:5000, Abcam 4448), anti-GLB1 (1:100, Abcam 139288), anti-phospho-histone 3 (1:500, Cell signaling 3377), anti-H3K9Me3 (1:1000, Active Motif 39162), anti-γH2AX (1:500, Cell signaling 9718) and anti-BrdU (1:500, Abcam ab1893). Secondary antibodies were: goat-anti-mouse Alexa 488 (1:250, Invitrogen A11029), goat-anti-mouse Alexa 594 (1:250, Invitrogen A11005), goat-anti-rabbit Alexa 488 (1:250, Invitrogen A11034) and goat-anti-rabbit Alexa 594 (1:250, Invitrogen A11037).

BrdU labeling

To detect cell proliferation, DOX-treated Tet-Plk4 HUVEC were incubated with 10 μM BrdU (Sigma B5002) for 24h. Cells were fixed in cold 100% MeOH for 10 min, and stained with anti-γ-tubulin antibodies as stated above. After γ-tubulin staining, cells were sequentially treated with 1N HCl on ice for 10 min, 2N HCl at RT for 10 min and phosphate/citric acid buffer (pH 7.4) at RT for 10 min. Treated cells were re-blocked with 5% bovine serum, and stained with anti-γ-tubulin and anti-BrdU antibodies as stated above.

Western Blots

Western blot analysis was performed as previously described, with slight modifications [21]. Briefly, HUVEC lysates were collected using cold PBS, and lysed using RIPA buffer supplemented with protease inhibitors (Cell signaling 5871S). Proteins were separated on a 10% sodium dodecyl sulfate–polyacrylamide gel and transferred to a polyvinylidene fluoride membrane (GE Healthcare RPN303F), which was blocked in 5% BSA at RT for 1h, then incubated with primary antibodies at 4°C overnight. Membrane was washed 3X 5 min with TBS

containing 0.1% tween-20 (TBST), incubated with secondary antibodies at RT for 1h, washed with 0.1% TBST for 1h at RT, and imaged via Clarity Western ECL Substrate (Bio-Rad 170-5061). Primary antibodies were: anti-p53 (1:1000, Abcam ab1101), anti-α-tubulin (1:15,000, Sigma T6199), anti-phospho-p53 (Ser33) (1:1000, Cell signaling 2526), anti-phospho-p53 (Ser15) (1:1000, Cell signaling 9284), anti-p21 (1:1000, Cell signaling 2947), anti-β-actin (1:10,000, Cell signaling 3700), anti-caspase-3 (1:1000, Cell signaling 9662), anti-cleaved-caspase3 (1:1000, Cell signaling 9664). Secondary antibodies were: HRP anti-rabbit (1:5000, Invitrogen G-21234), HRP anti-mouse (1:30,000, Invitrogen 81-6720).

3D Sprouting Angiogenesis Assay

The sprouting angiogenesis assay was performed as described [20,22]. DOX was added 3d prior to putting HUVEC onto beads. To isolate Tet-Plk4 HUVEC from sprouts and beads, fibrin matrix was digested with 0.25% trypsin for approximately 1.5 h, until the fibrin matrix was completely liquefied. Isolated cells were re-plated on cover slips, and fixed after overnight incubation in EGM-2 medium. To determine excess centrosome frequency in sprouts *in situ*, Tet-Plk4 HUVEC were infected with 100 μl/ml lentiviruses expressing a centrin-GFP fusion protein [20] overnight during DOX treatment. The number of centrosomes in 3D sprouts was determined using an Olympus FV1200 confocal microscope with a 40X oil objective.

To label cells with BrdU in sprouts, 10 μM BrdU in EGM-2 was added to wells 2d post embedding of HUVEC-coated beads. Cells were incubated with BrdU for 8d, then recovered by plasmin digestion. Briefly, the fibroblast layer was removed by 0.25% trypsin digestion, after which fibrin was then incubated with 1 mg/ml plasmin (Sigma P1867) for approximately 1h, until the fibrin matrix was completely liquefied. Cytodex beads were settled and removed from

supernatant, which was then centrifuged to collect recovered EC. The cell pellet was resuspended, a single cell suspension was generated by 0.05% trypsin digestion for 1 min, and EC were plated onto cover slips overnight before fixation and staining.

Senescence β-Galactosidase Staining Assay

The senescence β-Galactosidase (SA-β-gal) assay was performed according to manufacturer's directions (Cell Signaling 9860). Briefly, fixed cells were incubated overnight in 1 ml staining solution with X-gal. Cells in fibrin were fixed with 2% paraformaldehyde (PFA) for 15 min, and incubated in 500 µl staining solution for 1-2d. Images were acquired using an Olympus IX50 microscope with a bright field filter. To correlate centrosome status and SA-β-gal, centrin-GFP-expressing EC were examined under an Olympus FV1200 confocal microscope with a 40X oil objective to identify cells with centrosome over-duplication. Wells were then incubated with X-gal substrate, and the SA-β-gal staining of pre-identified centrosome over-duplicated cells was examined under an Olympus IX50 microscope under bright field. Centrosome images and SA-β-gal stained images were overlaid using ImageJ.

Software and Statistical Analysis

The Student's t-test and X^2 test were used to determine statistical significance in cases with 3 repeats and 2 repeats, respectively. Error bars represent standard deviations from the mean from independent experiments. Prism Graphpad was used to perform statistical analysis and generate graphs. ImageJ and R3.2.2 software were used to analyze H3K9Me3 staining patterns.

D. Results

Excess Centrosome Frequency Is Not Maintained in EC

We developed a tetracycline-inducible Plk4 expression system (Tet-Plk4) in HUVEC to conditionally induce centrosome over-duplication **(Fig 3.1A)** [20]. γ-tubulin was used to label centrosomes, and EC with more than 2 centrosomes (>2) were considered centrosome over-duplicated **(Fig 3.1B)** [20]. The γ-tubulin signal was confirmed as centrosome-specific by co-labeling EC with another centrosome-localized protein, centrin tagged with GFP, which showed strong overlap with γ-tubulin **(Supp. Fig 3.1)**. Treatment of Tet-Plk4 HUVEC with doxycycline (DOX) resulted in a significant increase in the percentage of EC with excess centrosomes compared to controls **(Fig 3.1C)**.

Next we asked whether EC maintain DOX-induced excess centrosomes over time. Tet-Plk4 HUVEC were treated with DOX for 24h, the DOX was removed, and EC were analyzed for centrosome numbers relative to elapsed time **(Fig 3.1D)**. At day 0, about 25% of treated EC had excess centrosomes, and there was a time-dependent decrease in the frequency of EC with excess centrosomes from days 2 to 6 **(Fig 3.1E)**. These results in primary human EC are consistent with previous data in mouse tumor EC [17], suggesting that centrosome over-duplication either leads to EC loss or reduces their competitive advantage in culture relative to non-over-duplicated EC.

Decrease of Excess Centrosome Frequency in EC Is p53-Dependent

Loss of centrosome integrity leads to p53 phosphorylation at Ser33 [8], so we tested whether centrosome over-duplication has similar effects on p53 phosphorylation. We found that DOX treatment elevated levels of p53 protein and dramatically increased p53 phosphorylation on Ser33 **(Fig 3.2A)**. Consistent with activated p53, levels of the p53 target p21, a protein that blocks the cell cycle by inhibiting cyclin-dependent kinases [23,24], were also elevated **(Fig**

3.2A). The upregulation of p53 levels by excess centrosomes in EC is consistent with previous reports showing that Plk4 over-expression elevates p53 in RPE-1 cells [25]. To test the association between centrosome over-duplication and p53 phosphorylation, we stained cells with γ-tubulin and phosphorylated p53 (pp53) (S33) after DOX treatment to assess pp53 (S33) levels on a per cell basis **(Fig 3.2B)**. We found that significantly more centrosome over-duplicated EC were positive for pp53 staining than EC with normal centrosome numbers **(Fig 3.2C)**, and the intensity of pp53 (S33) staining was significantly higher in EC with excess centrosomes **(Fig 3.2D)**. To confirm that the effects on p53 phosphorylation resulted from centrosome over-duplication and not some other aspect of Plk4 activity, we conditionally over-expressed $Plk4^{1\text{-}608}$, a truncated Plk4 protein that retains its kinase activity without inducing centrosome over-duplication [26]. After DOX treatment, pp53 (S33) levels in Tet-Plk4 HUVEC with 1-2 centrosomes were similar to that in Tet-$Plk4^{1\text{-}608}$ HUVEC, but remarkably lower than that in centrosome over-duplicated Tet-Plk4 HUVEC, indicating that *bona fida* centrosome over-duplication instead of Plk4 kinase activity induces p53 phosphorylation **(Supp. Fig 3.2A)**. Overall these results demonstrate that excess centrosomes lead to increased p53 phosphorylation at S33.

Because of the correlation between centrosome over-duplication and p53 phosphorylation, we hypothesized that the decrease in EC with excess centrosomes over time is dependent on p53. Knockdown of p53 via siRNA maintained excess centrosome frequency for several days as control EC frequencies dropped **(Fig 3.2E)**. By day 6, the excess centrosome percentage in p53 siRNA-treated cells had decreased to that of the controls **(Fig 3.2E)**, coinciding with the recovery of p53 levels after knockdown **(Supp. Fig 3.2B)**. These results demonstrate that p53 is required for the decrease in EC with centrosome over-duplication.

Excess Centrosomes Do Not Induce DNA Damage or Apoptosis

Excess centrosomes promote DNA segregation errors, which result in DNA damage and p53 activation [12,27]. A well-characterized output of DNA damage is p53 phosphorylation at Ser15 [28]. To test if excess centrosomes induced DNA damage, we determined the levels of pp53 (Ser15) in DOX-treated Tet-Plk4 HUVEC. DOX treatment significantly induced p53 phosphorylation at Ser33 but not at Ser15, indicating that centrosome over-duplication does not induce a p53-mediated DNA damage response **(Fig 3.3A)**. Using another marker of DNA damage, γH2AX [29], we found that UV treatment, but not centrosome over-duplication, significantly induced γH2AX levels **(Fig 3.3B-C)**. These results suggest that excess centrosomes induce p53 phosphorylation independent of DNA damage pathways.

p53 activation promotes apoptosis [30], and excess centrosomes may induce p53-driven apoptosis [15], so we asked whether the decrease in EC with excess centrosomes resulted from p53-induced apoptosis **(Fig 3.1E)**. To test this, we measured the levels of cleaved caspase-3, which is the activated form of caspase-3 during apoptosis [31]. While UV treatment of HUVEC induced caspase-3 cleavage, DOX treatment did not lead to caspase activation **(Fig 3.3D)**. Immunofluorescence staining for cleaved caspase-3 confirmed these results **(Fig 3.3E)**, suggesting that excess centrosomes do not induce apoptosis.

Excess Centrosomes Induce p53-Dependent Senescence

p53 activation can also promote permanent cell cycle arrest, or senescence [32,33]. To examine whether EC with excess centrosomes were proliferative, we assessed bromodeoxyuridine (BrdU) incorporation **(Fig 3.4A)**. Approximately 80% of control EC (1-2 centrosomes) were BrdU+, while only about 30% of centrosome over-duplicated EC were

BrdU+ **(Fig 3.4A-B)**. Strikingly, knockdown of p53 completely rescued the frequency of BrdU+ EC with centrosome over-duplication **(Fig 3.4B)**, suggesting that centrosome over-duplication leads to p53-dependent cell cycle arrest in EC. We also compared the proliferation of DOX-treated Tet-Plk4$^{1\text{-}608}$ and Tet-Plk4 HUVEC with 1-2 centrosomes, and found no differences **(Supp. Fig 3.3A)**, indicating that centrosome over-duplication, not Plk4 kinase activity, induces cell cycle arrest. Overall, these results show that centrosome over-duplication leads to p53-dependent cell cycle arrest in EC.

Senescence-associated beta-galactosidase (SA-β-gal) activity increases as cells become senescent [34]. To determine if centrosome over-duplication causes senescence in EC, we treated Tet-PLK4 HUVEC with DOX and assayed for SA-β-gal **(Fig 3.4C)**. DOX treatment led to a greater than 2-fold increase in the percentage of SA-β-gal positive EC compared to controls, and p53 knockdown blocked the SA-β-gal induction **(Fig 3.4D)**. We further confirmed this result by staining and quantifying the levels of galactosidase-beta 1(GLB1), which is the enzyme responsible for SA-β-gal activity [35], and found significantly increased levels of GLB1 in centrosome over-duplicated EC, and this increase was blocked by p53 knockdown **(Fig 3.4E-F)**. Overall, these results demonstrate that centrosome over-duplication in EC significantly induces the expression of senescence markers in a p53-dependent manner, suggesting that excess centrosomes trigger senescence in primary EC.

Senescent cells can have senescence-associated heterochromatin foci (SAHF), and tri-methylation of lysine 9 on histone 3 (H3K9Me3) is a common marker for heterochromatin [36,37]. We tested whether centrosome over-duplicated EC have SAHF by staining for H3K9Me3, using several senescence-inducing chemical agents as positive controls [38-40]. H3K9Me3 staining patterns in senescent cells were more uniformly distributed compared to

vehicle-treated cells **(Supp. Fig 3.3B-C, E)**. To quantitatively determine the H3K9Me3 distribution, we measured the H3K9Me3 fluorescence intensity at each pixel in the nucleus, and normalized it to the mean H3K9Me3 intensity in its respective nucleus. The percentage of pixels with intensity/mean value >1.5 or <0.5 in senescent nuclei is significantly lower than that in control cells **(Supp. Fig 3.3C-D)**, demonstrating that H3K9Me3 is more uniformly distributed in senescent EC nuclei. We next performed similar measurements in DOX-treated Tet-Plk4 HUVEC, and found that the H3K9Me3 distribution in centrosome over-duplicated EC is similar to that seen in senescent cells **(Supp. Fig 3.3F)**, indicating a senescence phenotype. Collectively, these results show that excess centrosomes lead to a p53-dependent senescence-like phenotype in EC.

Excess Centrosomes Induce p53 Phosphorylation and Senescence in EC in 3D

We next wanted to know whether the link between excess centrosomes and EC senescence held in a more physiological setting. We used a sprouting angiogenesis assay in which HUVEC extend and form lumenized sprouts in a fibrin matrix [22]. DOX treatment did not perturb the sprouting behavior of Tet-Plk4 HUVEC **(Fig 3.5A)**. Interestingly, EC maintained a higher percentage of excess centrosomes over a longer period of time in 3D compared with 2D. This effect was associated with differences in cell proliferation as read out by staining for the mitotic marker phospho-histone H3 **(Supp. Fig 3.4A-C)**. To detect p53 activation in 3D sprouts, we visualized centrosomes with centrin-GFP [20], then stained cells for pp53 (S33). Consistent with our 2D data, we found that centrosome over-duplicated EC had significantly higher levels of pp53 (S33) in 3D **(Fig 3.5B-C)**. BrdU incorporation analysis showed that significantly fewer EC with excess centrosomes were BrdU+ compared to EC with normal centrosome numbers in

3D **(Fig 3.5D)**. We next examined EC in sprouts for the senescence marker SA-β-gal, and found that DOX treatment led to a 3-fold increase in the percentage of SA-β-gal positive cells compared to controls **(Fig 3.5E-F)**. To correlate centrosome over-duplication and SA-β-gal, EC centrosomes were visualized with centrin-GFP. SA-β-gal staining was largely confined to EC with excess centrosomes in sprouts **(Fig 3.5G)**. Overall, these results suggest that excess centrosomes induce p53-dependent senescence in sprouting EC.

E. DISCUSSION

EC do not maintain a high frequency of centrosome over-duplication in culture, indicating that excess centrosomes somehow compromise the EC cell cycle [17]. Here we show that excess centrosomes induce p53 phosphorylation at Ser33, and loss of p53 allows EC to maintain a high frequency of excess centrosomes. Excess centrosome-induced p53 activation was independent of DNA damage, and did not induce apoptosis, but rather induced a senescence-like phenotype in 2D and in 3D sprouts. Thus excess centrosomes induce p53-dependent senescence without DNA damage in primary EC, revealing a novel effect of excess centrosomes may depend on whether cells have intact cell-cycle checkpoints.

It has been unclear whether cells have a surveillance mechanism for centrosome over-duplication. A proposed p53-dependent "tetraploidy checkpoint" downstream of drug-induced cytokinesis failure and subsequent excess centrosomes was later found to be a side effect of drug overdose [41,42]. Moreover, cells with excess centrosomes often cluster centrosomes and undergo bipolar cell divisions to produce viable progeny [12,20], indicating that in some scenarios cells may tolerate centrosome over-duplication and survive. This centrosome clustering mechanism is frequently observed in a variety of tumor cells [43,44], providing an explanation for a high frequency of excess centrosomes in these cells [11]. Our work shows that primary

human EC, unlike most tumor cells, undergo p53-dependent senescence downstream of excess centrosomes both in 2D culture and in 3D sprouts, showing that primary EC have a surveillance mechanism for centrosome over-duplication. This is consistent with a recent report showing that immortalized RPE-1 cells with excess centrosomes have increased total p53 levels [16].

Cell division after centrosome over-duplication can be deleterious to cells. Excess centrosomes often lead to multipolar spindle formation, which induces gross aneuploidy or cell death [11,12]. Alternatively, clustering of excess centrosomes produces DNA damage or aneuploidy and chromosome instability resulting from merotelic attachments [27], [12]. Here we show the existence of a p53-dependent "excess centrosome checkpoint" in primary cells that leads to senescence. We posit that in primary cells with excess centrosomes, this checkpoint prevents cell death and may maintain the integrity of blood vessels. Senescence is also predicted to prevent mitosis-associated defects such as aneuploidy and chromosome instability, and may be a mechanism to prevent transformation-inducing mutations downstream of excess centrosomes. The potential lack of this checkpoint in tumor cells may result in different outcomes for tumor cells with excess centrosomes.

Our finding that EC with excess centrosomes can undergo senescence in 3D sprouts may be relevant in the tumor microenvironment, since up to 30% of tumor EC have over-duplicated centrosomes [17,18]. Tumor vessels are disorganized, tortuous, leaky, and insufficiently perfused [45,46], and excess centrosome-induced senescence in tumor EC may contribute to these abnormalities. For example, tumor EC have altered migration properties [17,20] and may have increased secretion of IL-1, a hallmark of senescent cells [47,48]. This work describes a novel checkpoint that connects centrosome over-duplication, p53 activation and senescence. We think that primary cells, unlike tumor cells, maintain an intact checkpoint for centrosome over-

duplication. This may be a general defense mechanism allowing primary cell to survive while avoiding mutations leading to transformation.

F. Figures

Figure 3.1. Excess centrosome frequency is not maintained in EC.

(A) Schematic representation of tetracycline-inducible Plk4 (Tet-Plk4) in HUVEC. (B) Representative images of DOX-induced centrosome over-duplication in Tet-Plk4 HUVEC. (C) Frequency of excess centrosomes in indicated EC 2d post DOX treatment. (D) Experimental timeline; DOX added at day -3 for 24h. (E) Percent centrosome over-duplication in Tet-Plk4 HUVEC on indicated days. Statistics: two-tailed Student's t test. Error bars, standard deviation from mean. *, $p<0.05$; ns, not significant.

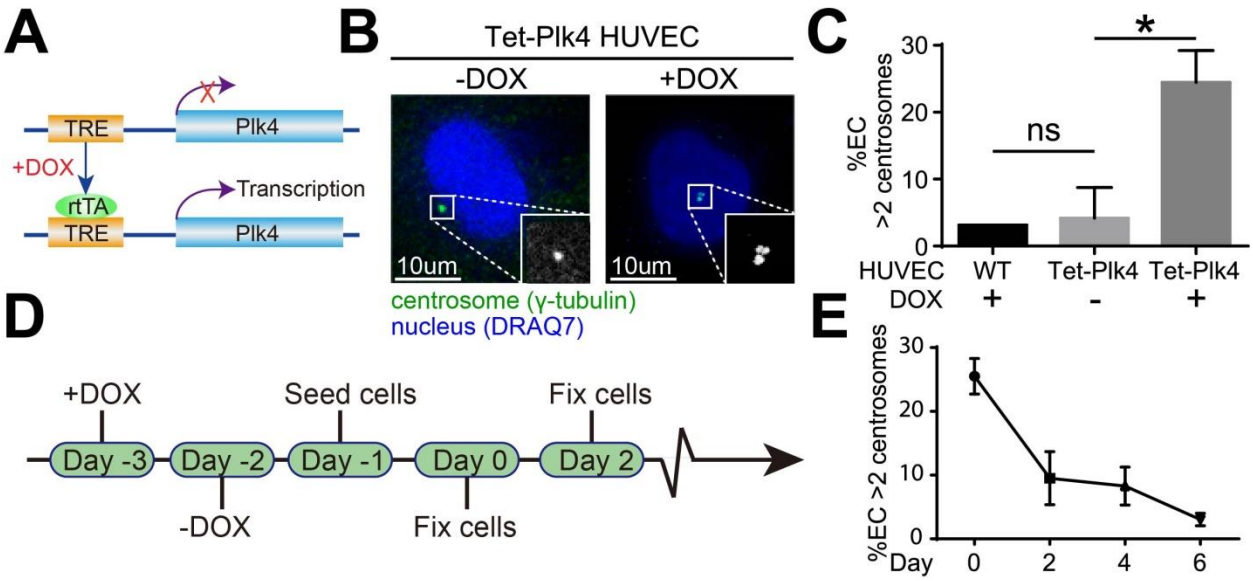
A
TRE
Plk4
+DOX
rtTA
TRE
Transcription
Plk4
B
Tet-Plk4 HUVEC
-DOX
+DOX
10um
10um
centrosome (γ-tubulin)
nucleus (DRAQ7)
C
%EC >2 centrosomes
30
20
10
0
ns
*
HUVEC WT Tet-Plk4 Tet-Plk4
DOX + - +
D
+DOX
Seed cells
Fix cells
Day -3
Day -2
Day -1
Day 0
Day 2
-DOX
Fix cells
E
%EC >2 centrosomes
30
20
10
0
Day 0 2 4 6

Figure 3.2. Decrease in excess centrosome frequency is p53-dependent.

(A) Western blot of phosphorylated p53 at Ser 33(pp53(S33)), total p53 and p21 in DOX-treated Tet-Plk4 HUVEC on d0. Normalized densitometry values are below each band. pp53(S33) normalized to total p53; total p53 and p21 normalized to α-tubulin. (B) Representative images of DOX-treated tet-Plk4 HUVEC on d0 stained for pp53(S33) (red), γ-tubulin (green) and DRAQ7 (blue). Yellow arrows, nuclei of EC with excess centrosomes. (C) Percent pp53+ cells in Tet-Plk4 HUVEC with 1-2 (n=524) or >2 (n=313) centrosomes on d0. (D) Log plot of mean fluorescence intensity of pp53(S33) in Tet-Plk4 HUVEC with 1-2 or >2 centrosomes on d0. (E) Percent excess centrosomes at indicated days in DOX-treated Tet-Plk4 HUVEC. Cells were transfected with control siRNA or p53 siRNA on d-1. Statistics: two-tailed Student's t test. Error bars, standard deviation from mean. *, $p<0.05$; ***, $p<0.01$; ****, $p<0.0001$; ns, not significant.

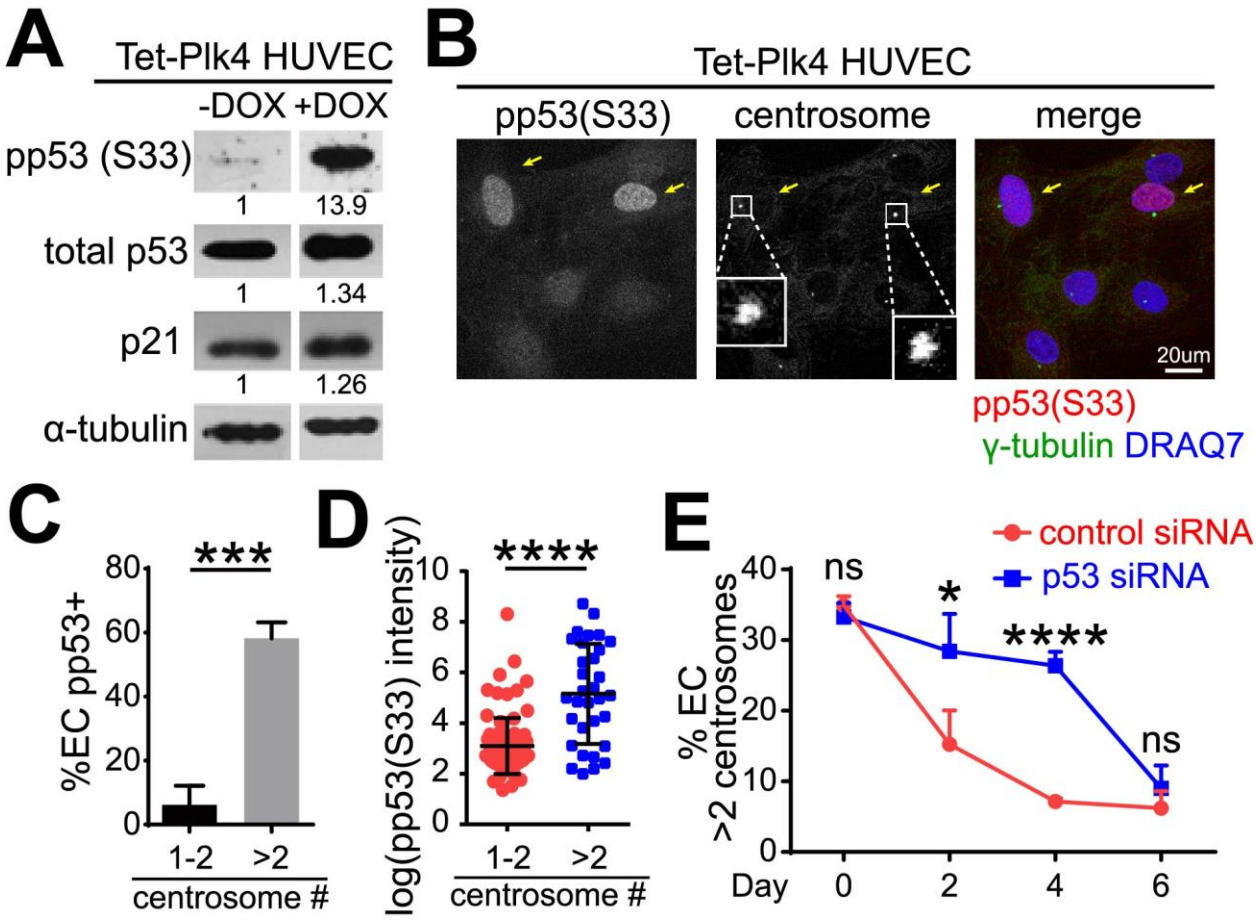
A
Tet-Plk4 HUVEC
-DOX +DOX
pp53 (S33)
1
13.9
total p53
1
1.34
p21
1
1.26
α-tubulin
B
Tet-Plk4 HUVEC
pp53(S33)
centrosome
merge
20um
pp53(S33)
γ-tubulin DRAQ7
C
***
%EC pp53+
80
60
40
20
0
1-2
>2
centrosome #
D
****
log(pp53(S33) intensity)
10
8
6
4
2
0
1-2
>2
centrosome #
E
control siRNA
p53 siRNA
% EC >2 centrosomes
40
30
20
10
0
ns
*
****
ns
Day
0
2
4
6

Figure 3.3. Excess centrosomes do not induce DNA damage or apoptosis.

(A) Western blot of p53 phosphorylation at Ser15 and Ser33. Tet-Plk4 HUVEC were DOX-treated on d-3 and collected on d0, and wild-type (WT) HUVEC were treated with UV. (B) Representative images showing γH2AX staining in Tet-Plk4 HUVEC with different centrosome numbers and WT HUVEC treated with UV. (C) Mean fluorescence intensity of γH2AX in indicated cells. (D) Western blot of full length and cleaved caspase-3 levels in Tet-Plk4 HUVEC treated with DOX or WT HUVEC treated with UV. (E) Representative images of cleaved caspase-3 staining in Tet-Plk4 HUVEC with >2 centrosomes or UV-treated WT HUVEC. Statistics, two-tailed Student's t test. Error bars, standard deviation from mean. ***, $p<0.001$; ns, not significant.

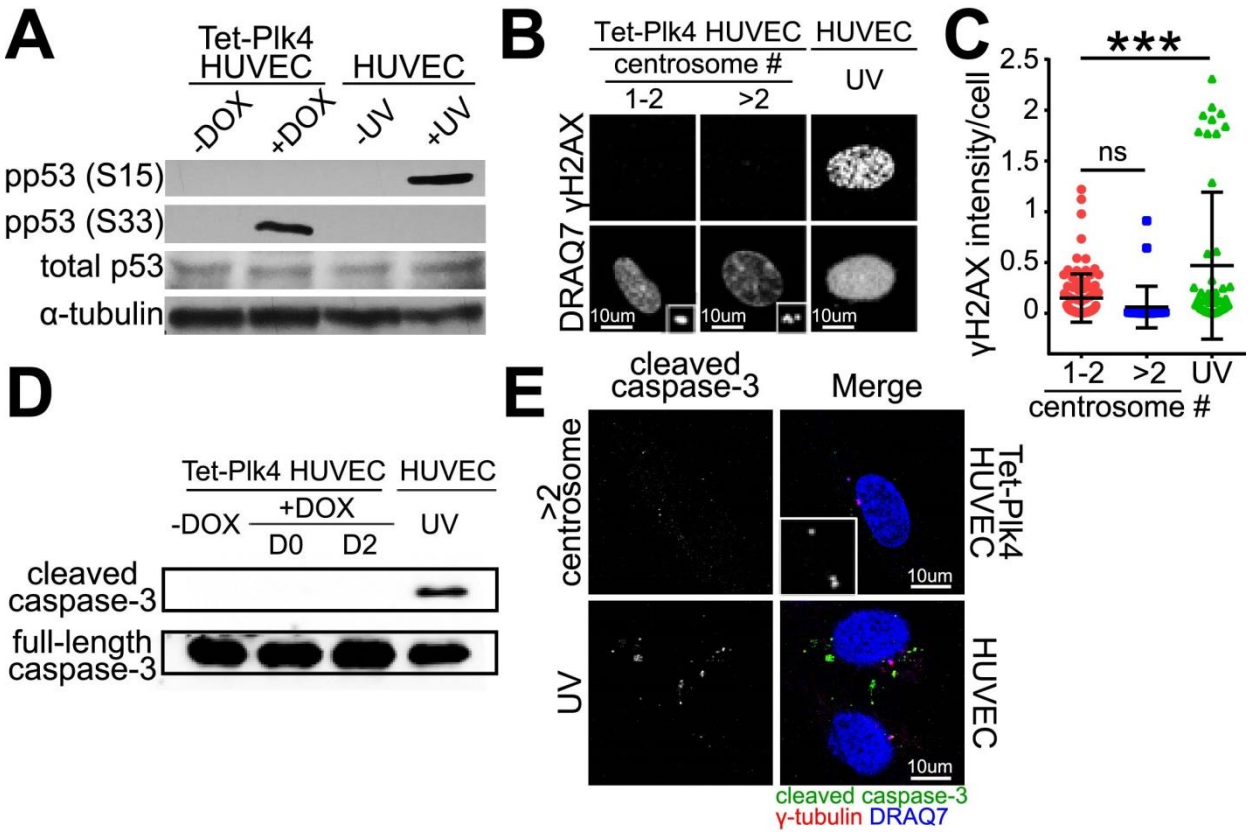
A
Tet-Plk4 HUVEC
HUVEC
-DOX
+DOX
-UV
+UV
pp53 (S15)
pp53 (S33)
total p53
α-tubulin
B
Tet-Plk4 HUVEC
HUVEC
centrosome #
1-2
>2
UV
γH2AX
DRAQ7
10um
C
***
ns
γH2AX intensity/cell
2.5
2
1.5
1
0.5
0
1-2
>2
UV
centrosome #
D
Tet-Plk4 HUVEC
HUVEC
-DOX
+DOX
D0
D2
UV
cleaved caspase-3
full-length caspase-3
E
cleaved caspase-3
Merge
>2 centrosome
UV
Tet-Plk4 HUVEC
HUVEC
10um
cleaved caspase-3
γ-tubulin DRAQ7

Figure 3.4. Excess centrosomes induce p53-dependent senescence.

(A) Representative image of DOX-treated Tet-Plk4 HUVEC stained for BrdU (red), centrosome (green), and DRAQ7 (blue). (B) Percent BrdU+ cells in control siRNA-treated (left) and p53 siRNA-treated (right) Tet-Plk4 HUVEC with indicated centrosome numbers. (C) Cytochemical staining of SA-β-gal in DOX-treated Tet-Plk4 HUVEC on d2. Black arrows, SA-β-gal+ EC. (D) Relative percent of SA-β-gal+ Tet-Plk4 HUVEC on d2. Results are fold change, with each value normalized to its respective control (control siRNA-treated d2 Tet-Plk4 HUVEC without DOX exposure). (E) Representative images of DOX-treated Tet-Plk4 HUVEC stained for GLB1 and pericentrin on d2. (F) Mean fluorescence intensity of GLB1 in control-siRNA treated (left) and p53-siRNA treated (right) Tet-Plk4 HUVEC with indicated centrosome numbers. Statistics, two-tailed Student's t test. Error bars, standard deviation from mean. *, $p<0.05$; **, $p<0.01$; ns, not significant.

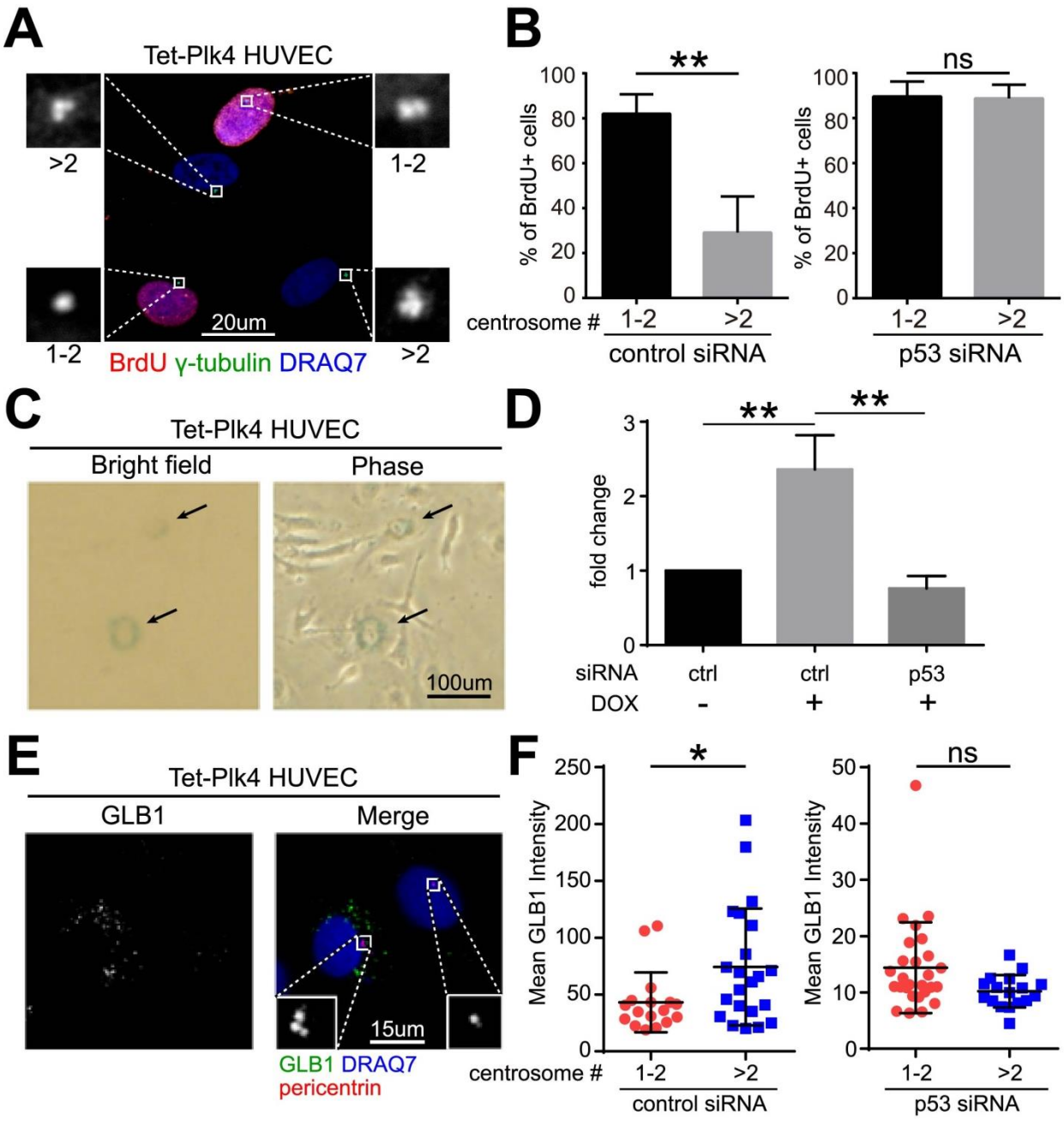
A
Tet-Plk4 HUVEC
>2
1-2
20um
1-2
>2
BrdU γ-tubulin DRAQ7
B
**
ns
% of BrdU+ cells
100
80
60
40
20
0
centrosome #
1-2
>2
control siRNA
p53 siRNA
C
Tet-Plk4 HUVEC
Bright field
Phase
100um
D
**
**
fold change
3
2
1
0
siRNA
ctrl
ctrl
p53
DOX
-
+
+
E
Tet-Plk4 HUVEC
GLB1
Merge
15um
GLB1 DRAQ7
pericentrin
F
*
ns
Mean GLB1 Intensity
250
200
150
100
50
0
50
40
30
20
10
0
centrosome #
1-2
>2
control siRNA
p53 siRNA

Figure 3.5. Excess centrosomes induce senescence markers in EC in sprouts.

(A) Representative images of sprouting EC in 3D. Tet-Plk4 HUVEC were treated with (+DOX, right) or without (-DOX, left) DOX on d-1 before embedding on d0, and stained with phalloidin. Z-stacks are depth-coded. (B) Representative images of sprout EC stained for phospho-p53 (Ser33) (pp53(S33), red) and labeled with centrin-GFP (green, centrosomes) in 3D. (C) Mean fluorescence intensity of phospho-p53 (Ser33) (pp53(S33)) in EC in sprouts. (D) Percent BrdU+ cells in Tet-Plk4 HUVEC recovered from 3D sprouts on d9. (E) Cytochemical staining of SA-β-gal in sprouting angiogenesis assay. Tet-Plk4 HUVEC were treated with DOX (+DOX) or not (-DOX). Black arrows; SA-β-gal+ EC in sprouts. (F) Relative percent SA-β-gal+ in sprouting Tet-Plk4 HUVEC with indicated treatments. Results are fold change, with each value normalized to its respective control (Tet-Plk4 HUVEC sprouts without DOX treatment). (G) Representative images of SA-β-gal+ EC coincident with EC with excess centrosomes. Centrosomes labeled with centrin-GFP. Statistics, two-tailed Student's t test (C, F), X^2 test (D). Error bars, standard deviation from mean. *, $p<0.05$; **, $p<0.01$.

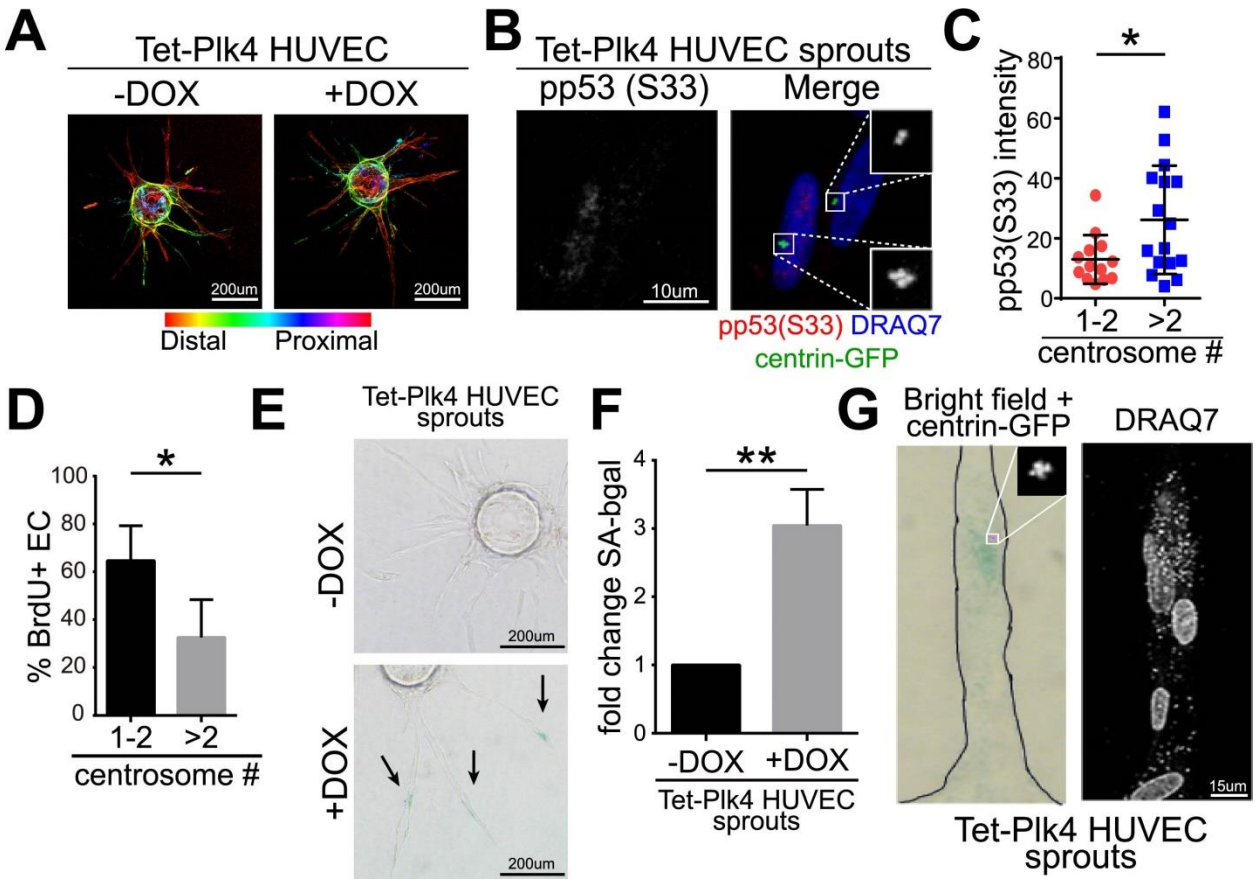
A
Tet-Plk4 HUVEC
-DOX
+DOX
200um
200um
Distal
Proximal
B
Tet-Plk4 HUVEC sprouts
pp53 (S33)
Merge
10um
pp53(S33) DRAQ7
centrin-GFP
C
*
pp53(S33) intensity
80
60
40
20
0
1-2
>2
centrosome #
D
*
% BrdU+ EC
100
80
60
40
20
0
1-2
>2
centrosome #
E
Tet-Plk4 HUVEC sprouts
-DOX
+DOX
200um
200um
F
**
fold change SA-bgal
4
3
2
1
0
-DOX
+DOX
Tet-Plk4 HUVEC sprouts
G
Bright field + centrin-GFP
DRAQ7
15um
Tet-Plk4 HUVEC sprouts

Supplementary Figure 3.1. Colocalization of centrin-GFP and γ-tubulin.

A representative image of Tet-Plk4 HUVEC with centrin-GFP (green) and γ-tubulin staining (red). Nucleus is stained with DRAQ7 (blue).

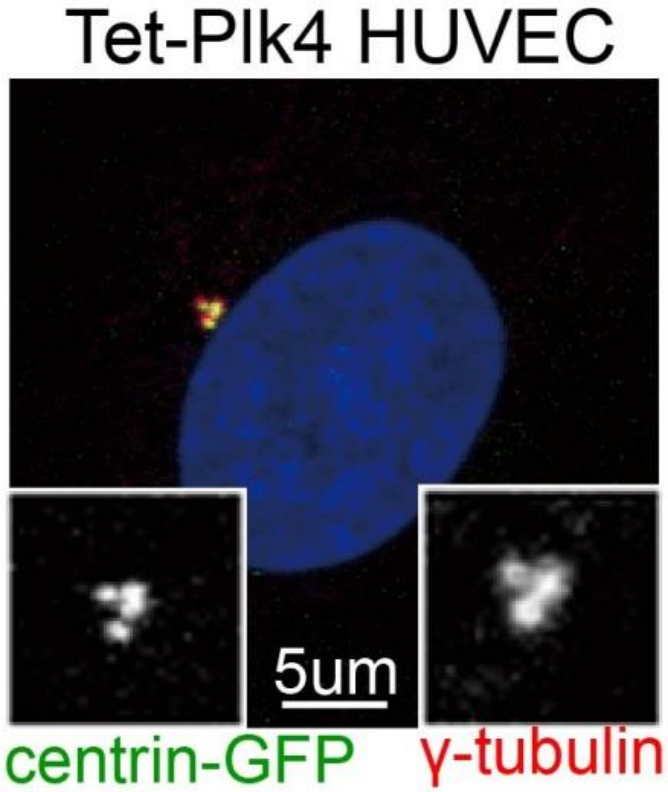
Tet-Plk4 HUVEC
5um
centrin-GFP
γ-tubulin

Supplementary Figure 3.2. Centrosome over-duplication instead of Plk4 kinase activity induces p53 phosphorylation.

(A) Mean fluorescence intensity of phospho-p53 (S33) (pp53 (S33)) in DOX-treated Tet-Plk4 or Tet-Plk4$^{1\text{-}608}$ HUVEC on d0. (B) Western blot of p53 in Tet-Plk4 HUVEC treated with control or p53 siRNA and collected on indicated days post-treatment. Statistics, two-tailed Student's t test. Error bars, standard deviation from mean. **, $p<0.01$. ****, $p<0.0001$.

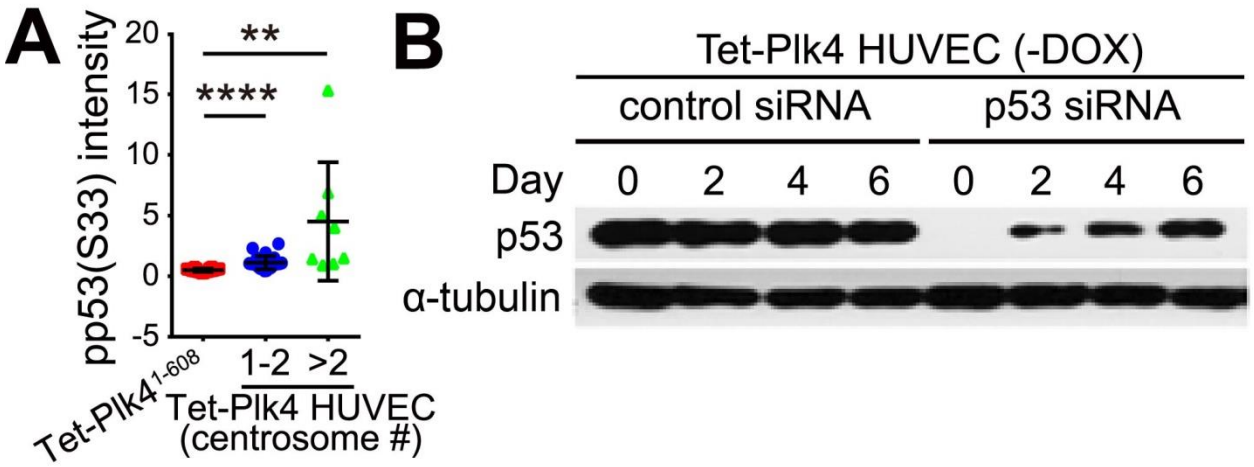
A
pp53(S33) intensity
20
15
10
5
0
-5
**
****
Tet-Plk4 1-608
1-2
>2
Tet-Plk4 HUVEC
(centrosome #)
B
Tet-Plk4 HUVEC (-DOX)
control siRNA
p53 siRNA
Day
0
2
4
6
0
2
4
6
p53
α-tubulin

Supplementary Figure 3.3. EC with excess centrosomes exhibit similar H3K9Me3 staining pattern with senescent EC.

(A) Percent BrdU+ cells in DOX-treated Tet-Plk4$^{1\text{-}608}$ or Tet-Plk4 HUVEC with 1-2 centrosomes. (B) Representative images of indicated chemical-treated HUVEC stained for SA-β-gal and H3K9Me3. Yellow dashed lines, path of line scans shown in (C, E). (C). Line scan of H3K9Me3 intensity of HUVEC with indicated treatments, normalized to respective means. (D) Percent pixels with intensity/mean >1.5 or <0.5 in each nucleus in HUVEC treated with vehicle or H_2O_2. (E) Line scan of H3K9Me3 intensity of HUVEC with indicated treatments, normalized to respective means. (F) Percent pixels with intensity/mean >1.5 or <0.5 in each nucleus in HUVEC treated with vehicle, etoposide or hydroxyurea (HU). (G) Representative images of DOX-treated Tet-Plk4 HUVEC stained for H3K9Me3 on d2. Yellow dashed lines, path of line scans shown in (H). (H) Line scan of H3K9Me3 intensity of HUVEC with indicated treatments, normalized to respective means. (I) Percent pixels with intensity/mean >1.5 or <0.5 in each nucleus in Tet-Plk4 HUVEC with 1-2 or >2 centrosomes. Statistics, two-tailed Student's t test. Error bars, standard deviation from mean. **, $p<0.01$; ***, $p<0.001$; ****, $p<0.0001$; ns, not significant.

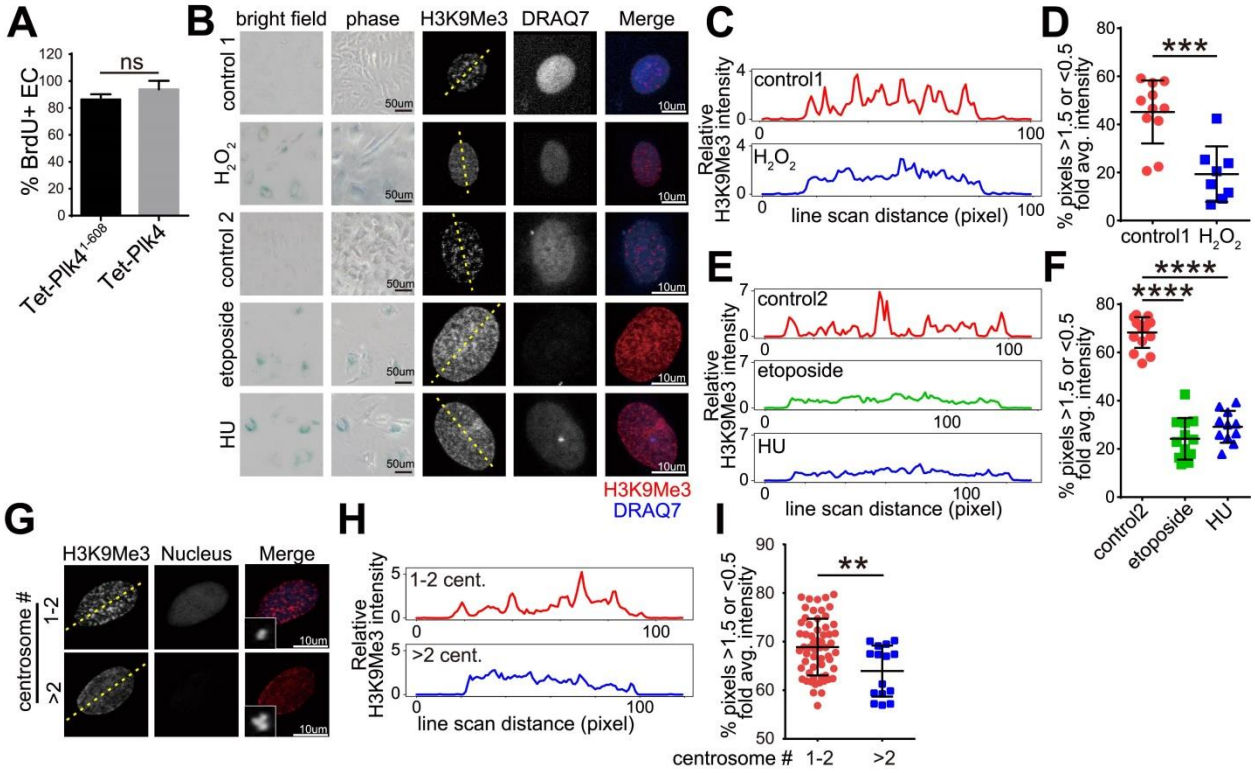
A
% BrdU+ EC
ns
Tet-Plk4 1-608
Tet-Plk4
B
bright field
phase
H3K9Me3
DRAQ7
Merge
control 1
H2O2
control 2
etoposide
HU
50um
10um
H3K9Me3
DRAQ7
C
control1
H2O2
Relative H3K9Me3 intensity
line scan distance (pixel)
D
***
% pixels >1.5 or <0.5 fold avg. intensity
control1
H2O2
E
control2
etoposide
HU
Relative H3K9Me3 intensity
line scan distance (pixel)
F
****
****
% pixels >1.5 or <0.5 fold avg. intensity
control2
etoposide
HU
G
H3K9Me3
Nucleus
Merge
centrosome #
1-2
>2
10um
H
1-2 cent.
>2 cent.
Relative H3K9Me3 intensity
line scan distance (pixel)
I
**
% pixels >1.5 or <0.5 fold avg. intensity
centrosome #
1-2
>2

Supplementary Figure 3.4. EC better maintain excess centrosome percentage in 3D sprouts than 2D.

(A) Percent excess centrosomes in Tet-Plk4 HUVEC in 2D or 3D (total) at indicated days. Cells in 3D were recovered from fibrin matrix by prolonged trypsin digestion (see methods). (B) Percent excess centrosomes in Tet-Plk4 HUVEC in 2D or 3D (sprouts) at indicated days. Excess centrosome percentage in 3D was determined via examining centrin-GFP signal *in situ* (see methods). (C) Percent phospho-histone 3+ (PH3+) cells in Tet-Plk4 HUVEC in 2D or 3D. Statistics, two-tailed Student's t test. Error bars, standard deviation from mean. ****, $p<0.001$.

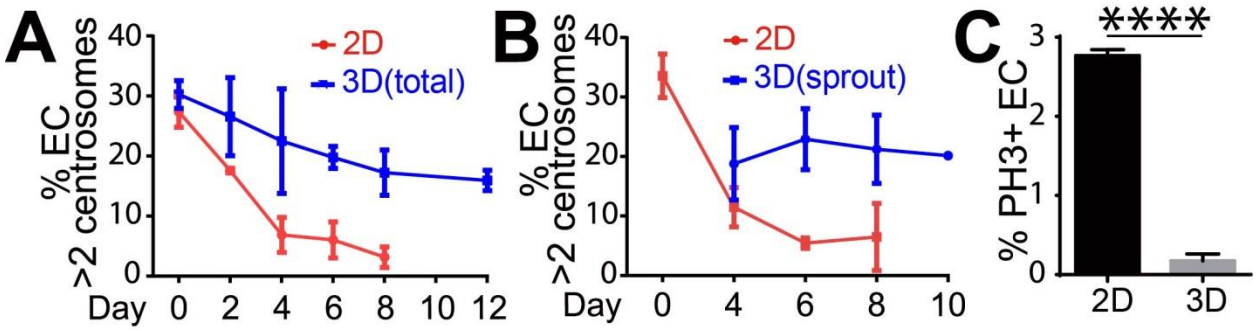
A
% EC >2 centrosomes
2D
3D(total)
Day 0 2 4 6 8 10 12
B
% EC >2 centrosomes
2D
3D(sprout)
Day 0 4 6 8 10
C
****
% PH3+ EC
2D
3D

REFERENCES

1. Yasutis KM, Kozminski KG (2013) Cell cycle checkpoint regulators reach a zillion. Cell Cycle 12: 1501-1509.

2. Kawabe T (2004) G(2) checkpoint abrogators as anticancer drugs. Molecular Cancer Therapeutics 3: 513-519.

3. Terzi MY, Izmirli M, Gogebakan B (2016) The cell fate: senescence or quiescence. Mol Biol Rep.

4. Loncarek J, Khodjakov A (2009) Ab ovo or de novo? Mechanisms of centriole duplication. Mol Cells 27: 135-142.

5. Bettencourt-Dias M, Glover DM (2007) Centrosome biogenesis and function: centrosomics brings new understanding. Nat Rev Mol Cell Biol 8: 451-463.

6. Nigg EA, Stearns T (2011) The centrosome cycle: Centriole biogenesis, duplication and inherent asymmetries. Nat Cell Biol 13: 1154-1160.

7. Nigg EA (2007) Centrosome duplication: of rules and licenses. Trends Cell Biol 17: 215-221.

8. Mikule K, Delaval B, Kaldis P, Jurcyzk A, Hergert P, et al. (2007) Loss of centrosome integrity induces p38-p53-p21-dependent G1-S arrest. Nat Cell Biol 9: 160-170.

9. Srsen V, Gnadt N, Dammermann A, Merdes A (2006) Inhibition of centrosome protein assembly leads to p53-dependent exit from the cell cycle. J Cell Biol 174: 625-630.

10. Anderhub SJ, Kramer A, Maier B (2012) Centrosome amplification in tumorigenesis. Cancer Lett 322: 8-17.

11. Godinho SA, Kwon M, Pellman D (2009) Centrosomes and cancer: how cancer cells divide with too many centrosomes. Cancer Metastasis Rev 28: 85-98.

12. Ganem NJ, Godinho SA, Pellman D (2009) A mechanism linking extra centrosomes to chromosomal instability. Nature 460: 278-282.

13. Sluder G, Thompson EA, Miller FJ, Hayes J, Rieder CL (1997) The checkpoint control for anaphase onset does not monitor excess numbers of spindle poles or bipolar spindle symmetry. J Cell Sci 110 (Pt 4): 421-429.

14. Salmon ED, Cimini D, Cameron LA, DeLuca JG (2005) Merotelic kinetochores in mammalian tissue cells. Philos Trans R Soc Lond B Biol Sci 360: 553-568.

15. Cuomo ME, Knebel A, Morrice N, Paterson H, Cohen P, et al. (2008) p53-Driven apoptosis limits centrosome amplification and genomic instability downstream of NPM1 phosphorylation. Nat Cell Biol 10: 723-730.

16. Holland AJ, Fachinetti D, Zhu Q, Bauer M, Verma IM, et al. (2012) The autoregulated instability of Polo-like kinase 4 limits centrosome duplication to once per cell cycle. Genes Dev 26: 2684-2689.

17. Kushner EJ, Ferro LS, Liu JY, Durrant JR, Rogers SL, et al. (2014) Excess centrosomes disrupt endothelial cell migration via centrosome scattering. J Cell Biol 206: 257-272.

18. Hida K, Hida Y, Amin DN, Flint AF, Panigrahy D, et al. (2004) Tumor-associated endothelial cells with cytogenetic abnormalities. Cancer Research 64: 8249-8255.

19. Taylor SM, Nevis KR, Park HL, Rogers GC, Rogers SL, et al. (2010) Angiogenic factor signaling regulates centrosome duplication in endothelial cells of developing blood vessels. Blood 116: 3108-3117.

20. Kushner EJ, Ferro LS, Yu Z, Bautch VL (2016) Excess centrosomes perturb dynamic endothelial cell repolarization during blood vessel formation. Mol Biol Cell 27: 1911-1920.

21. Roberts DM, Anderson AL, Hidaka M, Swetenburg RL, Patterson C, et al. (2004) A vascular gene trap screen defines RasGRP3 as an angiogenesis-regulated gene required for the endothelial response to phorbol esters. Mol Cell Biol 24: 10515-10528.

22. Nakatsu MN, Davis J, Hughes CC (2007) Optimized fibrin gel bead assay for the study of angiogenesis. J Vis Exp: 186.

23. Xiong Y, Hannon GJ, Zhang H, Casso D, Kobayashi R, et al. (1993) P21 Is a Universal Inhibitor of Cyclin Kinases. Nature 366: 701-704.

24. Vermeulen K, Van Bockstaele DR, Berneman ZN (2003) The cell cycle: a review of regulation, deregulation and therapeutic targets in cancer. Cell Proliferation 36: 131-149.

25. Ganem NJ, Cornils H, Chiu SY, O'Rourke KP, Arnaud J, et al. (2014) Cytokinesis failure triggers hippo tumor suppressor pathway activation. Cell 158: 833-848.

26. Guderian G, Westendorf J, Uldschmid A, Nigg EA (2010) Plk4 trans-autophosphorylation regulates centriole number by controlling betaTrCP-mediated degradation. J Cell Sci 123: 2163-2169.

27. Janssen A, van der Burg M, Szuhai K, Kops GJ, Medema RH (2011) Chromosome segregation errors as a cause of DNA damage and structural chromosome aberrations. Science 333: 1895-1898.

28. Dai C, Gu W (2010) p53 post-translational modification: deregulated in tumorigenesis. Trends Mol Med 16: 528-536.

29. Kuo LJ, Yang LX (2008) Gamma-H2AX - a novel biomarker for DNA double-strand breaks. In Vivo 22: 305-309.

30. Vousden KH, Lu X (2002) Live or let die: the cell's response to p53. Nat Rev Cancer 2: 594-604.

31. Wolf BB, Schuler M, Echeverri F, Green DR (1999) Caspase-3 is the primary activator of apoptotic DNA fragmentation via DNA fragmentation factor-45/inhibitor of caspase-activated DNase inactivation. Journal of Biological Chemistry 274: 30651-30656.

32. Rufini A, Tucci P, Celardo I, Melino G (2013) Senescence and aging: the critical roles of p53. Oncogene 32: 5129-5143.

33. Salama R, Sadaie M, Hoare M, Narita M (2014) Cellular senescence and its effector programs. Genes Dev 28: 99-114.

34. Dimri GP, Lee X, Basile G, Acosta M, Scott G, et al. (1995) A biomarker that identifies senescent human cells in culture and in aging skin in vivo. Proc Natl Acad Sci U S A 92: 9363-9367.

35. Lee BY, Han JA, Im JS, Morrone A, Johung K, et al. (2006) Senescence-associated beta-galactosidase is lysosomal beta-galactosidase. Aging Cell 5: 187-195.

36. Narita M, Nunez S, Heard E, Lin AW, Hearn SA, et al. (2003) Rb-mediated heterochromatin formation and silencing of E2F target genes during cellular senescence. Cell 113: 703-716.

37. Aird KM, Zhang R (2013) Detection of senescence-associated heterochromatin foci (SAHF). Methods Mol Biol 965: 185-196.

38. Chen Q, Ames BN (1994) Senescence-like growth arrest induced by hydrogen peroxide in human diploid fibroblast F65 cells. Proc Natl Acad Sci U S A 91: 4130-4134.

39. te Poele RH, Okorokov AL, Jardine L, Cummings J, Joel SP (2002) DNA damage is able to induce senescence in tumor cells in vitro and in vivo. Cancer Research 62: 1876-1883.

40. Yeo EJ, Hwang YC, Kang CM, Kim IH, Kim DI, et al. (2000) Senescence-like changes induced by hydroxyurea in human diploid fibroblasts. Experimental Gerontology 35: 553-571.

41. Andreassen PR, Lohez OD, Lacroix FB, Margolis RL (2001) Tetraploid state induces p53-dependent arrest of nontransformed mammalian cells in G1. Mol Biol Cell 12: 1315-1328.

42. Wong C, Stearns T (2005) Mammalian cells lack checkpoints for tetraploidy, aberrant centrosome number, and cytokinesis failure. BMC Cell Biol 6: 6.

43. Ring D, Hubble R, Kirschner M (1982) Mitosis in a cell with multiple centrioles. J Cell Biol 94: 549-556.

44. Kwon M, Godinho SA, Chandhok NS, Ganem NJ, Azioune A, et al. (2008) Mechanisms to suppress multipolar divisions in cancer cells with extra centrosomes. Genes Dev 22: 2189-2203.

45. McDonald DM, Choyke PL (2003) Imaging of angiogenesis: from microscope to clinic. Nature Medicine 9: 713-725.

46. Nagy JA, Chang SH, Dvorak AM, Dvorak HF (2009) Why are tumour blood vessels abnormal and why is it important to know? British Journal of Cancer 100: 865-869.

47. Garfinkel S, Brown S, Wessendorf JHM, Maciag T (1994) Posttranscriptional Regulation of Interleukin-1-Alpha in Various Strains of Young and Senescent Human Umbilical Vein Endothelial-Cells. Proc Natl Acad Sci U S A 91: 1559-1563.

48. Mariotti M, Castiglioni S, Bernardini D, Maier JA (2006) Interleukin 1 alpha is a marker of endothelial cellular senescent. Immun Ageing 3: 4.

CHAPTER IV-Cell-Autonomous Effects of p53 Loss on Angiogenesis[3]

A. Introduction

Blood vessel formation is dependent on angiogenesis, the process where new vessels sprout and extend from pre-existing ones. Angiogenesis is a highly coordinated program involving a series of cell migration and cell proliferation events in endothelial cells (EC), an essential component of blood vessels [1]. Many signaling pathways, such as vascular endothelial growth factor (VEGF-A) and NOTCH, participate in the regulation of angiogenesis, which is normally inactive in adults, but can be re-activated in certain situations such as wound healing or tumor progression [1,2]. Tumors are usually highly vascularized, and require tumor blood vessels for oxygen and nutrients after reaching the size of 2 mm in diameter [3]. Tumor vasculature is morphologically and functionally abnormal with tortuosity, leakiness and uneven lumens, contributing to tumor dissemination [4]. It is not completely understood how tumor vessels acquire these abnormalities, but the tumor micro-environment is believed to contribute to the defects.

p53 is a well-known cell cycle regulatory protein that senses and responds to cell stress by initiating downstream gene expression to either inhibit the cell cycle or induce cell death [5]. It is a tumor suppressor that is mutated in about half of identified tumors, indicating its critical role in controlling tumor progression. In addition to regulating cell cycle, p53 inhibits cell

[3]I performed most of the experiments. Diana Chong isolated and mounted mouse retina. Hong Lee performed the random migration assay in HUVEC treated with p53 shRNA.

migration in mouse embryonic fibroblasts [6-8], therefore likely limiting tumor cell invasion and metastasis.

p53 also regulates tumor angiogenesis in a cell non-autonomous manner. Clinical data show that tumors with mutated p53 are more vascularized than those with wild-type p53, and correlate with poor prognosis [9]. Tumor cells secrete many angiogenic factors, such as vascular endothelial growth factor-A (VEGF-A) and basic fibroblast growth factor (bFGF), into the tumor microenvironment to promote angiogenesis, and p53 can repress the expression of these factors [10]. In addition, p53 upregulates the release of a variety of antiangiogenic proteins from tumor cells, such as thromobospondin-1 (TSP-1) [11,12]. Therefore p53 mutations in tumor cells promote angiogenesis in a cell non-autonomous manner. However, the EC-autonomous effects of p53 in angiogenesis remain elusive.

Here we present the novel findings about EC-autonomous roles of p53 in angiogenesis. We found that p53 inhibits sprouting, EC migration and EC proliferation *in vitro*. Contradictory to the *in vitro* results, p53 global knockout (KO) mice had decreased angiogenesis *in vivo*, and EC-selective p53 KO did not have significant effects on angiogenesis *in vivo*.

B. Materials and Methods

Cell culture

Human umbilical vein endothelial cells (HUVEC) were cultured in endothelial cell growth media-2 (EGM-2, Lonza cc-3162). Tetracyclin-inducible Polo-like kinase 4 (Tet-Plk4) HUVEC were made as previously described [13]. Doxycycline (DOX; Sigma D9891) was added at 1 μg/ml in EGM-2 to induce centrosome over-duplication in Tet-Plk4 HUVEC. RNAi Max transfection agent (Life technologies 13778-075) was used to transfect HUVEC with non-

targeting (Life technologies 4390847) or p53 siRNA (Life technologies 4427038-s605) according to the manufacturer protocols. Control or p53 shRNA (Open Biosystems, clone ID: V3LHS_333920) were introduced into HUVEC via infection of lentiviruses purchased from the UNC Lenti-shRNA Core Facility.

Sprouting angiogenesis assay

Sprouting angiogenesis assays were performed as previously described with slight modifications [14]. Briefly, Tet-Plk4 HUVEC were mixed with Cytodex microcarrier beads, incubated and agitated at a 20-min interval for 4 hours. Beads coated with HUVEC were plated on a 6-cm dish, resuspended in 2 mg/ml fibrinogen (Fisher Scientific 820224) in PBS the next day, and embedded in a fibrin matrix by adding thrombin (Sigma T7201). Human lung fibroblasts (Lonza cc2512) were plated on top of fibrin, and EGM-2 medium was changed every other day. HUVEC cells were cultured in fibrin for 6 days, fixed with 4% paraformaldehyde, stained with phalloidin (Invitrogen A-12381), and imaged using an Olympus FV1200 microscope with a 10X objective. Images were analyzed using ImageJ.

Cell migration assay

Random cell migration assay were performed as previously described [15]. HUVEC, infected with shRNA viruses or transfected with siRNA, were seeded on a glass-bottom dish coated with 2 μg/ml fibronectin (Sigma F2006). Cells were live-imaged at 5 min intervals for 3 hours using an Olympus FV1200 microscope with a 20X objective. Images were acquired with a DIC filter, and cell tracks were analyzed with mTrackJ software (Meijering Laboratory).

Mouse strains and tissue preparations

All experiments involving animals were performed with the approval of the University of North Carolina, Chapel Hill Institutional Animal Care and Use Committee. The p53 KO mice were purchased from The Jackson Laboratory (#002101), and retinas were harvested at P4 or P5. To induce EC-selective p53 KO, p53 flox mice ($p53^{fl/fl}$; JAX #008462) were mated to Cdh5-$Cre^{ERT2+/-}$ mice (JAX #006137), and tamoxifen was injected at a dose of 0.25 mg/mL at P1 and P2, with retinas harvested at P5. Retinas were fixed, processed and stained with Alexa Fluor 488-conjugated isolectin (Invitrogen I21411) as previously described [16]. Images were acquired using an Olympus FV1200 microscope with a 10X objective, and analyzed using ImageJ.

C. Results

Down-regulation of p53 in EC induces angiogenesis in vitro

To determine the EC autonomous effects of p53 on angiogenesis, we reduced p53 levels in EC via siRNA knock-down (KD) and performed 3D sprouting angiogenesis assays. p53 siRNA-treated HUVEC had increased sprouting, demonstrated by more and longer sprouts than controls **(Fig. 4.1A-C)**. We previously showed that excess centrosomes in EC compromise angiogenesis [13]. To determine if p53 knockdown rescues excess centrosomes-induced angiogenesis defects, Tet-Plk4 HUVEC, which lead to centrosome over-duplication with doxycycline (DOX) treatment, were transfected with p53 siRNA. DOX treatment did not significantly reduce sprout number/bead or sprout length **(Fig. 4.1D-E)**, which is not consistent with previous results probably due to different methods [13]. However, Tet-Plk4 HUVEC treated with p53 siRNA had more and longer sprouts than EC with control siRNA **(Fig. 4.1D-E)**. We also validated our finding with p53 shRNA, which led to more and longer sprouts compared with

control (**Fig. 4.1F**). Overall, we find that knockdown of p53 in EC induces sprouting, suggesting a cell-autonomous effect of p53 on angiogenesis.

Down-regulation of p53 promotes EC migration and proliferation

Angiogenesis is dependent on cell migration, and p53 inhibits cell migration in mouse embryonic fibroblasts [6]. To understand the mechanisms of p53 loss-induced sprouting, we first investigated the effects of p53 loss on EC migration. Down-regulation of p53 by shRNA increased the migration distance in random migration assays **(Fig. 4.2A-B)**. Similarly, p53 siRNA treatment significantly induced cell migration compared with control siRNA **(Fig. 4.2C)**, indicating that p53 knockdown promotes sprouting by increasing cell migration. p53 is also known as a critical cell cycle suppressor [5]. To determine if cell proliferation contributes to p53 loss-induced sprouting, we analyzed HUVEC growth curves and found that HUVEC treated with p53 siRNA had increased growth relative to controls **(Fig. 4.2D)**. Collectively, these results suggest that loss of p53 promotes sprouting by increasing cell migration and proliferation.

Knockout of p53 does not promote angiogenesis in vivo

To determine if loss of p53 induces angiogenesis *in vivo,* we examined sprouting and branching in postnatal mouse retina vessels (**Fig 4.3A**). We analyzed sprout number at the vascular front and the branch number near the vascular front in wild-type (WT, $p53^{+/+}$), p53 heterozygous ($p53^{+/-}$) and p53 KO ($p53^{-/-}$) B6 mice. We found that the sprouting and branching parameters in $p53^{+/-}$ mice retina were not significantly different from those in WT retina, while P5 $p53^{-/-}$ retina had less sprouts/mm at the front compared to the P5 $p53^{+/-}$ retinas (**Fig 4.3B-C**). In addition, P4 and P5 $p53^{-/-}$ retinas had decreased branch numbers compared with P4 and P5

$p53^{+/-}$ retinas, respectively (**Fig 4.3D-E**). These results indicate that loss of p53 inhibits angiogenesis *in vivo* in the mouse retina, which is not consistent with our *in vitro* data.

We reasoned that loss of p53 in other cell types besides EC led to the decreased angiogenesis *in vivo*. To test this, we generated EC-selective p53 conditional KO mice by crossing Cdh5-$Cre^{ERT2+/-}$ mice with $p53^{fl/fl}$ mice, and injected tamoxifen at P1 and P2 to induce recombination-mediated p53 excision in EC. EC-selective p53 KO did not have significant effects on the retinal vasculature at P5, indicating that EC-autonomous KO of p53 do not affect EC angiogenesis *in vivo* (**Fig 4.3F-G**).

D. Discussion

Mutated p53 induces angiogenesis in a cell non-autonomous manner [10], but it is not known whether mutated p53 in EC have cell-autonomous effects on angiogenesis. Here we show that knockdown of p53 in EC induces sprouting *in vitro*, likely through increased EC migration and EC proliferation. Contradictory to the *in vitro* results, global p53 global deletion inhibited angiogenesis *in vivo*, and EC-selective p53 KO did not have apparent effects on retinal angiogenesis *in vivo*.

Tumor vessels, although morphologically and phenotypically abnormal, are required for tumor growth, and tumor angiogenesis is considered a hallmark of cancer [17]. One mechanism for the high vascularization of tumors may depend on lost/mutated p53, which happens in about 50% of tumors and contributes to tumor vascularization in a cell non-autonomous manner [10,18]. Tumor EC were considered genetically normal until recent evidence showed that p53 signaling is also compromised in tumor stromal cells, including tumor EC [19]. However, the effects of compromised p53 in tumor EC are unknown. Here we show that knockdown of p53 in

EC promotes angiogenic sprouting *in vitro*, indicating that compromised p53 signaling in tumor EC may contribute to tumor angiogenesis in a cell autonomous manner.

We found that p53 knockdown promotes EC migration and proliferation, two essential components of angiogenesis. These results are consistent with previous findings that loss of p53 increases cell migration in mouse embryonic fibroblasts (MEF) [6-8], and the fact that p53 inhibits cell cycle [5]. The next step will be focused on understanding the mechanisms of p53 loss-induced EC migration and proliferation in EC. p53 loss-induced increased MEF migration is dependent on increased Rho signaling and decreased cell-cell junction [8], and it is likely that the same mechanisms exist in EC.

Although we found increased sprouting induced by p53 knockdown *in vitro*, we did not identify these effects of p53 *in vivo*. p53 global KO mice had reduced postnatal retinal angiogenesis compared to controls, and EC-selective p53 deletion mice were not different from controls in retinal angiogenesis. It is possible that retina angiogenesis reflects a distinct physiological developmental process that differs from tumor. To test this hypothesis, we will cross EC-selective p53 KO mice to a transgenic mouse that develops spontaneous tumors, such as MMTV-PyMT mice which develop spontaneous breast tumors, and examine tumor vessel density. We hypothesize to see higher vascularization in EC-selective p53 KO tumors.

In summary, we found that loss of p53 induces sprouting *in vitro*, likely via increased EC migration and proliferation in a cell autonomous manner, but does not affect retinal angiogenesis *in vivo* when deleted in EC. Future work will focus on understanding the mechanisms.

E. Figures

Figure 4.1. Down-regulation of p53 in EC induces angiogenesis *in vitro*.

(A) Representative images of sprouting HUVEC. HUVEC were transfected with control siRNA or p53 siRNA. Z-stacks are depth-coded. (B) Mean sprout number/bead of wild-type (WT) HUVEC treated with control or p53 siRNA. (C) Average length of WT HUVEC sprout treated with control or p53 siRNA. (D) Mean sprout number/bead of Tet-Plk4 HUVEC treated as indicated. (E) Average length of Tet-Plk4 HUVEC sprout treated as indicated. (F) Representative images of sprouting WT HUVEC treated with control shRNA or p53 shRNA (p53#20). Statistics: unpaired two-tailed Student's t test. ns, not significant; *, $p<0.05$; **, $p<0.01$; ***, $p<0.001$; ****, $p<0.0001$.

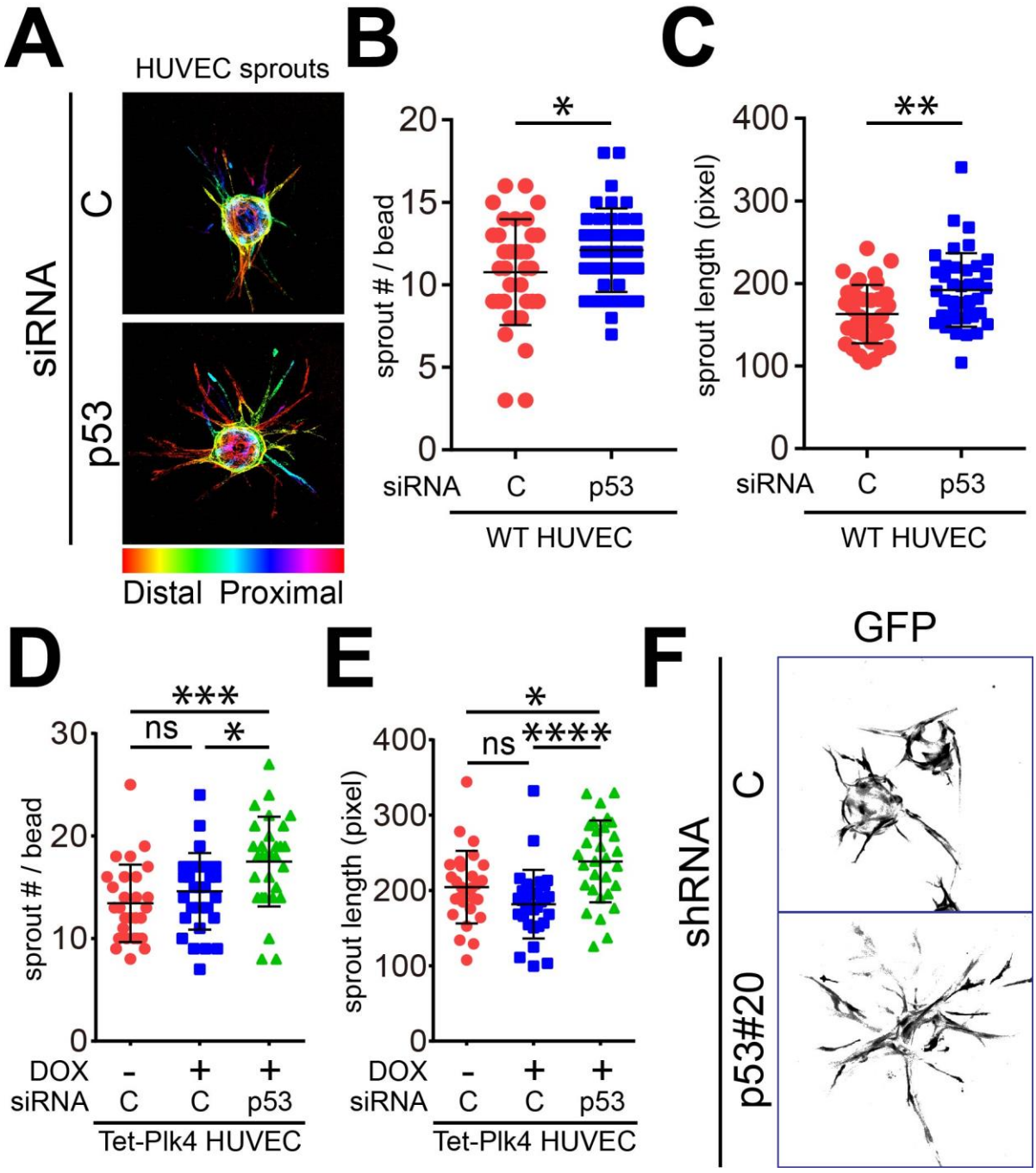
A
HUVEC sprouts
siRNA
C
p53
Distal Proximal
B
sprout # / bead
20
15
10
5
0
*
siRNA C p53
WT HUVEC
C
sprout length (pixel)
400
300
200
100
0
**
siRNA C p53
WT HUVEC
D
sprout # / bead
30
20
10
0
***
ns
*
DOX - + +
siRNA C C p53
Tet-Plk4 HUVEC
E
sprout length (pixel)
400
300
200
100
0
*
ns
****
DOX - + +
siRNA C C p53
Tet-Plk4 HUVEC
F
GFP
shRNA
C
p53#20

Figure 4.2. Knockdown of p53 promotes cell migration and proliferation.

(A) Representative random migration tracks of HUVEC treated with control shRNA or p53 shRNA (p53#19 or p53#20). (B) Migration distance of HUVEC treated with control shRNA or p53 shRNA. (C) Migration distance of HUVEC treated with control siRNA or p53 siRNA. (D) Density of HUVEC treated with control siRNA or p53 siRNA on indicated days. Statistics: unpaired two-tailed Student's t test (B, C) or two-way ANOVA (D). **, $p<0.01$; ****, $p<0.0001$; ns, not significant.

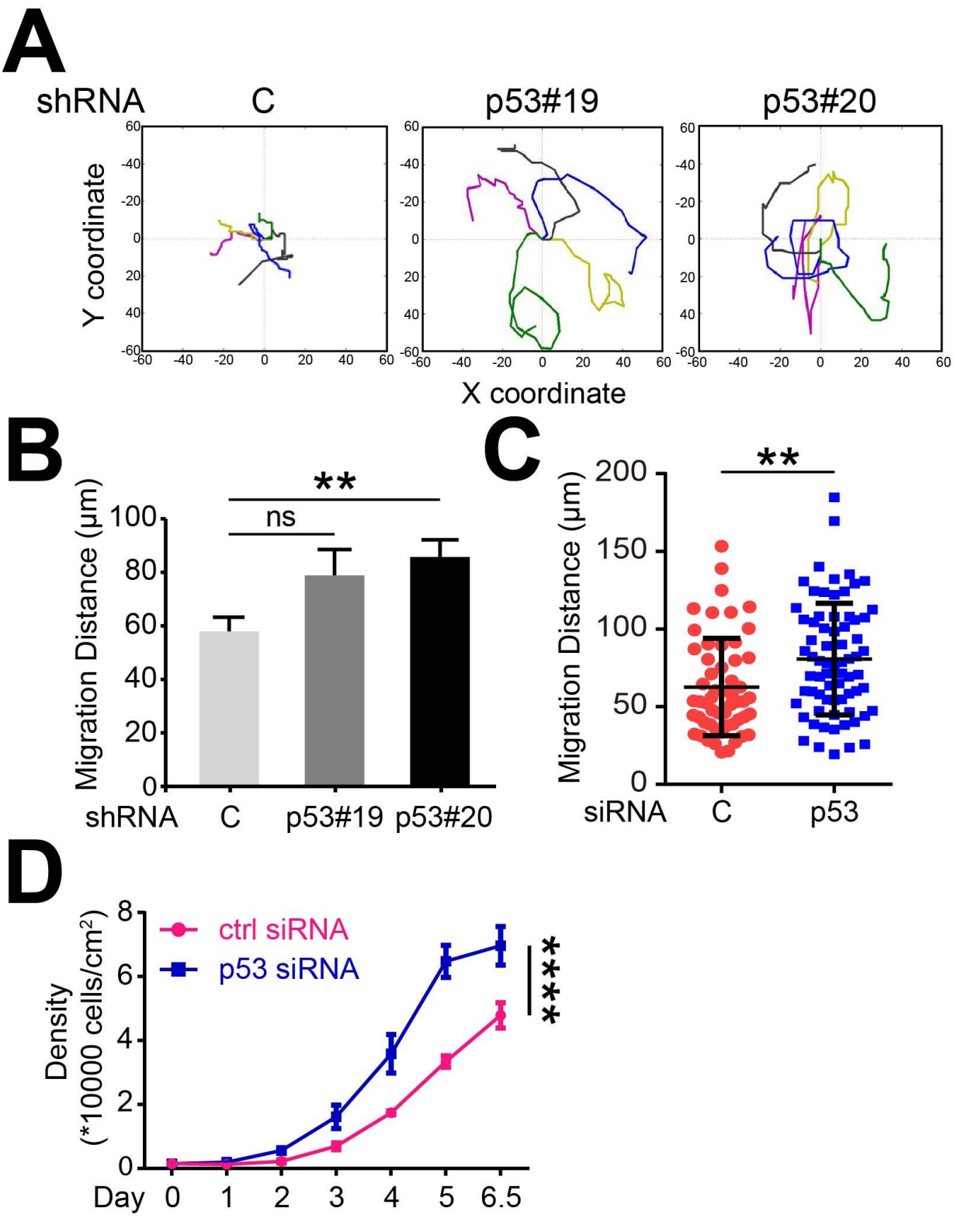
A
shRNA
C
p53#19
p53#20
Y coordinate
X coordinate
B
Migration Distance (μm)
**
ns
shRNA
C
p53#19
p53#20
C
Migration Distance (μm)
**
siRNA
C
p53
D
Density
(*10000 cells/cm²)
ctrl siRNA
p53 siRNA
****
Day

Figure 4.3. Knockout of p53 does not promote angiogenesis *in vivo*.

(A) Representative images of retina from P5 mice with indicated genotypes. (B,C) Sprout number/mm in P4 (B) or P5 (C) retina with indicated p53 genotypes. (D,E) Branch number/mm in P4 (D) or P5 (E) retina with indicated p53 genotypes. (F,G) Sprouting (F) or branching (G) parameter in P5 retina with indicated genotypes. Mice were injected with 0.25 mg/mL tamoxifen at P1 and P2. Statistics: unpaired two-tailed Student's t test. ****, $p<0.0001$; ns, not significant.

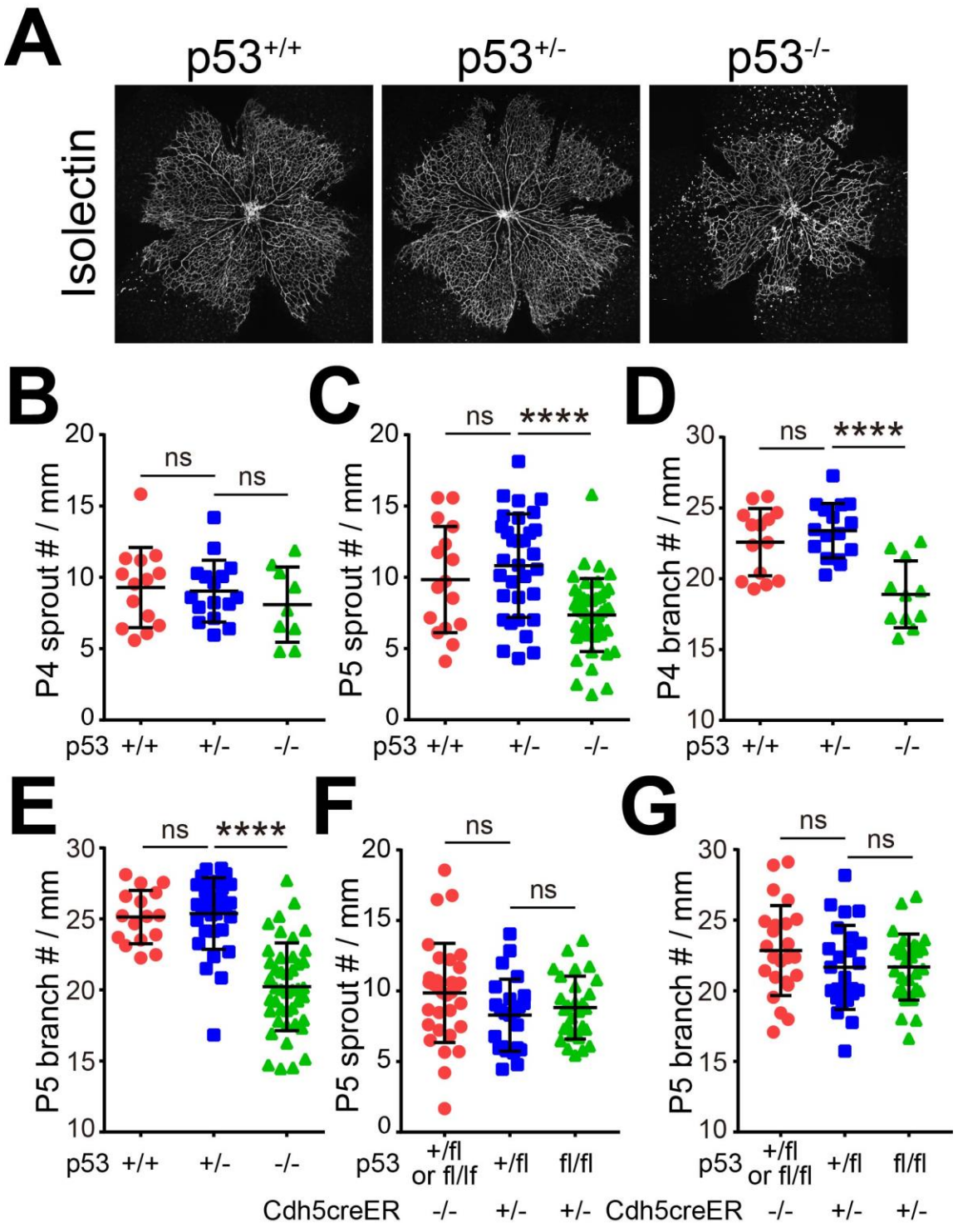
A
p53+/+
p53+/-
p53-/-
Isolectin
B
P4 sprout # / mm
ns
ns
p53 +/+ +/- -/-
C
P5 sprout # / mm
ns
****
p53 +/+ +/- -/-
D
P4 branch # / mm
ns
****
p53 +/+ +/- -/-
E
P5 branch # / mm
ns
****
p53 +/+ +/- -/-
F
P5 sprout # / mm
ns
ns
p53 +/fl or fl/lf +/fl fl/fl
Cdh5creER -/- +/- +/-
G
P5 branch # / mm
ns
ns
p53 +/fl or fl/fl +/fl fl/fl
Cdh5creER -/- +/- +/-

REFERENCES

1. Potente M, Gerhardt H, Carmeliet P (2011) Basic and therapeutic aspects of angiogenesis. Cell 146: 873-887.

2. Carmeliet P, Jain RK (2011) Molecular mechanisms and clinical applications of angiogenesis. Nature 473: 298-307.

3. Kerbel RS (2000) Tumor angiogenesis: past, present and the near future. Carcinogenesis 21: 505-515.

4. Narang AS, Varia S (2011) Role of tumor vascular architecture in drug delivery. Adv Drug Deliv Rev 63: 640-658.

5. Chen JD (2016) The Cell-Cycle Arrest and Apoptotic Functions of p53 in Tumor Initiation and Progression. Cold Spring Harb Perspect Med 6.

6. Guo F, Gao Y, Wang L, Zheng Y (2003) p19Arf-p53 tumor suppressor pathway regulates cell motility by suppression of phosphoinositide 3-kinase and Rac1 GTPase activities. Journal of Biological Chemistry 278: 14414-14419.

7. Wang B, Feng P, Xiao ZW, Ren EC (2009) LIM and SH3 protein 1 (Lasp1) is a novel p53 transcriptional target involved in hepatocellular carcinoma. Journal of Hepatology 50: 528-537.

8. Muller PA, Vousden KH, Norman JC (2011) p53 and its mutants in tumor cell migration and invasion. J Cell Biol 192: 209-218.

9. Gasparini G, Weidner N, Bevilacqua P, Maluta S, Dallapalma P, et al. (1994) Tumor Microvessel Density, P53 Expression, Tumor Size, and Peritumoral Lymphatic Vessel Invasion Are Relevant Prognostic Markers in Node-Negative Breast-Carcinoma. Journal of Clinical Oncology 12: 454-466.

10. Teodoro JG, Evans SK, Green MR (2007) Inhibition of tumor angiogenesis by p53: a new role for the guardian of the genome. Journal of Molecular Medicine-Jmm 85: 1175-1186.

11. Alvarez AA, Axelrod JR, Whitaker RS, Isner PD, Bentley RC, et al. (2001) Thrombospondin-1 expression in epithelial ovarian carcinoma: association with p53 status, tumor angiogenesis, and survival in platinum-treated patients. Gynecol Oncol 82: 273-278.

12. Sundaram P, Hultine S, Smith LM, Dews M, Fox JL, et al. (2011) p53-responsive miR-194 inhibits thrombospondin-1 and promotes angiogenesis in colon cancers. Cancer Research 71: 7490-7501.

13. Kushner EJ, Ferro LS, Yu Z, Bautch VL (2016) Excess centrosomes perturb dynamic endothelial cell repolarization during blood vessel formation. Mol Biol Cell 27: 1911-1920.

14. Nakatsu MN, Davis J, Hughes CC (2007) Optimized fibrin gel bead assay for the study of angiogenesis. J Vis Exp: 186.

15. Kushner EJ, Ferro LS, Liu JY, Durrant JR, Rogers SL, et al. (2014) Excess centrosomes disrupt endothelial cell migration via centrosome scattering. J Cell Biol 206: 257-272.

16. Pelton JC, Wright CE, Leitges M, Bautch VL (2014) Multiple endothelial cells constitute the tip of developing blood vessels and polarize to promote lumen formation. Development 141: 4121-4126.

17. Hanahan D, Weinberg RA (2011) Hallmarks of cancer: the next generation. Cell 144: 646-674.

18. Vogelstein B, Lane D, Levine AJ (2000) Surfing the p53 network. Nature 408: 307-310.

19. Dudley AC, Shih SC, Cliffe AR, Hida K, Klagsbrun M (2008) Attenuated p53 activation in tumour-associated stromal cells accompanies decreased sensitivity to etoposide and vincristine. Br J Cancer 99: 118-125.

CHAPTER V-General Discussion

A. Summary

Tumors with a diameter larger than 2 mm require blood vessels to deliver oxygen and nutrients for their survival [1], and tumor angiogenesis is considered as a hallmark of cancer [2]. Tumor vasculature is phenotypically and functionally abnormal, and recently tumor EC, which are an important component of tumor vasculature, were identified with cytogenetic abnormalities including aneuploidy, compromised p53 signaling and centrosome over-duplication [3-5], indicating that tumor EC possess unstable genetic information, which may contribute to their morphological and functional abnormalities. However, it is not entirely clear what are the causes and effects of excess centrosomes and abrogated p53 signaling in tumor EC. Previous results from our lab demonstrated that excess levels of VEGF-A induce centrosome over-duplication in EC [6]. However, it is not clear whether and how other tumor environmental factors contribute to centrosome over-duplication.

Here we show that high levels of BMP2/6/7, hypoxia and loss of p53 promote centrosome over-duplication, suggesting that the high percentage of excess centrosomes in tumor EC comes from a combination of several signaling inputs. We also show that excess centrosomes induce p53-dependent senescence in primary EC. This result indicates that the response to centrosome over-duplication is dependent on the transformation status of the cells, and excess centrosome-induced senescence contributes to the morphological and functional abnormalities of tumor vasculature. In addition, we investigated the potential effects of compromised p53 signaling in tumor EC, and found that knockdown of p53 contributes to angiogenesis in a cell

autonomous manner *in vitro*. In summary, my work promotes the understanding of centrosome over-duplication in tumor EC, and contributes to the study on tumor microenvironment.

B. Tumor-derived factors promote excess centrosomes

~30% of tumor EC are centrosome over-duplicated [3,5], likely because of the signaling input from tumor microenvironment, which is a complex milieu consisted of different cell types, growth factors and cytokines [7,8]. Previous studies in our lab demonstrated that high levels of VEGF-A induce excess centrosomes in EC, but the frequency of excess centrosomes induced by VEGF-A only (<10%) is significantly lower than that in primary tumor EC (~30%) [6]. Therefore other environmental/genetic factors may also contribute to centrosome over-duplication. In Chapter II, I tested the effects of reduced p53 and several tumor environmental factors, including high levels of BMP2/6/7, hypoxia and inflammation, on centrosome over-duplication in EC.

I found that elevated levels of some BMP ligands, similar to high levels of VEGF and FGF ligands, induce excess centrosomes in EC. The mechanisms downstream of these ligands-induced excess centrosomes are likely very complex, since each of these ligands has multiple targets, and can activate several signaling pathways. One potential target is ERK, which VEGF-A and BMP pathways may share to induce excess centrosomes. Our previous data showed that VEGF-mediated effects were ERK-dependent [6], and BMP also up-regulates ERK [9]. Therefore it is likely that some of the signaling pathways downstream of VEGF and BMP converge to induce excess centrosomes. Alternatively, these two pathways may have some different targets, one of which can be SMAD that is correlated with centrosome over-duplication status as I showed in Chapter II. Future work will examine the different and/or shared signaling

pathways downstream of VEGF-A and BMP. First, although I demonstrated the correlation between SMAD phosphorylation and excess centrosomes, it is essential to test whether it is required and/or sufficient to drive excess centrosomes. Second interesting question is whether ERK is downstream of SMAD in terms of BMP-induced excess centrosomes. Finally, it will be interesting to test whether VEGF and BMP can additively or even synergistically promote excess centrosomes.

Tumors are highly vascularized, but in a hypoxic state because tumor blood vessels are functionally abnormal [10,11]. Here I show that hypoxia can induce centrosome over-duplication in EC, and this is the first study linking cell metabolism with centrosome over-duplication. I also demonstrate that hypoxia-induced excess centrosomes in a VEGF-A-independent manner, suggesting that there is a cell-autonomous effect of hypoxia on centrosome over-duplication. Future studies will focus on understanding the mechanisms of hypoxia-induced centrosome over-duplication, and several candidates, including Aurora kinase A and miR-210, are potentially involved. Aurora kinase A is activated in hypoxia-mimetic conditions [12], and its ectopic overexpression leads to centrosome over-duplication [13,14]. Over-expression of miR-210, which is a downstream target of hypoxia-inducible factors, also causes centrosome over-duplication [15]. One will need to express Aurora kinase A siRNA or anti-sense oligonucleotide of miR-210 to test their effects on centrosome over-duplication in EC [16].

C. Excess centrosomes induce p53-dependent senescence

Results from Chapter II provide several potential mechanisms of excess centrosomes in tumor EC. Our previous results demonstrated that excess centrosomes in EC disrupt cell migration, polarity and sprouting behavior, indicating that excess centrosomes may account for

the morphological and functional abnormalities of tumor vasculature [5,17]. However, centrosome is closely associated with cell cycle, and the effects of excess centrosomes on EC cycle remain elusive. Interestingly, we observed that isolated tumor EC cannot maintain a high percentage of excess centrosomes, indicating a negative impact of excess centrosomes on EC cell cycle [5]. Here we show that excess centrosomes activate the tumor suppressor gene p53 in a DNA damage-independent manner, and lead to the phosphorylation of p53 at Ser33. Activation of p53 further induces senescence, but not apoptosis, in both 2D cultured EC and 3D EC sprouts.

Before my work, several independent studies with different methods demonstrated cells have a p53-dependent surveillance mechanism for loss of centrosomes. By knocking down various centrosomal structure proteins, Mikule et al showed that loss of centrosome integrity-induced p53-dependent cell cycle arrest [18]. A similar study indicates that inhibition of centrosome assembly by silencing pericentrin leads to p53-dependent senescence [19]. Meanwhile, chemical and genetic inhibition of Plk4, which is required for centrosome duplication, activates p53 and induces senescence [20,21]. However, it has been controversial whether cells have a surveillance mechanism for centrosome over-duplication. A originally proposed p53-dependent “tetraploidy” checkpoint downstream of drug-induced excess centrosomes and subsequent cytokinesis failure was later found to be a side effects of drug overdose [22,23]. Moreover, cells with excess centrosomes often cluster centrosomes and undergo bipolar cell divisions to produce viable progeny [17,24], indicating that in some scenarios cells may tolerate centrosome over-duplication and survive. Nevertheless, recent evidence suggests that excess centrosomes can induce p53-dependent cell cycle arrest [25,26]. Here we use primary human EC to show that excess centrosomes lead to p53 phosphorylation at Ser33 and senescence in EC, indicating that EC have a surveillance mechanism for centrosome

over-duplication, similar to that for loss of excess centrosomes. Future work will be needed to test whether primary cells other than EC have similar surveillance mechanisms for excess centrosomes. For example, it is possible that primary epithelial cells also activate p53 upon centrosome over-duplication. This hypothesis is consistent with the fact that excess centrosomes are linked with a variety of tumors, which presumably lose this checkpoint mechanism during tumor development [27]. In addition, I used a tetracycline-inducible system to over-express Plk4 to induce excess centrosomes as published previously [17]. To generalize my finding, future work will need to use other methods to promote excess centrosomes.

Previous results showed that centrosome over-duplication can cause chromosome segregation errors, which induce DNA damage and activate p53[24,28,29]. However, here we show that centrosome over-duplication did not induce DNA damage, evidenced by the lack of p53 phosphorylation at Ser15 and lack of γH2AX. This finding indicates that DNA damage is not the reason for excess centrosome-induced senescence, unlike most conditions such as proliferative senescence [30] and oncogenic protein-induced premature senescence [31]. Meanwhile and more importantly, the absence of DNA damage suggests that centrosome over-duplicated cells undergo cell cycle arrest before mitosis, thus avoiding mitotic events that potentially lead to chromosome segregation problems. This idea is consistent with the finding that mitotic events are not required for loss of centrosome integrity-induced cell cycle arrest [18]. Therefore, the surveillance mechanism for centrosome abnormality may exist in interphase. This can be advantageous to cells because arresting cells in interphase will significantly reduce the possibility of generating tumorigenic mutations. Future work will be needed to test this hypothesis. One experiment can be first arresting cells at the beginning of S phase by double

thymidine block, then inducing the expression of Plk4 and measuring the levels of phosphorylated p53 (Ser33) at different time points.

The mechanisms of excess centrosome-induced p53-dependent senescence remains elusive, but several studies provided potential targets, including p38 mitogen-activated protein kinase (MAPK) and hippo pathway, to investigate. Loss of centrosome integrity-induced p53 phosphorylation at Ser33 is dependent on p38 MAPK [18]. In addition, p38 MAPK mediates oncogene-induced senescence partially by inducing p53 phosphorylation at Ser33 [32]. Therefore it is likely that excess centrosomes also activate p38 MAPK to phosphorylate p53 at Ser33, finally leading to EC senescence.

Evidence suggests that the Hippo pathway is another potentially important mechanism, particularly LATS2 which is a serine/threonine kinase mediating Hippo signaling. The core Hippo pathway is a kinase cascade, in which MST1/2 (Hpo) phosphorylates Lats1/2 (Wts) that further phosphorylates YAP/TAZ (Yki), leading to the cytoplasmic retention or degradation of YAP/TAZ [33]. Dephosphorylated YAP/TAZ enters nuclei and promotes gene expression by interacting with transcription factors [33]. Evidence suggests that LATS2 may be involved in excess centrosome-induced p53-dependent senescence. First, LATS2 localizes at centrosomes [34], suggesting LATS2 can directly detect centrosome alterations and initiate downstream signaling. In addition, LATS2 is closely involved in cell cycle regulation, and limits centrosome over-duplication. *Lats2*$^{-/-}$ embryos and mouse embryonic fibroblasts display centrosome over-duplication and genomic perturbations [35], and LATS2 is also phosphorylated by Aurora-A kinase [34], which is important for centrosome duplication [13]. Thirdly, LATS2 and p53 are associated with each other. LATS2 stabilizes p53 by inhibiting its E3 ligase MDM2, and perturbation of centrosome function leads to the translocation of LATS2 from centrosome to

nucleus and the accumulation of p53 [36]. Meanwhile, accumulation of p53 promotes LATS2 expression, creating a positive feedback loop [36]. Furthermore, down-regulation of LATS2 abrogates oncogenic Ras-induced p53-dependent senescence, indicating an important role of LATS2 in senescence [37]. Finally, cytokinesis failure, which leads to excess centrosomes, activates LATS2, leading to the stabilization of p53, further suggesting that LATS2 is a mediator in excess centrosomes-induced p53-dependent senescence [38]. Based on all previous results, I hypothesize that change in centrosome number and/or structure induces LATS2 translocation from centrosomes to nucleus, leading to an accumulation of p53 and p53-dependent senescence. Future work will be needed to test this hypothesis.

Another important implication from my study is about the phosphorylation of p53. p53 have many different post-translational modifications (PTM) that are closely associated with the regulation and functions of p53 [39]. For example, the phosphorylation at Ser15 is induced by DNA damage, and activates p53-regulated gene expression [40]. Here we show that centrosome over-duplication induced p53 phosphorylation at Ser33 but not Ser15, coinciding with senescence. Consistent with our results, other studies also linked p53 Ser33 phosphorylation with senescence. Loss of centrosome integrity activates p53 phosphorylation at Ser33, and leads to senescence [18,19]. In addition, oncogenic Ras induces p53 Ser33 phosphorylation and senescence simultaneously [32]. Therefore, p53 Ser33 phosphorylation may be specifically associated with senescence. Future experiments are required for testing this relationship. One method is to use CRISPR to mutate serine 33 of p53 to alanine, and to detect whether Ser33 is required for p53-dependent senescence under several stresses. In parallel, one can generate a phospho-mimetic mutant of p53 by mutating serine 33 to aspartic acid, and examine whether this mutant is sufficient to induce senescence. Downstream targets of phosphorylated p53 at Ser33

need to be identified by biochemical methods and/or bioinformatics to fully understand the pathway.

D. A hypothesized model for the development of abnormal tumor vasculature

My dissertation mainly illustrates the causes and effects of excess centrosomes in EC, and found that several environmental factors induce excess centrosomes, which lead to p53-dependent senescence **(Fig. 5.1)**. Based on previous literature and my dissertation work, here I hypothesize a model to explain how tumor vasculature develops and becomes abnormal. Tumors that are larger than 2 mm in diameter cannot acquire enough resources for their growth, and recruit normal surrounding blood vessels by secreting various angiogenic factors, such as VEGF-A, bFGF, BMP2/6/7. Normal blood vessels penetrate into tumors, encountering a hypoxic and excessive growth factor-filling tumor microenvironment, which induces centrosome over-duplication in EC. This leads to p53-dependent senescence in tumor EC, serving as a protective mechanism to prevent genetic alterations in centrosome over-duplicated tumor EC and to maintain tumor blood vessel integrity. However, senescence potentially compromises EC functions, leading to a leaky, tortuous and functionally compromised tumor vasculature, and aggravating tumor hypoxia. Meanwhile, senescent EC contribute to the inflammation in tumor microenvironment, potentially creating a more suitable environment for EC to develop excess centrosomes. Through mechanisms that are not completely understood, some senescent EC develop p53 mutations/attenuation and maybe other genetic alterations, allowing centrosome over-duplicated EC to reinitialize cell cycle and to proliferate. Unfortunately during mitosis, cells with excess centrosomes have high potential to form multi-polar spindle or merotelic attachment, which results in the accumulation of genetic variations, further contributing to the abnormal

structure and function in tumor vasculature. The abrogated p53 signaling also generates a selection advantage for tumor EC so that many tumor EC have both centrosome over-duplication and abrogated p53 signaling. Together, these effects lead to cytogenetic and phenotypical abnormalities in tumor vasculature, and may also help tumor EC develop drug resistance, reducing the efficiency of anti-angiogenic therapies.

E. Figure

Figure 5.1. Causes and effects of excess centrosomes in EC

EC, which line the inner surface of blood vessels, acquire excess centrosomes upon stimulation of several environmental factors including high BMP2/6/7, high VEGF and hypoxia. Excess centrosomes in EC lead to p53 activation, and finally induce p53-dependent senescence.

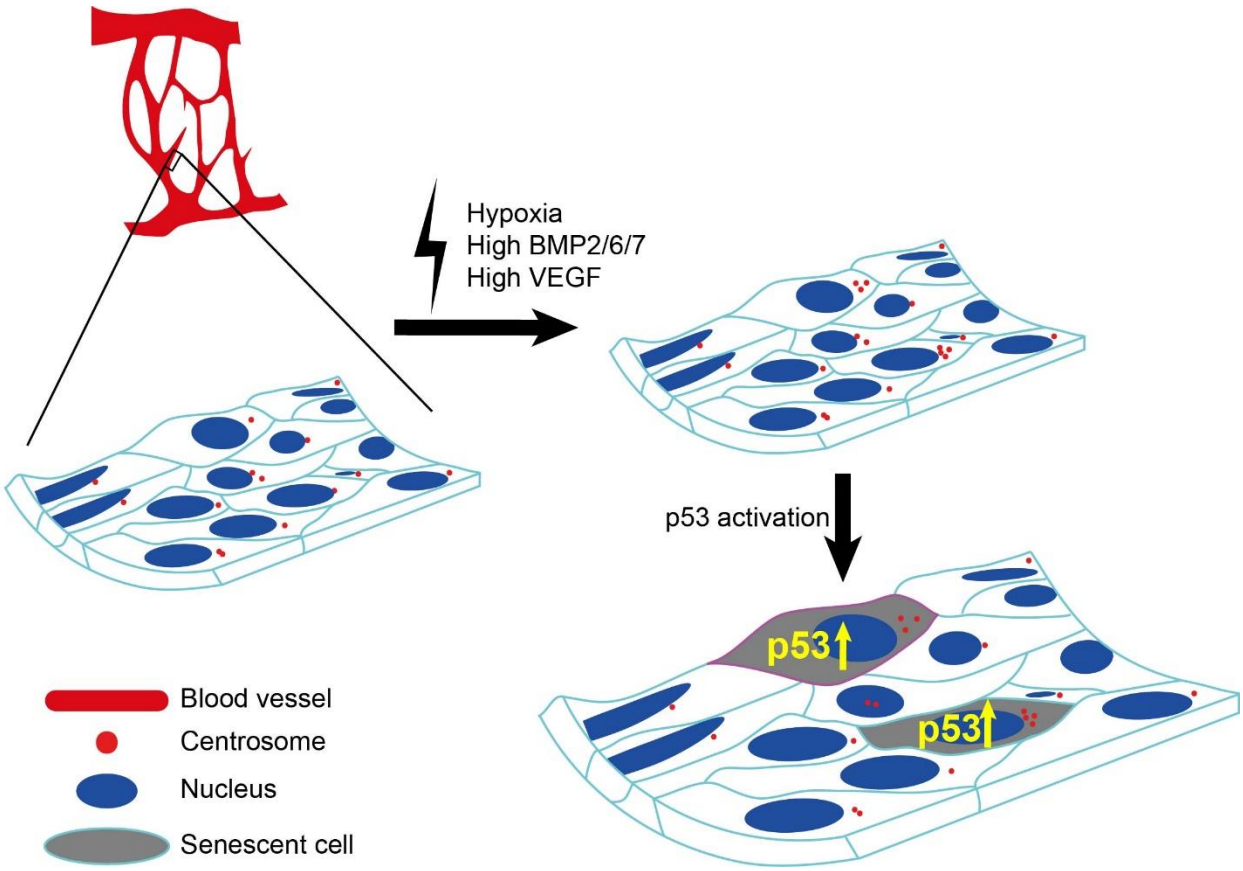
Hypoxia
High BMP2/6/7
High VEGF
p53 activation
p53
p53
Blood vessel
Centrosome
Nucleus
Senescent cell

REFERENCES

1. Folkman J (1971) Tumor angiogenesis: therapeutic implications. N Engl J Med 285: 1182-1186.

2. Hanahan D, Weinberg RA (2011) Hallmarks of cancer: the next generation. Cell 144: 646-674.

3. Hida K, Hida Y, Amin DN, Flint AF, Panigrahy D, et al. (2004) Tumor-associated endothelial cells with cytogenetic abnormalities. Cancer Research 64: 8249-8255.

4. Dudley AC, Shih SC, Cliffe AR, Hida K, Klagsbrun M (2008) Attenuated p53 activation in tumour-associated stromal cells accompanies decreased sensitivity to etoposide and vincristine. Br J Cancer 99: 118-125.

5. Kushner EJ, Ferro LS, Liu JY, Durrant JR, Rogers SL, et al. (2014) Excess centrosomes disrupt endothelial cell migration via centrosome scattering. J Cell Biol 206: 257-272.

6. Taylor SM, Nevis KR, Park HL, Rogers GC, Rogers SL, et al. (2010) Angiogenic factor signaling regulates centrosome duplication in endothelial cells of developing blood vessels. Blood 116: 3108-3117.

7. Balkwill FR, Capasso M, Hagemann T (2012) The tumor microenvironment at a glance. Journal of Cell Science 125: 5591-5596.

8. Zhang XJ, Nie DT, Chakrabarty S (2010) Growth factors in tumor microenvironment. Frontiers in Bioscience-Landmark 15: 151-165.

9. Bragdon B, Moseychuk O, Saldanha S, King D, Julian J, et al. (2011) Bone morphogenetic proteins: a critical review. Cell Signal 23: 609-620.

10. Vaupel P, Kallinowski F, Okunieff P (1989) Blood-Flow, Oxygen and Nutrient Supply, and Metabolic Microenvironment of Human-Tumors - a Review. Cancer Research 49: 6449-6465.

11. Hockel M, Schlenger K, Aral B, Mitze M, Schaffer U, et al. (1996) Association between tumor hypoxia and malignant progression in advanced cancer of the uterine cervix. Cancer Research 56: 4509-4515.

12. Xu J, Li H, Wang B, Xu Y, Yang J, et al. (2010) VHL inactivation induces HEF1 and Aurora kinase A. J Am Soc Nephrol 21: 2041-2046.

13. Zhou HY, Kuang J, Zhong L, Kuo WL, Gray JW, et al. (1998) Tumour amplified kinase STK15/BTAK induces centrosome amplification, aneuploidy and transformation. Nat Genet 20: 189-193.

14. Meraldi P, Honda R, Nigg EA (2002) Aurora-A overexpression reveals tetraploidization as a major route to centrosome amplification in p53(-/-) cells. Embo Journal 21: 483-492.

15. Nakada C, Tsukamoto Y, Matsuura K, Nguyen TL, Hijiya N, et al. (2011) Overexpression of miR-210, a downstream target of HIF1 alpha, causes centrosome amplification in renal carcinoma cells. Journal of Pathology 224: 280-288.

16. Horwich MD, Zamore PD (2008) Design and delivery of antisense oligonucleotides to block microRNA function in cultured Drosophila and human cells. Nat Protoc 3: 1537-1549.

17. Kushner EJ, Ferro LS, Yu Z, Bautch VL (2016) Excess centrosomes perturb dynamic endothelial cell repolarization during blood vessel formation. Mol Biol Cell 27: 1911-1920.

18. Mikule K, Delaval B, Kaldis P, Jurcyzk A, Hergert P, et al. (2007) Loss of centrosome integrity induces p38-p53-p21-dependent G1-S arrest. Nat Cell Biol 9: 160-170.

19. Srsen V, Gnadt N, Dammermann A, Merdes A (2006) Inhibition of centrosome protein assembly leads to p53-dependent exit from the cell cycle. J Cell Biol 174: 625-630.

20. Lambrus BG, Uetake Y, Clutario KM, Daggubati V, Snyder M, et al. (2015) p53 protects against genome instability following centriole duplication failure. J Cell Biol 210: 63-77.

21. Wong YL, Anzola JV, Davis RL, Yoon M, Motamedi A, et al. (2015) Cell biology. Reversible centriole depletion with an inhibitor of Polo-like kinase 4. Science 348: 1155-1160.

22. Andreassen PR, Lohez OD, Lacroix FB, Margolis RL (2001) Tetraploid state induces p53-dependent arrest of nontransformed mammalian cells in G1. Mol Biol Cell 12: 1315-1328.

23. Wong C, Stearns T (2005) Mammalian cells lack checkpoints for tetraploidy, aberrant centrosome number, and cytokinesis failure. BMC Cell Biol 6: 6.

24. Ganem NJ, Godinho SA, Pellman D (2009) A mechanism linking extra centrosomes to chromosomal instability. Nature 460: 278-282.

25. Cuomo ME, Knebel A, Morrice N, Paterson H, Cohen P, et al. (2008) p53-Driven apoptosis limits centrosome amplification and genomic instability downstream of NPM1 phosphorylation. Nat Cell Biol 10: 723-730.

26. Holland AJ, Fachinetti D, Zhu Q, Bauer M, Verma IM, et al. (2012) The autoregulated instability of Polo-like kinase 4 limits centrosome duplication to once per cell cycle. Genes Dev 26: 2684-2689.

27. Nigg EA, Raff JW (2009) Centrioles, centrosomes, and cilia in health and disease. Cell 139: 663-678.

28. Janssen A, van der Burg M, Szuhai K, Kops GJ, Medema RH (2011) Chromosome segregation errors as a cause of DNA damage and structural chromosome aberrations. Science 333: 1895-1898.

29. Vitre BD, Cleveland DW (2012) Centrosomes, chromosome instability (CIN) and aneuploidy. Curr Opin Cell Biol 24: 809-815.

30. d'Adda di Fagagna F, Reaper PM, Clay-Farrace L, Fiegler H, Carr P, et al. (2003) A DNA damage checkpoint response in telomere-initiated senescence. Nature 426: 194-198.

31. Di Micco R, Fumagalli M, Cicalese A, Piccinin S, Gasparini P, et al. (2006) Oncogene-induced senescence is a DNA damage response triggered by DNA hyper-replication. Nature 444: 638-642.

32. Kwong J, Hong L, Liao R, Deng Q, Han J, et al. (2009) p38alpha and p38gamma mediate oncogenic ras-induced senescence through differential mechanisms. J Biol Chem 284: 11237-11246.

33. Yu FX, Guan KL (2013) The Hippo pathway: regulators and regulations. Genes Dev 27: 355-371.

34. Toji S, Yabuta N, Hosomi T, Nishihara S, Kobayashi T, et al. (2004) The centrosomal protein Lats2 is a phosphorylation target of Aurora-A kinase. Genes Cells 9: 383-397.

35. McPherson JP, Tamblyn L, Elia A, Migon E, Shehabeldin A, et al. (2004) Lats2/Kpm is required for embryonic development, proliferation control and genomic integrity. EMBO J 23: 3677-3688.

36. Aylon Y, Michael D, Shmueli A, Yabuta N, Nojima H, et al. (2006) A positive feedback loop between the p53 and Lats2 tumor suppressors prevents tetraploidization. Genes Dev 20: 2687-2700.

37. Aylon Y, Yabuta N, Besserglick H, Buganim Y, Rotter V, et al. (2009) Silencing of the Lats2 tumor suppressor overrides a p53-dependent oncogenic stress checkpoint and enables mutant H-Ras-driven cell transformation. Oncogene 28: 4469-4479.

38. Ganem NJ, Cornils H, Chiu SY, O'Rourke KP, Arnaud J, et al. (2014) Cytokinesis failure triggers hippo tumor suppressor pathway activation. Cell 158: 833-848.

39. Meek DW, Anderson CW (2009) Posttranslational modification of p53: cooperative integrators of function. Cold Spring Harb Perspect Biol 1: a000950.

40. Tibbetts RS, Brumbaugh KM, Williams JM, Sarkaria JN, Cliby WA, et al. (1999) A role for ATR in the DNA damage-induced phosphorylation of p53. Genes Dev 13: 152-157.